

BIODEGRADATION OF PHENOLIC COMPOUNDS USING AN INDIGENOUS MIXED MICROBIAL CULTURE

A THESIS

submitted by

P.SARAVANAN

for the award of the degree

of

DOCTOR OF PHILOSOPHY



**DEPARTMENT OF CHEMICAL ENGINEERING
INDIAN INSTITUTE OF TECHNOLOGY GUWAHATI**

MAY 2008

BIODEGRADATION OF PHENOLIC COMPOUNDS USING AN INDIGENOUS MIXED MICROBIAL CULTURE

A THESIS

submitted by

P. SARAVANAN

for the award of the degree

of

DOCTOR OF PHILOSOPHY



**DEPARTMENT OF CHEMICAL ENGINEERING
INDIAN INSTITUTE OF TECHNOLOGY GUWAHATI**

MAY 2008

I dedicate this thesis to my parents,

wife and daughter





**INDIAN INSTITUTE OF TECHNOLOGY
GUWAHATI**

Department of Chemical Engineering

STATEMENT

I do hereby declare that the matter embodied in this thesis is the result of investigations carried out by me in the Department of Chemical Engineering, Indian Institute of Technology Guwahati, India, under the supervision of Dr. Prabirkumar Saha and Dr. K. Pakshirajan.

In keeping with the general practice of reporting scientific observations, due acknowledgements have been made wherever the work described is based on the findings of other investigators.

May, 2008.

P. Saravanan



INDIAN INSTITUTE OF TECHNOLOGY
GUWAHATI

Department of Chemical Engineering

CERTIFICATE

It is certified that the work described in this thesis entitled “*Biodegradation of phenolic compounds using an indigenous mixed microbial culture,*” by P. Saravanan for the award of degree of Doctor of Philosophy is an authentic record of the results obtained from the research work carried out under our supervision in the Department of Chemical Engineering, Indian Institute of Technology Guwahati, India, and this work has not been submitted elsewhere for a degree.

May, 2008

Dr. Prabirkumar Saha

Assistant Professor

(Thesis Supervisor)

Department of Chemical Engineering

IIT Guwahati

Dr. K. Pakshirajan

Assistant Professor

(Thesis Supervisor)

Department of Biotechnology

IIT Guwahati

ACKNOWLEDGEMENTS

Ph.D is again learning process. Throughout these years, I have received much support from my supervisors, family and friends... It would be difficult to individually acknowledge all those who deserve it, without any serious omissions. However, I will try to express my gratitude to those who supported me in making this thesis possible.

It is with my deepest sense of appreciation that I express my foremost acknowledgement to my research advisors, Dr. Prabirkumar Saha, Department of Chemical Engineering and Dr. Pakshirajan, Department of Biotechnology for their continuous care, support and encouragement throughout my research work. I am obliged for the ample freedom they allowed me in conducting my work.

I am thankful to my doctoral committee members, Prof. A. K. Ghosal, Dr. A. Singh and Prof. B. K. Patel for their constructive criticism and precious suggestions. I owe my gratitude to the Heads of the Department of Chemical Engineering, Prof. D. S. De and Prof. A. K. Ghosal for providing me with the necessary facilities in their respective tenures.

I take this opportunity to express my love and gratitude to my loving parents and brothers (especially to my eldest brother) for being there near to me all through my career.

I would express my humble indebted thanks to my friend, Gopinath for his suggestions, constant encouragement and moral support to, throughout my Ph. D work.

I cherish my close association with my friends Aadal, Monash, Ashok, Kitcha, Atul, Satish, Shiva, Debasis (the only Bengali friend to me) and other friendly faces always abound in my memories.

I reserve this final paragraph to my loving wife Sujatha and my daughter Sangamithirai. I am so lucky to have them in my life. I had a lot of support from my wife through out my research without which I could not have completed my research in time. In fact, the arrival of my daughter in our life kindled me to make this thesis at the earliest.

P. Saravanan

May 2008

ABSTRACT

Biological treatment of wastewater containing phenolic compounds, using indigenous mixed microbial consortium, is the main theme of this thesis. Biological degradation has been advocated to be a better alternative for phenol degradation as opposed to other popular methods for wastewater treatment. Merits of biological treatment and demerits of other methods are also properly discussed in the thesis. Phenol and *m*-cresol have been identified as two crucial phenolic compounds that are found commonly in various industrial effluents. Although past researchers have mostly studied biodegradation of single pollutant using pure single microbial species, it has been argued in this thesis that various organic pollutants usually exist together in industrial wastewater and best degradation of all these can be ensured only with a mixed microbial consortium. Hence, an indigenous mixed microbial consortium has been isolated and enriched from a wastewater treatment plant located at Guwahati, India and has been used for the present study. The mixed culture was identified as mixed strains of predominantly *Pseudomonas* sp. Degradation of phenol and *m*-cresol were studied both as single substrate and mixed substrate using the culture. The study was initiated in 250 mL batch shake flask with 100 mL working volume and scaled up to 4 L batch stirred tank reactor (BSTR) and internal loop airlift bioreactor (ILAR) of 2.5 L capacity.

The experimental data on biodegradation of phenol and *m*-cresol, investigated in batch shake flasks as single and dual substrate, were analyzed for process modeling. The specific growth rates of the culture at various phenol concentrations were fitted to various models such as Haldane, Han-Levenspiel, Edward, Luong and Yano-Koga. The bio kinetic constants estimated using these models showed good potential of the

mixed microbial culture in phenol degradation. For biodegradation of phenol/*m*-cresol as mixed substrate, a 2^2 full factorial design with the two substrates as the factors at two different levels and two different initial concentration ranges, were employed. Statistical analyses of the specific growth rate of the culture in the mixed substrate system were performed in the form Analysis of Variance (ANOVA) and Student 't' test, which gave good interpretation in terms of main and interaction effects of the substrates.

Photocatalytic oxidation in presence of semiconductor has been identified as another popular and effective method of phenol degradation. It has been intended to study and compare the efficiency of photocatalytic degradation of phenol with that of biological degradation process. Two efficient semiconductors *viz.*, an internationally popular brand TiO₂ Degussa P-25[®] and a locally made TiO₂ Anjatox[®], were chosen to carry the necessary study in this direction. The photocatalytic activities of the two semiconductors were studied and compared, and performance in terms of phenol degradation efficiency of the photocatalytic process was evaluated and compared with that of the biodegradation process using the mixed culture.

Based on the batch shake flask and BSTR studies, a 2.5 L internal loop airlift reactor (ILALR) was designed and evaluated for its performance in phenolics degradation. Prior to the biodegradation experiments in the ILAR, hydrodynamic studies such as residential time distribution (RTD) and determination of volumetric mass transfer coefficient (k_1a) were carried out with both de-ionized water and fermentation medium supporting growth of the mixed culture. This hydrodynamic study proved helpful in finding the optimum residence time and air flow rate into the reactor for further biodegradation experiments.

The ILALR was operated under batch, fed batch and continuous mode to study biodegradation of phenol and *m*-cresol as both single and mixed substrate systems. The results of this batch study were compared with that of the batch shake flask study, and several demerits were observed in batch operation of the ILALR. The fed-batch operations were carried out to overcome the shortcomings in the batch operation. Results showed that the mixed microbial culture was able to degrade both phenol and *m*-cresol quickly and efficiently in this mode of operation.

To maintain parity with industrial scale operation, continuous operation of the ILALR was also carried out for the treatment of phenol/*m*-cresol as both single and mixed substrate systems under two Hydraulic Retention Times (HRTs). The continuous operation of the ILALR rendered even better results than fed-batch operation. Shock loading experiments at the said HRTs revealed stable and good performance of the system in treating high strength phenolics even under such extreme conditions.

Keywords: Biodegradation; indigenous mixed microbial culture; *Pseudomonas* spp.; phenol; *m*-cresol; mixed substrate system; substrate inhibition model; batch stirred tank reactor; photoreactor, internal loop airlift bioreactor.

CONTENTS

Acknowledgement	i
Abstract	ii
List of Figures	x
List of Tables	xv
Abbreviations and Notations	xviii
1. INTRODUCTION	1
1.1. Generalities.....	1
1.2. Biological Processes Involving Microbes	5
1.3. Heterogeneous Photocatalysis	6
1.4. Bioreactor for Wastewater Treatment.....	9
1.5. Objective and Scope.....	13
1.6. Organization of Thesis.....	14
2. LITERATURE REVIEW	18
2.1. Sources and Major Components of Phenolic Wastewater.....	18
2.2. Major Treatment Techniques for Phenolic Wastewater	20
2.2.1. Adsorption.....	20
2.2.2. Air Stripping.....	20
2.2.3. Electrochemical Oxidation.....	21
2.2.4. Advanced Oxidation Processes.....	22
2.2.4.1 . Ozonation/UV.....	22
2.2.4.2 . Ultrasonication.....	23
2.2.4.3 . Solar Photocatalytic Oxidation.....	23

2.3.	Pros and Cons of the above Wastewater Treatment Techniques...	24
2.4.	Biological Treatment Processes Involving Microbes.....	25
2.4.1.	Biodegradation by Yeast and Fungi.....	26
2.4.2.	Biodegradation of Phenolics by Bacteria.....	27
2.5.	Design of Experiments.....	35
2.5.1.	Factorial Design of Experiments.....	35
2.5.2.	Analysis of Variance.....	36
2.5.3.	Students 't' Test	37
2.6.	Microbial Growth Kinetics and Substrate Inhibition Models for Single Substrate Biodegradation Systems.....	40
2.7.	Treatment of Phenolics in Airlift Bioreactors.....	44
3.	MATERIALS AND METHODS	50
3.1.	Chemicals and Reagents.....	50
3.2.	Indigenous Mixed Microbial Culture and Culture Conditions...	50
3.3.	Enrichment of the Culture to Degrade Phenolic Compounds.....	51
3.4.	Characterization and Identification of the Indigenous Mixed Microbial Culture.....	51
3.4.1.	Biochemical Characterization.....	51
3.4.2.	Scanning Electron Microscopy (SEM).....	52
3.5.	Biodegradation Studies in Batch Shake Flasks.....	52
3.5.1.	Single Substrate System.....	52
3.5.2.	Mixed Substrate System.....	53
3.6.	Phenol Biodegradation in a Batch Stirred Tank Reactor.....	54
3.6.1.	Experimental Set up.....	54
3.7.	Feasibility of the Indigenous Mixed Culture to Treat a Refinery Industry Wastewater.....	54
3.8.	Phenol Degradation in a Solar Photoreactor.....	55
3.8.1.	Characterization of the Photocatalysts.....	56
3.8.1.1.	X-Ray Diffraction (XRD) Analysis.....	56

3.8.1.2. BET Surface Area Analysis.....	56
3.8.1.3. Particle Size Distribution.....	56
3.9. Biodegradation Studies in an Internal Loop Airlift Bioreactor (ILALR).....	57
3.9.1. Experimental Setup.....	57
3.9.2. Hydrodynamic Studies with the ILALR.....	57
3.9.2.1. Residential Time Distribution (RTD).....	57
3.9.2.2. Volumetric Mass Transfer Coefficient (k_La) Determination.....	58
3.9.2.3. Bubble Diameter Analysis in the Riser and Downcomer Sections of the ILALR.....	58
3.9.3. Batch Biodegradation Studies with the ILALR.....	59
3.9.3.1. Single Substrate System.....	59
3.9.3.2. Mixed Substrate System.....	59
3.9.4. Fed-batch Biodegradation Study with the ILALR.....	60
3.9.4.1. Single Substrate System.....	60
3.9.4.2. Mixed Substrate System.....	60
3.9.5. Continuous Degradation Studies with the ILALR.....	61
3.9.5.1. Single Substrate System.....	61
3.9.5.2. Mixed Substrate System.....	61
3.9.5.3. Stability Studies on the Performance of the ILALR.....	62
3.10. Analytical Methods.....	63
3.10.1. Determination of Biomass.....	63
3.10.2. HPLC Analysis.....	63
3.10.3. Chemical Oxygen Demand (COD) and Heavy Metal Analysis.....	64
4 RESULTS AND DISCUSSION	75
4.1. Characterization Results of the Indigenous Mixed Microbial Culture.....	75
4.2. Batch Biodegradation of the Phenolics in Shake Flasks.....	76

4.2.1.	Culture Growth and Phenol Degradation Kinetics – Single Substrate System	76
4.2.1.1.	Effect of Initial Concentration of Phenol.....	76
4.2.1.2.	Kinetics of Phenol Biodegradation.....	78
4.2.1.3.	Modeling the Kinetics of Growth of the Culture.....	78
4.2.1.4.	Modeling the Kinetics of Phenol Degradation..	81
4.2.1.5.	Analysis of Probable Intermediates during Phenol Degradation.....	82
4.2.2.	Culture Growth and <i>m</i> -Cresol Degradation Kinetics....	83
4.2.2.1.	Effect of Initial Concentration of <i>m</i> -Cresol.....	83
4.2.2.2.	Modeling the Kinetics of <i>m</i> -Cresol Biodegradation.....	85
4.2.2.3.	Modeling the Kinetics of the Culture Growth...	85
4.2.3.	Culture Growth and Mixed Substrates Degradation Kinetics.....	88
4.2.3.1.	Simultaneous Degradation Profiles of Phenol and <i>m</i> -Cresol.....	88
4.2.3.2.	Growth of the Culture in the Mixed Substrate System.....	89
4.2.3.3.	Statistical Analysis of the Specific Growth Rate of the Culture.....	90
4.2.3.4.	Biomass Yield and Specific Degradation Rate of the Substrates.....	93
4.2.3.5.	Sum Kinetics Model Fitting of Experimental Specific Degradation Rate.....	95
4.2.4.	Evaluation of the Culture to Treat a Refinery Effluent	97
4.3.	Performance of Batch Stirred Tank Reactor in Degrading Phenol	99
4.3.1.	Effect of Initial Phenol Concentration on the Culture Growth and its Degradation.....	99
4.3.2.	Modeling the Culture Growth and Phenol Degradation Kinetics.....	101

4.4.	Solar Photocatalytic Degradation of Phenol by TiO ₂ -Based Heterogeneous Catalyst.....	103
4.4.1.	Characterization Results of the Photocatalysts.....	104
4.4.2.	Effect of Photocatalyst Concentration on Phenol Degradation.....	106
4.4.3.	Effect of Initial Concentration of Phenol.....	106
4.4.4.	Analysis of Intermediates during phenol degradation....	107
4.5.	Biodegradation of Phenolics in Internal Loop Airlift Reactor.....	108
4.5.1.	Hydrodynamics and Mass Transfer Studies.....	108
4.5.1.1.	Residence Time Distribution (RTD).....	109
4.5.1.2.	Volumetric Oxygen Mass Transfer Coefficient (k_La) in the ILALR.....	110
4.5.2.	Batch Biodegradation of Phenol and <i>m</i> -Cresol in the ILALR.....	113
4.5.2.1.	Phenol Biodegradation and the Culture Growth	113
4.5.2.2.	<i>m</i> -Cresol Biodegradation and the Culture Growth.....	115
4.5.2.3.	Biodegradation of Phenol and <i>m</i> -Cresol in Mixed Substrate System.....	116
4.5.3.	Fed-batch Biodegradation of Phenolics.....	118
4.5.3.1.	Single Substrate System.....	119
4.5.3.2.	Mixed Substrate System.....	120
4.5.4.	Biodegradation of Phenol and <i>m</i> -Cresol in the Continuously Operated ILALR	121
4.5.4.1.	Single Substrate System.....	122
4.5.4.2.	Performance of the ILALR under Shock Loading Conditions of Phenol/ <i>m</i> -Cresol.....	123
4.5.4.3.	Mixed Substrate System.....	125
5	SUMMARY AND CONCLUSIONS	169
	BIBLIOGRAPHY	173
	APPENDIX A	190
	LIST OF PUBLICATIONS	194

LIST OF FIGURES

Figures	Title	Page No.
1.1	TiO ₂ -semiconductor photocatalytic process.....	17
2.1	Biodegradation pathway for the metabolism of 3,5 xylenol, <i>m</i> -cresol and <i>p</i> -cresol by <i>Pseudomonas putida</i>	49
3.1	Phenol degradation profile followed during the enrichment period.....	70
3.2	<i>m</i> -Cresol degradation profile followed during the enrichment period.....	70
3.3	Schematic of the simple batch stirred tank reactor.....	71
3.4	Schematic of the solar photoreactor.....	71
3.5	Schematic of the ILALR.....	72
3.6	Photograph of the ILALR used in the study	73
3.7	Schematic of the ILALR in continuous operation.....	73
3.8	Calibration curve obtained for phenol estimation using the HPLC	74
3.9	Calibration curve obtained for <i>m</i> -cresol estimation using the HPLC.....	74
4.1	Photograph of the Gram stained culture taken under light microscope clearly showing the predominant presence of distinct rod shaped Gram-negative bacteria of <i>Pseudomonas</i> spp.....	139
4.2	SEM image of the enriched mixed microbial culture confirming the presence of rod shaped <i>Pseudomonas</i> spp. bacteria along with its typical sizes.....	139
4.3	Time profile of phenol biodegradation by the culture in the batch shake flasks.....	140
4.4	Variation of phenol degradation rate with initial phenol concentrations.....	140

4.5	Biomass (OD ₆₀₀) of the culture as a function of time at different initial phenol concentrations.....	141
4.6	Experimental and model predicted specific growth rate of the culture at different initial phenol concentrations.....	141
4.7	Experimental and predicted phenol degradation rate of the culture due to the various models.....	142
4.8	Intermediates formed and their concentrations during (middle) and end of batch biodegradation of phenol.....	142
4.9	Time profile of <i>m</i> -cresol degradation by the culture in batch shake flasks.....	143
4.10	Biomass (OD ₆₀₀) of the culture as a function of time at different initial <i>m</i> -cresol concentrations.....	144
4.11	Comparison of specific growth and degradation rates at different initial <i>m</i> -cresol concentrations.....	145
4.12	Experimental and model predicted specific growth rate of the culture at different initial <i>m</i> -cresol concentrations.....	145
4.13	Experimental and various model predicted specific degradation rate of the culture at different <i>m</i> -cresol concentrations.....	146
4.14	Phenol and <i>m</i> -cresol biodegradation patterns shown by the culture at low initial concentration ranges of the substrates.....	146
4.15	Phenol and <i>m</i> -cresol biodegradation patterns shown by the culture at high initial concentration ranges of the substrates.....	147
4.16	Biomass profile of the culture when grown in medium containing both phenol and <i>m</i> -cresol.....	147
4.17	Interaction effect between phenol and <i>m</i> -cresol on the culture specific growth rate in their low concentration ranges.....	148
4.18	Interaction effect between phenol and <i>m</i> -cresol on the culture specific growth rate in their high concentration ranges.....	148
4.19	Interaction effect between phenol and <i>m</i> -cresol in their low concentration ranges on specific phenol degradation rate.....	149
4.20	Interaction effect between phenol and <i>m</i> -cresol in their high concentration ranges on specific phenol degradation rate.....	149

4.21	COD removal profile of the pH adjusted refinery wastewater as a function of time.....	150
4.22	Time profile of phenol degradation at different initial phenol concentrations in the BSTR.....	150
4.23	Time profile of biomass output at different initial phenol concentrations in the BSTR.....	151
4.24	Comparison of specific growth and substrate degradation rates at different initial phenol concentrations.....	151
4.25	Experimental and predicted specific growth rate of the culture obtained by applying Haldane and Han-Levenspiel substrate inhibition models.....	152
4.26	Experimental and predicted specific substrate degradation rate obtained by applying Haldane and Han-Levenspiel substrate inhibition models.....	152
4.27	XRD pattern of the Anjatox [®] TiO ₂ photocatalyst.....	153
4.28	XRD pattern of the Degussa P-25 [®] TiO ₂ photocatalyst.....	153
4.29	Particle size distribution of Degussa P-25 [®] TiO ₂ photocatalyst...	154
4.30	Particle size distribution of Anjatox [®] TiO ₂ photocatalyst.....	154
4.31	Effect of concentration of Anjatox [®] and Degussa P-25 [®] TiO ₂ photocatalysts on phenol degradation.....	155
4.32	Effect of initial concentration of phenol on its degradation using Degussa P-25 [®] TiO ₂ at an optimum concentration of 3 g/L.....	155
4.33	Effect of initial concentration of phenol on its degradation using Anjatox [®] TiO ₂ at an optimum concentration of 9 g/L.....	156
4.34	Intermediates identified in the photocatalytic degradation along with its concentrations.....	156
4.35	Results of RTD in the ILALR at various superficial gas flow rate.	157
4.36	Photograph of the bubble used for the analysis.....	157
4.37	DO profile (C _L) in estimating k _L a in the ILALR for a non-living system by the dynamic gassing out method.....	158
4.38	Variation of k _L a in the ILALR for nonliving system at different superficial airflow rates.....	158

4.39	DO profile (C_L) obtained by the dynamic gassing out method in estimating k_La in the ILALR for a living system.....	159
4.40	Batch biodegradation profile of phenol obtained in the ILALR.....	159
4.41	Biomass profile of the culture obtained at various initial phenol concentrations in the batch operated ILALR.....	160
4.42	Comparison of specific growth and degradation rates at different initial phenol concentrations in the ILALR.....	160
4.43	Batch biodegradation profile of <i>m</i> -cresol obtained in the ILALR..	161
4.44	Biomass profile of the culture obtained at various initial <i>m</i> -cresol concentrations in the batch operated ILALR.....	161
4.45	Comparison of specific growth and degradation rates at different initial <i>m</i> -cresol concentrations in the ILALR.....	162
4.46	Biodegradation patterns of phenol and <i>m</i> -cresol in the mixed substrate system in the ILALR.....	162
4.47	Biomass concentration profile due to phenol and <i>m</i> -cresol in the mixed substrate system in the ILALR.....	163
4.48	Biodegradation of phenol and <i>m</i> -cresol as single substrate system in the fed-batch operated ILALR.....	163
4.49	Biomass profile obtained in the fed-batch operated ILALR during degradation of phenol and <i>m</i> -cresol in single substrate system.....	164
4.50	Biodegradation of phenol and <i>m</i> -cresol in mixed substrate system in the ILALR operated under fed-batch mode.....	164
4.51	Biomass profile of the culture in mixed substrate system in the fed-batch operated ILALR.....	165
4.52	Phenol degradation in single substrate system in the continuously operated ILALR at 8.3 h HRT along with the shock loading effect in the reactor.....	165
4.53	Phenol degradation in single substrate system in the continuously operated ILALR at 4.1 h HRT along with the shock loading effect in the reactor.....	166

4.54	<i>m</i> -Cresol degradation in single substrate system in the continuously operated ILALR at 8.3 h HRT along with the shock loading effect in the reactor.....	166
4.55	<i>m</i> -Cresol degradation in single substrate system in the continuously operated ILALR at 4.1 h HRT along with the shock loading effect in the reactor.....	167
4.56	Degradation of phenol and <i>m</i> -cresol in mixed substrate system in the continuously operated ILALR at 8.3 h HRT.....	167
4.57	Degradation of phenol and <i>m</i> -cresol in mixed substrate system in the continuously operated ILALR at 4.1 h HRT.....	168



LIST OF TABLES

Tables	Title	Page No.
1.1.	Band positions of some common semiconductor photocatalysts in aqueous solution at pH1.....	16
3.1	Composition of the mineral salt medium used in the study.....	65
3.2	2 ² full factorial design with three center point replicates adopted in the mixed substrate biodegradation study for both the initial concentration ranges.....	65
3.3	Characteristics of the refinery wastewater	66
3.4	Geometrical details of the internal loop airlift reactor	66
3.5	Combinations of the phenolics concentrations adopted to study the batch degradation of the mixed substrates in the ILALR.....	67
3.6	Concentrations of the phenolics in single substrate and mixed substrate system along with volume treated in each step in the ILALR operated under fed batch mode.....	67
3.7	Various stages of continuous operation in the ILALR treating synthetic wastewater containing either phenol/ <i>m</i> -cresol	68
3.8	2 ² full factorial design matrix along with the stages and time of operation for studying degradation of phenol/ <i>m</i> -cresol as mixture at 8.3 h HRT	69
3.9	2 ² full factorial design matrix along with the stages and time of operation for studying degradation of phenol/ <i>m</i> -cresol as mixture at 4.1 h HRT.....	69

4.1	Results of the various biochemical characterization tests to identify the predominant microbial species in the enriched mixed culture	128
4.2	Determination coefficient (R^2) and rate constant values obtained by fitting three-half order kinetic model to the experimental phenol degradation profile.	129
4.3	Estimated growth kinetic parameters during phenol degradation using various models	129
4.4	Comparison of the estimated kinetics parameter of the culture during phenol degradation in batch shake flasks with those found in the literature.....	130
4.5	Estimated biokinetic parameters obtained from different models during biodegradation of phenol by the culture	132
4.6	Culture growth kinetic parameters obtained from different models during biodegradation of <i>m</i> -cresol.....	132
4.7	Estimated substrate degradation kinetic parameters obtained from different models during biodegradation of <i>m</i> -cresol.....	133
4.8	Calculated specific growth rate of the culture obtained for high and low initial concentration ranges of phenol and <i>m</i> -cresol.....	133
4.9	ANOVA of the culture specific growth rate in low concentration ranges of the substrates.....	134
4.10	ANOVA of the culture specific growth rate in high concentration ranges of the substrates.....	134
4.11	Students ' <i>t</i> ' test of the culture specific growth rate in low concentration ranges of the substrates.....	135
4.12	Students ' <i>t</i> ' test of the culture specific growth rate in the high concentration ranges of the substrates.....	135
4.13	Total biomass yield (g/g) values in low concentration ranges of the substrates.....	135
4.14	Total biomass yield (g/g) values in high concentration ranges of the substrates.....	136

4.15	Specific degradation rates of phenol and <i>m</i> -cresol obtained in low and high initial concentration ranges of the substrates.....	136
4.16	Typical characteristics of the refinery wastewater.....	137
4.17	Biokinetic constants estimated by fitting Haldane and Han-Levenspiel substrate inhibition models on the experimental data on growth of the culture.....	137
4.18	Specific growth rate of the culture obtained at different combinations of phenol and <i>m</i> -cresol concentrations in the ILALR.....	138
4.19	Observed degradation rates of phenol and <i>m</i> -cresol in the mixed substrate system in the fed-batch operated ILALR.....	138



ABBREVIATIONS AND NOTATIONS

ANOVA	Analysis Of Variance
BSTR	Batch Stirred Tank Reactor
COD	Chemical Oxygen Demand
DO	Dissolved Oxygen
HRT	Hydraulic Retention Time
ILALR	Internal Loop Airlift Bioreactor
RTD	Residential Time Distribution
C_e	Liquid Phase Oxygen Concentration in Equilibrium with Gas Phase (mg/L)
C_L	Concentration of DO in the Liquid (mg/L)
K	Constant in Edward and Yano-Koga Models
K_s	Half Saturation Coefficient (mg/L)
K_i	Inhibition Constant (mg/L)
S	Substrate Concentration at Time t (mg/L)
S_0	Substrate concentration at time t = 0 (mg/L)
S^*	Substrate Concentration at which Specific Growth Rate is Maximum (mg/L)
X	Biomass Concentration at Time t (mg/L)
X_0	Biomass Concentration at Time t = 0 (mg/L)
m, n	Empirical Constants in Han-Levenspiel Model

k_La	Volumetric Mass Transfer Coefficient (s^{-1})
q	Specific Substrate Degradation Rate (h^{-1})
q_{max}	Maximum Specific Substrate Degradation Rate (h^{-1})
t	Time (h)
μ	Specific Growth rate (mg/L)
μ_{max}	Maximum Specific Growth Rate (h^{-1})



CHAPTER 1

INTRODUCTION

1.1. Generalities

Generation of gaseous, liquid and solid wastes is an unavoidable consequence of industrial, agricultural and domestic activities. Nevertheless, the environmental impact of these activities must be minimized to ensure sustainable quality of life.

While conservation and better utilization of resources would ultimately have the greatest influence on sustainability of the planet; reduced generation, improved treatment and utilization of wastes will remain the essential components of an overall strategy for maintenance of environmental quality.

One of the most alarming phenomena is the growth of industrial sectors, which discharge a huge amount of wastewater contaminated with the toxic organic substances like phenolics. The major industries that discharge phenolic wastewater include petroleum refineries, petrochemicals, textile, dye manufacturing, phenolics resin manufacturing, glass fiber units, varnish industries and smelting related to metallurgical operations (Nuhoglu and Yalcin, 2005; Juang and Tsai, 2006; Yan *et al.*, 2006; Bai *et al.*, 2007). Phenol and cresol are the two most important phenolic compounds that are present in wastewater discharged from these industries (Yan *et al.*, 2006; Pakshirajan *et al.*, 2008). They are toxic to human beings and aquatic

biota (Kumaran and Paruchuri, 1996; Monteiro *et al.*, 2000). Humans, who are acutely exposed to phenol by the oral route, suffer damage in blood, liver, kidney and cardiac toxicity including weak pulse, cardiac depression and reduced blood pressure. Ingestion of 1 g phenol is reported to be lethal for humans (Kumaran and Paruchuri, 1996). Moreover, consumption of water containing high phenolic compounds may lead to cancer. Due to these adverse health effects of phenolics, the World Health Organization (WHO) has set a permissible upper limit of 1 mg/L to regulate the phenol concentration in drinking waters (Nuhoglu and Yalcin, 2005). Therefore, removal of these phenolics to sufficiently low levels in wastewater is mandatory. Appropriate strategies of wastewater treatment have to be employed in order to counterbalance these growing environmental problems.

For the last two decades, rigorous pollution control and legislation in many countries have resulted in an intensive search for new and more efficient water treatment technologies. Important wastewater treatment technologies that have come up in recent times, include but are not limited to flocculation, precipitation, adsorption on granular activated carbon, reverse osmosis, combustion and Advanced Oxidation Process (AOP) *viz.*, Photo Fenton, photocatalysis and sonication. Some of these are briefed below:

Adsorption

Adsorption is a process that occurs when a gas or liquid solute accumulates on the surface of a solid or a liquid (adsorbent), forming a molecular or atomic film (the adsorbate). The mass transfer in the opposite direction could remove the adsorbed compounds in the adsorbent. Adsorption is indicative in most natural physical, biological, and chemical systems, and is widely used in industrial applications such as

activated charcoal, synthetic resins and water and wastewater treatment. In wastewater treatment process it is generally practised as a tertiary treatment mainly for removing colour.

Photo Fenton Reaction

Decomposition of H_2O_2 , using ferrous iron (Fe II) or ferric iron (Fe III) under acidic conditions yields $\cdot OH$. This radical oxidizes the organic pollutant and eventually decomposes them to CO_2 and H_2O . The rate of removal (decomposition) of organic pollutants and the extent of mineralization using the Fe II/ H_2O_2 , and Fe III/ H_2O_2 reagents are improved considerably by irradiation with near-UV radiation and visible light. This process is called the Photo-Fenton reaction (EPA, 1998).

Photocatalytic Oxidation

In a semiconductor-sensitized AOP process, metal semiconductors are employed to destroy environmental contaminants by means of light-induced redox reactions. These reactions involve generation of conduction band electrons and valence band holes by UV irradiation of semiconductor materials such as titanium dioxide (TiO_2). In this process, the formation and availability of $\cdot OH$ are maximized by addition of oxidants such as H_2O_2 and O_3 (EPA, 1998).

Ultrasonication

Implosion of cavity bubbles in sonicated water containing dissolved gases results in formation of hydrogen and hydroxyl radicals by fragmentation of water molecules. These radicals in turn combine and generate other oxidative species such as peroxy and super oxide radicals as well as hydrogen peroxide; the quantities of each depend

on the ambient conditions and the operating parameters. Such $\bullet\text{OH}$ radicals are used for the degradation of the organic compounds (Kidak and Ince, 2006).

However, the major disadvantages of the above popular treatment technologies are:

- Some of these techniques are physico-chemical processes involving transfer of pollutants from aqueous to solid/gas phase, and they do not necessarily destroy the pollutant completely.
- Complete destruction of pollutants is not achieved in AOPs, which very often results in production of toxic intermediates. In addition to this, they cannot be adopted as a complete treatment technique due to their less efficiency in treating the pollutants.
- Chemical oxidation processes selectively destroy pollutants in slow to moderate rate. Even otherwise, fast and non-selective chemical oxidation processes add up appreciable reactor or energy costs leading to more operational and maintenance problems.

Biological Treatment

Biological treatment with pure and mixed microbial strains is an attractive alternative for the treatment of contaminated ground, surface, and wastewaters containing recalcitrant substances such as phenolics (Monteiro *et al.*, 2000; Banerjee *et al.*, 2001; Hao *et al.*, 2002; Abuhamed *et al.*, 2004; Kumar *et al.*, 2005; Rodriguez *et al.*, 2006). Aerobic degradation of phenol using pure microbial cultures has been studied extensively by many researchers; for example, *Pseudomonas putida* has been widely studied for its potential for phenol biodegradation (Hannaford and Kuek, 1999; Monteiro *et al.*, 2000; Banerjee *et al.*, 2001; Abuhamed *et al.*, 2004; Kumar *et al.*, 2005; Nuhoglu and Yalcin, 2005; Karigar *et al.*, 2006; Rodriguez *et al.*, 2006; Tsai

and Juang, 2006). However, pure cultures can hardly achieve 100% biodegradation and leave hazardous residuals after incomplete degradation (Wang and Loh, 1999). On the other hand, mixed microbial culture may be well capable of complete degradation of phenolics leaving no hazardous residues in the process. CO₂ and H₂O are generated as a result of complete degradation of organic pollutants (Ryan *et al.*, 2005; Bai *et al.*, 2007). Therefore, a mixed microbial culture would always be preferred for better applicability in wastewater treatment.

In view of the above, the theme of the research is quest for environmental friendly and economically viable process for treatment of industrial wastewaters containing phenolic compounds using mixed microbial consortium.

1.2. Biological Processes Involving Microbes

In a biological process, microbial community is confronted with a mixture of substrate composed of toxic and non-toxic compounds. The substrate is consumed by the microorganism through an enzyme-catalysed reaction. Thereby, the population of community increases. In addition to the presence of a capable microorganism, environmental conditions must also be suitable for the enzyme-catalysed reactions to proceed at a significant rate. On the other hand, growth in the microbial community depends on the changes in the feed substrate and the physico-chemical conditions (pH, temperature *etc.*) of the process. Normally, the concentration of the toxic compounds is much lower than those of the non-toxic substances. Regarding the performance of a microbial wastewater treatment system, the basic questions that one may pose are:

- Will toxic (inhibitory) compounds be degraded in the presence of non-toxic compounds? If so, to what degree?
- What should be the optimum loading rate or flow rate through the reactor to achieve complete degradation of the toxic compounds?

By studying the degradation kinetics of various toxic compounds and growth kinetics of microorganisms, knowledge about the kinetic properties of different biological systems can be gathered and these information may be helpful to understand more complex systems in a step-by-step manner. The effect of various substrates, on the microbial degradation of organic pollutants, has been the subject of a number of studies (Juang and Tsai, 2006; Yan *et al.*, 2006; Bai *et al.*, 2007). Although some of these authors, dealing with microbial growth kinetics, emphasized the ecological point of view, they almost totally neglected the facts that (i) microorganisms mostly encounter systems containing mixture of substrates (ii) growth may not be controlled by only a single substrate but by two or more substrates simultaneously and (iii) microbial growth kinetics might change due to adaptation conditions (Kar *et al.*, 1997; Juang and Tsai, 2006; Yan *et al.*, 2006; Bai *et al.*, 2007). Hence the neglected facts by the other researchers were considered for research in the present thesis work.

1.3. Heterogeneous Photocatalysis

Heterogeneous photocatalysis is a technology based on the irradiation on a catalyst, usually a semiconductor, which may be photo excited to form electron-donor sites (reducing sites) and electron-acceptor sites (oxidizing sites). Hence it provides great scope as redox reagent. The process is heterogeneous because there are two active phases - solid and liquid. The molecular orbitals of semiconductors have a band structure. The bands of interest in photocatalysis are the occupied valence band (VB)

and the unoccupied conductance band (CB), separated by an energy distance referred to as the band gap energy (E_{bg}). When the semiconductor is illuminated with light ($h\nu$) of greater energy than that of the band gap, an electron is promoted from the VB to the CB leaving a positive hole in the valence band as illustrated in Fig.1.1. After separation, the electron (e^-) and hole (h^+) pair may recombine and generate heat or can become involved in electron transfer reactions with other species in solution, *e.g.*, the oxidation or reduction of electron-donor (D) or electron-acceptor (A) species respectively shown in Fig.1.1. For oxidation reactions to occur, the VB must have a higher oxidation potential than the material under consideration. The redox potential of the VB and the CB for different semiconductors varies between +4.0 and -1.5 volts versus Normal Hydrogen Electrode (NHE) respectively. Therefore, by careful selection of the semiconductor photocatalyst, a wide range of species can be treated *via* this process.

Metal oxides and sulphides represent a large class of semiconductor materials suitable for photocatalytic purposes (Robertson 1996). Table 1.1 lists some selected semiconductor materials, which are normally used for photocatalytic reactions. The table also lists their Valence band (VB) and Conductance Band (CB) potentials, band gap energy and wavelength required to activate the catalyst.

To produce this gap, the radiation must be of a wavelength (λ) equal or lower than that calculated by the Planck's equation:

$$\lambda = \frac{hc}{E_{bg}} \quad (1.1)$$

where E_{bg} is the semiconductor band-gap energy, h is the Planck's constant and c is the speed of light.

Among the listed semiconductors, TiO_2 has been proven to be the most suitable for widespread environmental applications. It is biologically and chemically inert, stable to photo and chemical corrosion and inexpensive. Furthermore, TiO_2 is of special interest since it can use natural (solar) UV radiation. This is because TiO_2 has an appropriate energetic separation between its valence and conduction bands, which can be surpassed by the energy of a solar photon. The VB and CB energies of the TiO_2 are estimated to be +3.1 and -0.1 volts, respectively, which means that its band gap energy is 3.2 eV and therefore absorbs in the near UV light ($\lambda < 387$ nm). Although ZnO seems to be a suitable alternative to TiO_2 , it dissolves in acidic solutions and hence cannot be used for technical applications (Bahnemann *et al.*, 1991). Other semiconductor particles (*e.g.*, CdS or GaP) absorb larger fractions of the solar spectrum than TiO_2 and can form chemically activated surface-bond intermediates, but unfortunately, such catalysts are degraded during the repeated catalytic cycles usually involved in heterogeneous photocatalysis.

Titanium dioxide is widely used as white paint pigment, as sun blocking material, as cosmetic, or as binder in vitamin tablets, among its many other uses. This semiconductor exists in three crystalline forms: anatase, rutile, and brookite. Anatase and rutile are the most common forms, and the former is the most effective in wastewater treatment (Matthews, 1991). The band gap energies are approximately 3.2 eV for anatase and 3.0 eV for rutile but the driving force for oxidative processes are similar. Anatase is thermodynamically less stable than rutile, but its formation is kinetically favoured at lower temperature ($< 600^\circ\text{C}$). This could explain its higher surface area and higher surface density of active sites for adsorption and catalysis.

A popular brand of Titanium dioxide, viz., Degussa P-25[®] has become the standard for photoreactivity in environmental applications (Hoffmann *et al.*, 1995; Mills and Hunte, 1997; Litter, 1999). The product is 99.5% pure TiO₂ (anatase - rutile ratio 70:30). It is a non-porous substance, round with edged cubic particles. It is important to note that 90% of the materials do not exist as isolated particles. Rather they exist as irreducible complex primary aggregates, typically of approximately 0.1 μm in diameter. The VB and CB positions for Degussa P-25[®] have been calculated as +2.9 and -0.3 V, respectively (Martin *et al.*, 1994).

The catalytic or photo catalytic oxidation with UV/sunlight yields a good amount of intermediates. It was also reported by the researchers that intermediates such as alcohols, aldehydes, catechol, resorcinol and organic acids like oxalic, acetic, maleic fumaric, *etc.*, are found in considerable amount (Alnaizy and Akgerman, 2000) after photocatalytic reactions. Many researchers have extensively studied the activity of Degussa P-25[®] for treatment of various organic pollutants (Courco *et al.*, 1996; Guillard *et al.*, 1999; Robert and Malato, 2002; Gernjak *et al.*, 2004; Malato *et al.*, 2007; Marugan *et al.*, 2007; Nieto *et al.*, 2007; Kuo *et al.*, 2008; Monteagudo *et al.*, 2008). But the photocatalytic activity of cheaper and locally available TiO₂ has not been studied for its activity to degrade organics. Hence the present thesis has a scope of studying lab scale treatment of phenol with the said TiO₂ products and comparing their performances in terms of phenol degradation with that of biodegradation using a mixed culture.

1.4. Bioreactors for Wastewater Treatment

In the last few decades, various bioreactor designs have been proposed for wastewater treatment with an aim to ensure increased oxygen transfer rate and minimal power

consumption. One of the most promising bioreactors is the airlift bioreactor, which was first patented by Lefrancois *et al.* (1955). They are pneumatically agitated reactors where fluid circulation is carried out in a defined cyclic pattern (through a loop of conduits). They do not need any mechanical agitation and a low energy is sufficient for required aeration in the process. Compared to conventional reactors such as the stirred tanks or bubble columns, shear stress in ILALR is relatively constant and mild throughout the reactor. This fact is favorable to microbial growth (Kanai *et al.*, 1996). All these advantages explain why so many researchers have focused their attention on ALRs (Camarasa *et al.*, 2001; Couvert *et al.*, 2004; Quan *et al.*, 2004; Vinod and Reddy, 2005; Sun *et al.*, 2006; Viggiani *et al.*, 2006; Jajuee *et al.*, 2007; Feng *et al.*, 2007).

Airlift reactors differ from the bubble columns reactors by the fact that the rising fluid is separated from the down coming fluid. Airlift bioreactors comprise of four distinct zones, each with its own distinct flow pattern. The first zone, in which the gas is sparged, is known as *the riser*, as the gas-liquid dispersion travels upward in co-current fashion. This section has the higher fractional gas hold up where most of the gas-liquid mass transfers takes place. The liquid leaving the top of the riser enters a gas disengagement zone, *the gas-liquid separator*, where, some or most of the dispersed gas is removed depending on its specific design. The gas free liquid (or a dispersion of lesser gas hold up) then flows into *the down comer* and travels to the base of the device, through *the bottom*, where it re-enters the riser. Thus, the liquid phase circulates continuously around the loop. Airlift bioreactors are commonly used in aerobic fermentation processes because of their simple structure, low shear stress and ease of maintenance in comparison to the conventional stirred tank bioreactor.

In general, stirred tank reactors and airlift reactors are commonly used in industry for various types of applications. The applications include the catalytic conversion of hydrocarbons, coal gasification, synthesis of hydrocarbons from carbon monoxide and hydrogen, absorption processes, extraction, fermentation in bioengineering field. In recent years, airlift reactors have become more popular than that of the stirred tank reactor (Annettone, 2006).

The overall setup of an airlift reactor can take one of the two basic forms: (i) Internal and (ii) External. An internal airlift reactor is essentially a bubble column with a baffle or a draught tube separating the rising fluid from the sinking fluid. An external airlift reactor consists of a bubble column as the riser and a recirculation pipe that exists outside of the bubble column as the down comer. Due to the popularity of airlift reactors and bubble columns, many studies have been done in an attempt to link the efficiency of the various applications to the geometry of the column and the operating conditions under which it is running. The parameters that characterize the hydrodynamics inside an airlift reactor are the mixing efficiency, dispersion coefficient, mixing time and volumetric mass transfer rate. Mean bubble diameter is also an important parameter because of its impact on the other parameters, especially the mass transfer rate. These parameters are affected by the geometry of the reactor and the operating conditions. The operating conditions that mostly affect hydrodynamics in an airlift reactor or a bubble column are the gas flow rates and the liquid flow rates.

Quan et al. (2004) performed a study using an internal loop airlift reactor immobilized with *Achromobacter* sp to degrade phenol and 2,4 dichlorophenol. They obtained a removal efficiency of about 99.6% at a hydraulic retention time (HRT) of 8 h for a

maximum phenol concentration of 200 mg/L. Vinod and Reddy (2005) studied the biodegradation of phenolic wastewater using microorganisms in a fluidized-bed bioreactor (FBR). Experiments were conducted at wastewater flow rate of 510 mL/h and with a feed concentration of phenol as high as 1254 mg/L. Although they obtained better treatment efficiency, a fluidized bed bioreactor has a complicated operational protocol and is thus difficult in adopting it to real wastewater treatment. Jajuee et al. (2007) studied the kinetics of biodegradation of *p*-xylene and naphthalene and oxygen transfer in an airlift immobilized bioreactor. The reactor was operated under continuous mode. The biodegradation rates were 81 mg/L and 40 mg/L of *p*-Xylene and naphthalene, respectively.

Similar studies were carried out on ILALR by other researchers; however, their studies had the following limitations:

- They adopted pollutants with lower concentration as a single substrate, instead of mixed substrate with higher concentration.
- They employed pure strain of microbes for treating phenolics instead of a mixed culture, which may yield complete treatment of phenolics even at high concentrations in shorter duration of time.
- They used immobilized culture instead of adopting free cell culture, which facilitates simplicity of reactor operation and enhance better mass transfer between the gas and liquid phase. In addition, free cell culture system has feasibility for adapting it for real wastewater treatment.
- They did not evaluate the reactor stability towards shock loading of pollutants, which helps to study the stability of reactor towards higher pollutant concentrations.

- They did not operate the reactor continuously, similar to that of a real wastewater treatment plant.

The above limitations are properly addressed in the present study and are reported accordingly.

1.5. Objective and Scope

Based on the detailed literature review, the overall objective of the present study was to evaluate the degradation (both bio and solar photocatalytic oxidation) of phenolic compounds, viz., phenol and *m*-cresol. The biodegradation study was carried out using an indigenous mixed microbial culture and the photocatalytic oxidation was carried out with Degussa P-25[®] and ANJATOX[®].

This research contributes to the study and development of a new degradation system that employs an indigenous mixed microbial consortium in an internal loop airlift bioreactor for the treatment of recalcitrant organic substances present in aqueous milieu. To achieve the said objective, following investigations were performed.

- Isolation, acclimatization and characterization of indigenous mixed microbial culture potent to degrade phenolic compounds - phenol and *m*-cresol.
- Batch shake flask studies on the culture growth and biodegradation of individual phenolic compounds in single substrate system.
- Evaluation of biomass yield and simultaneous degradation of a mixture of phenol and *m*-cresol by the mixed culture in batch shake flasks containing mixed substrate system
- Estimation of biokinetic parameters involved in the culture growth and phenolics biodegradation in batch shake flasks.

- Feasibility study of the mixed culture to treat a real industrial wastewater.
- Assessment of a simple batch stirred tank reactor (BSTR) as compared to that of a photo catalytic reactor for degrading phenol.
- Design and evaluation of an internal loop air lift reactor (ILALR) with the mixed culture in treating phenol and *m*-cresol, both individually and in mixtures, under batch, fed-batch and continuous modes of operation.
- Stability study of the ILALR under shock-loading conditions of the phenolics.

1.6. Organization of the Thesis

The presentation of the work has been divided in four chapters. The literature that supports the present work is presented in Chapter 2. Details of the materials and methods adopted in the present study are described in Chapter 3. This chapter provides technical information about the quantification of phenol, *m*-cresol and intermediates. It also elaborates the details of the photocatalytic reactor, batch stirred tank reactors and internal loop airlift bioreactor. Chapter 4 contains the results and discussions. This chapter starts with a discussion on the identification and characterization of the mixed microbial consortium. The results of phenol and *m*-cresol degradation in batch shake flasks, batch stirred tank reactor and finally in the internal loop airlift reactor are all presented and discussed in this chapter. This chapter addresses the efficiency of the biological process in treating phenolics, both in single and mixed substrate systems. It also elaborates the performance of photocatalytic reactor and batch stirred tank reactor in degrading phenol. Finally, the chapter emphasizes the performance of airlift bioreactor in treating the phenolics in single and mixed substrate systems under batch, fed batch and continuous modes of operation. Chapter 5 draws summary and appropriate conclusion based on the previous results

and discussion. This chapter also provides some useful recommendations for future research in the relevant area.



Table 1.1: Band positions of some common semiconductor photocatalysts in aqueous solution at pH1.

Semiconductor	Valence band (V vs NHE)	Conductance band (V vs NHE)	Band gap energy (eV)	Band gap wavelength (nm)
TiO ₂	+3.1	-0.1	3.2	387
SnO ₂	+4.1	+0.3	3.9	318
ZnO	+3.0	-0.2	3.2	387
ZnS	+1.4	-2.3	3.7	335
WO ₃	+3.0	+0.2	2.8	443
CdS	+2.1	-0.4	2.5	496
CdSe	+1.6	-0.1	1.7	729
GaAs	+1.0	-0.4	1.4	886
GaP	+1.3	-1.0	2.3	539

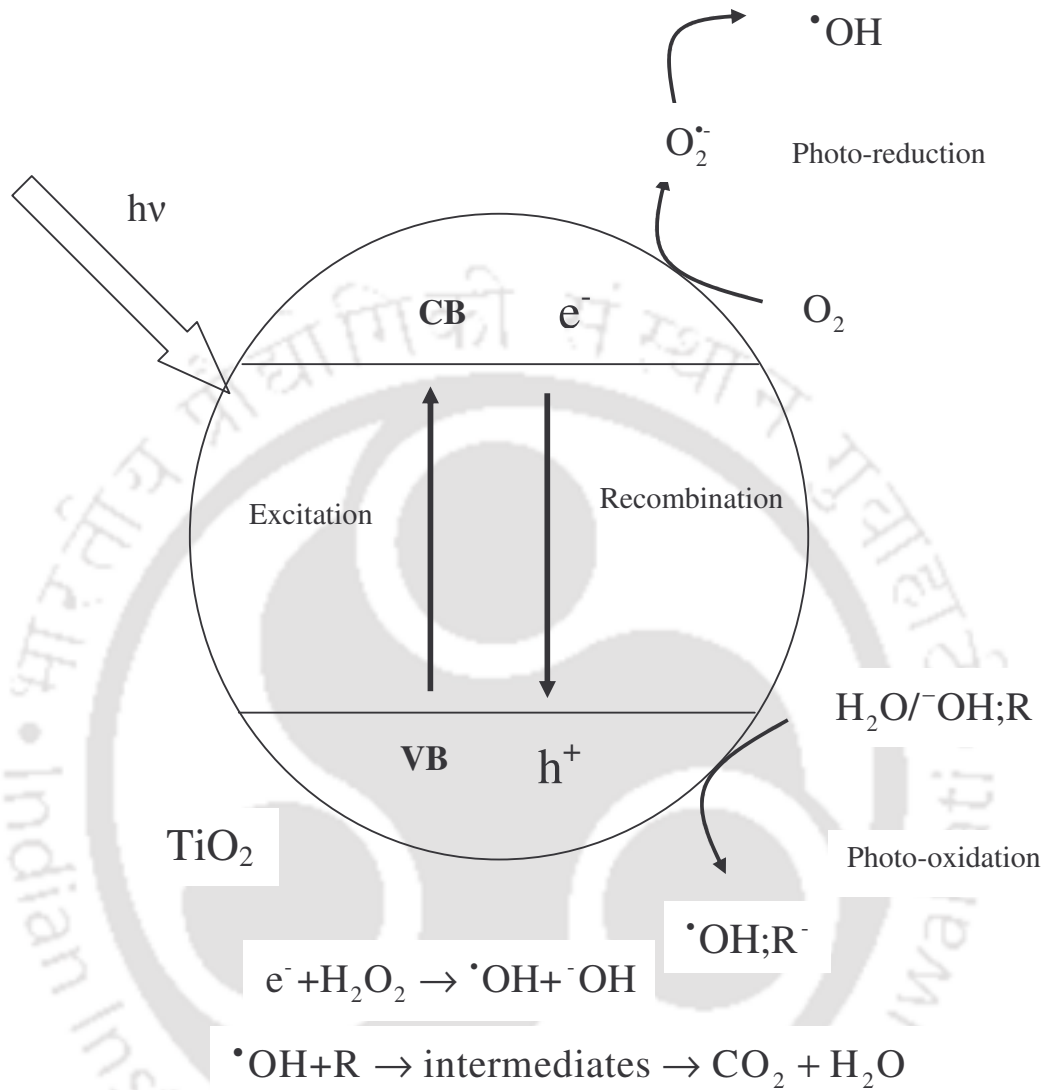


Fig. 1.1: TiO₂-semiconductor photocatalytic process (Bahnemann et al., 1991)

CHAPTER 2

LITERATURE REVIEW

2.1. Sources and Major Components of Phenolic Wastewater

Phenol and *m*-cresol are characteristic pollutants in wastewater from crude oil refineries, ceramic plants, steel plants, coal conversion processes, manufacturing units of phenolic resins, pesticides and explosives, *etc.* These chemicals are toxic and hazardous even at low concentrations. The generation of such phenolics and their major adverse effects are reported by many researchers (Hill and Robinson, 1975; Li and Humphrey, 1989; Kumaran and Paruchuri, 1996; Kar *et al.*, 1997; Monteiro *et al.*, 2000; Kim *et al.*, 2002; Murialdo *et al.*, 2003; Kumar *et al.*, 2005; Rodriguez *et al.*, 2006; Bai *et al.*, 2007; Feng *et al.*, 2007). The harmful characteristics of phenolic compounds lie in concentrations level they present (García *et al.*, 2000), which are very inferior to toxic concentrations, and contribute a disagreeable smell and taste to chlorinated water. Normally, the taste cannot be detected in concentrations if they are present in the range of 0.1 to 0.01 mg/L. Phenols are considered toxic to most of the aquatic life forms and the ingestion of 1 g of phenol can have fatal consequences in humans. Even though they are high toxic in nature, phenolics have a wide range of uses:

- *Plastics, resins and plasticizers*: Phenol in this type of industry is used above all in the production of plastics and phenol-formaldehyde resins. In addition, cresols are used in the making of tricresyl phosphate, which is a plasticizer useful for cellulose acetate, nitrocellulose, ethane thiol cellulose and vinyl plastics.
- *Preserving agent for wood, disinfectants and insecticides*: Creosote oil, a distillation obtained from the process of coal-making at high temperatures, is used for preserving wood in addition to being a source of cresylic acid and cresols used as disinfectants and insecticides.
- *Vegetable hormones and detergents*: Phenol is used directly in the production of these types of compounds.
- *Medicines*: A clear example of a derivative of phenol is acetylsalicylic acid - a compound from which aspirin is obtained.
- *Dyes, photography and explosives*: These industries have many uses for phenol although the total consumption is not very high. Some aminophenols are used as dyes and photographic developers. Trinitrophenol, for example, is used as a dye and as an explosive.

All these above said industries discharge phenolics in their wastewaters. Hence, it is advocated for efficient treatment methods to reduce phenol concentration in wastewater to acceptable levels. Following is a short account on the state-of-the-art wastewater treatment methods.

2.2. Major Treatment Techniques for Phenolic Wastewater

2.2.1. Adsorption

Carbon adsorption is an advanced wastewater treatment method used for the removal of recalcitrant organic compounds as well as residual inorganic compounds such as nitrates, sulfides and heavy metals. This is a separation method in which the contaminants, dissolved in water phase, are transferred to the surface of active carbon, the most commonly used adsorbent, where it is accumulated for subsequent extraction or destruction of the contaminants. The application of adsorption process includes but is not limited to control of color and odors, removal of organic compounds or trihalomethanes precursors, removal of chlorine *etc.* Numerous literatures have been reported regarding the treatment of phenolics on activated carbon (Calleja *et al.*, 1993; Dargaville *et al.*, 1996; Viraraghavan and Alfaro, 1998; Przepiórski, 2006; Vázquez *et al.*, 2007). Phenol was found to be a well adsorbable compound onto activated carbon, but only in low concentrations (Cañizares *et al.*, 1999; Sacher *et al.*, 2001).

2.2.2. Air Stripping

Air stripping involves the transfer of volatile organics from liquid phase to the air phase by greatly increasing the air/water contact area. Typical aeration methods include packed towers, diffusers, trays and spray aeration. It is a well established and more widely understood technology than chemical oxidation (Metcalf and Eddy, 2003). If air emissions are not required to be regulated, air stripping is by far the simplest and cheapest solution for the removal of volatile compounds from water. Air stripping has been used in the treatment of trichloroethylene (TCE), dichloromethane (DCM), 1,2-dichloroethylene (DCE), 1,2-dichloroethane (DCA), chlorobenzene (Cl-Bz), and dichloroethyl ether (DCEE). The results showed that they could be removed

easily from water solutions except DCEE (Li *et al.*, 2000) However, treatment of phenolic effluents by means of air stripping has not been reported due to its low volatile nature.

2.2.3. Electrochemical Oxidation

The use of electrochemical oxidation for the destruction of organic compounds in water solutions has been tried on bench and pilot plant scale operation (Boudenne *et al.*, 1996; Brillas *et al.*, 1998), but is not used commercially because of its high operating cost. One of the main advantages of the electrochemical processes is that electrons are generated or assimilated by the electrodes. Thus it supplies a clean reactant and does not increase the number of chemical molecules involved in the process. The electrochemical oxidation of organic compounds is thermodynamically favored against the competitive reaction of oxygen production by oxidation of water. However, the kinetics of oxidation of water is much faster than the kinetics of oxidation of the organic compounds, among other reasons because of its higher concentration. The mechanism of the electrochemical processes involves three stages: electrocoagulation, electrofloatation and electrooxidation, and these are depicted by Eqns. (2.1) – (2.3) (Boudenne *et al.*, 1996; Brillas *et al.*, 1998):



Nevertheless, it suffers from some disadvantages, such as:

- As stated before, the electrochemical treatment is expensive in comparison with other processes and the mechanism in water is rather complex.
- The effluent needs to be a conductor. Therefore, a salt should be added in the effluent in case it does not have good conductivity.

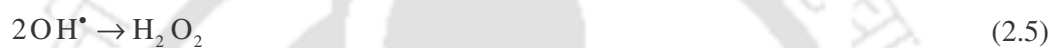
2.2.4. Advanced Oxidation Processes

The phrase *advanced oxidation processes* (AOP) refer specifically to processes in which oxidation of organic contaminants occurs primarily through reactions with hydroxyl radicals (Glaze *et al.*, 1995). It involves two stages of oxidation: (1) the formation of strong oxidants (*e.g.*, hydroxyl radicals) and (2) the reaction of these oxidants with organic contaminants in water (Alnaizy and Akgerman, 2000). In water treatment applications, AOPs usually refer to a specific subset of processes that involve O_3 , H_2O_2 , and/or UV light. However, often AOPs are also referred to a more general group of processes that also involve semiconductor catalysis, cavitation, E-beam irradiation, and Fenton's reaction (Legrini *et al.*, 1993; Fox and Dulay, 1993). All these processes can produce hydroxyl radicals, which can react with and destroy a wide range of organic contaminants, including phenolics. Although many of the processes noted above have different mechanisms for destroying organic contaminants, in general, the effectiveness of an AOP is proportional to its ability to generate hydroxyl radicals (Legrini *et al.*, 1993; Fox and Dulay, 1993).

2.2.4.1. Ozonation / UV

The O_3 system is one of the AOP for the destruction of organic compounds in wastewater. Basically, aqueous systems saturated with ozone are irradiated with UV

light of 253.7 nm. The extinction coefficient of O₃ at 253.7 nm is 3300 Lmol/cm, much higher than that of H₂O₂ (18.6 L.mol/cm). The decay rate of ozone is about a factor of 1000 higher than that of H₂O₂ (Guittonneau *et al.*, 1991). The AOP with UV radiation and ozone is initiated by the photolysis of ozone. The photodecomposition of ozone leads to two hydroxyl radicals, which do not act as they recombine producing hydrogen peroxide, as shown in the following Eqns. (2.4) and (2.5) (Peyton and Glaze, 1988):



2.2.4.2. Ultrasonication

Implosion of cavity bubbles in sonicated water containing dissolved gases results in formation of hydrogen and hydroxyl radicals by fragmentation of water molecules. These radicals in turn combine and generate other oxidative species such as peroxy and super oxide radicals ($\bullet\text{OH}$) as well as hydrogen peroxide; the quantities of each depend on the ambient conditions and the operating parameters. Such $\bullet\text{OH}$ radicals are used for the degradation of the organic compounds (Kidak and Ince, 2006).

2.2.4.3. Solar Photocatalytic Oxidation

In the past years, there have been a number of studies and reviews about this process (Legrini *et al.*, 1993; Fox and Dulay., 1993; Hoffmann *et al.*, 1995; Bahnemann., 2004; Herrmann *et al.*, 2007). Photocatalytic oxidation is based on the use of UV light and a semiconductor. Many catalysts have been tested, although titanium dioxide (TiO₂) in the anatase form seems to possess the most interesting features, such as high

stability, good performance and low cost (Fox and Dulay, 1993; Legrini *et al.*, 1993; Hoffmann *et al.*, 1995; Bahnemann., 2004).

Matthews (1990) reported that more than 90% of nitro benzene (NB) mineralization was achieved with TiO₂ and sunlight. Minero *et al.* (1994) studied the photocatalytic degradation of NB on TiO₂ and ZnO and reported complete mineralization with TiO₂. Titanium dioxide has become the most studied and used photocatalyst, because it is easily available, chemically robust and durable. It can be used to degrade, *via* photocatalysis, a wide range of organic compounds (Leyva *et al.*, 1998; Robert and Malato, 2002; Hincapié *et al.*, 2005; Herrmann *et al.*, 2007). Photocatalytic degradation of phenolic compounds by employing Degussa P-25[®] in presence of sunlight has been successfully studied by many researchers (Minero *et al.*, 1994; Curcó *et al.*, 1996). Vione *et al.* (2005) studied the degradation of phenol and benzoic acid in presence of sunlight with a commercial TiO₂ photocatalyst Wackherr's "Oxyde de titane standard". In his study he observed that the Wackherr's TiO₂ showed a better photocatalytic activity over Degussa P-25[®] in degrading phenol and benzoic acid.

2.3. Pros and Cons of the above Wastewater Treatment Techniques

In adsorption, the pollutant in the wastewater is selectively transferred into the solid phase (adsorbent) instead of eliminating it from the wastewater. It once again produces a large amount of solid waste, which further requires a safe disposal. Electrochemical oxidation is an uneconomical process with lack of feasibility towards commercialization. The advanced oxidation processes has many drawbacks as listed below:

- No full scale application exists
- Supplement oxidant such as O_3 and H_2O_2 are required to achieve a maximum removal efficiency, which results in increased cost.
- Pretreatment is required to avoid fouling of semiconductor catalysts
- If semiconductor catalyst is used as slurry then separation is required
- Rigorous studies are needed to determine the optimum dosage
- Complete degradation of organics is not achieved
- Large amount of toxic intermediates are produced

2.4. Biological Treatment Processes Involving Microbes

Biological treatment is more attractive method than that of conventional one because of its high potential to degrade phenolics completely that produces innocuous end products and generates minimum secondary waste (Goudar *et al.*, 2000). Biological treatment, generally by means of activated sludge (Wiesmann and Putnaerglis, 1986; Givens *et al.*, 1991) in adequate conditions (Wu *et al.*, 1994) has unquestionable advantages for the destruction of organic compounds. However, many organic pollutants cannot effectively be eliminated by activated sludge process for effluents with phenols, nitro-aromatic, ether, aliphatic compounds and textile waters. The restrictions are due to the high toxicity inherent in these wastes. There are two kinds of microbial processes in the biological treatment of organic compounds: aerobic and anaerobic (Eckenfelder *et al.*, 1989; Wang, 1992). The aerobic processes are more popular because of their efficiency and operational simplicity (Ruiz-Ordez *et al.*, 2001). In case of phenol solutions of slightly high concentrations (50 to 100 mg/L), aerobic treatment process has been used successfully (Urano and Kato, 1986; Kameya *et al.*, 1995). Implementation of a novel bioreactor to remove such high toxic

phenolics has been studied recently by some researchers (Quan *et al.*, 2004; Ryan, *et al.*, 2005; Vinod and Reddy, 2005; Jajuee *et al.*, 2007). The biodegradation process can be categorized based on the type of microorganism involved in the process, *viz.*, yeast, bacteria, etc. A short account of the culture-specific survey has been included in the following subsections.

2.4.1. Biodegradation by Yeast and Fungi

Biodegradation of phenolics by using yeast such as *Candida spp.* (Hofmann and Krüger, 1985; Krug and Straube, 1986; Neujahr *et al.*, 1974), *Fusarium sp.* (Anselmo *et al.*, 1985) and *Trichosporon cutaneum* (Gaal and Neujahr, 1979; Neujahr and Gaal, 1973; Spänning and Neujahr, 1987) has been studied by various researchers. Ruiz-ordez *et al.* (2001) studied phenol biodegradation using *Candida tropicalis* in a multistage bubble column. A semi continuous system was implemented to treat effluents with relatively high concentrations (>9,000 mg/L) of phenol, by replacing about 22% of the bioreactor operational volume periodically. They observed that phenol removal efficiency of their system was higher than 98.7%. Yan *et al.* (2006) evaluated the biodegradation of phenol and *m*-cresol using a pure culture of *Candida tropicalis*. Their results showed that *C. tropicalis* could degrade 2000 mg/L phenol alone and 280 mg/L *m*-cresol alone in single substrate system within 66 and 52 h, respectively. The capacity of the strain to degrade phenol was obviously higher than that to degrade *m*-cresol. The capacity of *C. tropicalis* for *m*-cresol biodegradation was increased up to 320 mg/L with the presence of 60–100 mg/L phenol. In addition, the intrinsic kinetics of cell growth and substrate degradation was investigated with phenol and *m*-cresol as single and mixed substrates in batch cultures.

Santos and Valter (2004) studied the biodegradation of phenol by a filamentous fungi isolated from industrial effluents. They isolated about thirty filamentous fungal strains from effluents of a stainless steel industry (Minas Gerais, Brazil) and tested for phenol tolerance. They also tested fifteen strains of the genera *Fusarium* sp., *Aspergillus* sp., *Penicillium* sp. and *Graphium* sp., which are capable of degrading phenol up to 10 mM. However they observed that *Fusarium* sp. presented the highest percentage phenol degradation, with 75% degradation of 10 mM phenol in 168 h for *Fusarium* sp. A higher starting cell density of *Graphium* sp. FIB4 lead to a less degradation time and increased degradation rate.

2.4.2. Biodegradation of Phenolics by Bacteria

Hopper and Taylor (1975) studied the pathways for the degradation of *m*-cresol and *p*-cresol by *Pseudomonas putida* and observed that catechol, 3-methylcatechol, and 4 methylcatechol were formed in the path way of the *m*-cresol biodegradation. They also proposed the pathway for metabolism of 3,5xylenol, *m*-cresol and *p*-cresol by *Pseudomonas putida*. The proposed pathway is illustrated in Fig.2.1.

Several studies have shown that phenolics can be aerobically degraded by a wide variety of microorganisms, including pure bacterial cultures such as *Acinetobacter calcoaceticus* (Paller *et al.*, 1995), *Alcaligenes eutrophus* (Hughes *et al.*, 1984; Léonard and Lindley, 1998), *Bacillus stearothermophilus* (Buswell, 1975), *Pseudomonas putida* (Hill and Robinson, 1975; Yang and Humphrey, 1975; Gotz and Reuss, 1997; Banerjee *et al.*, 2001; Kumar *et al.*, 2005), *Pseudomona sresinovorans* (Dikshitulu *et al.*, 1993), *Ralstonia eutropha* (Léonard *et al.*, 1999).

The degradation of phenolics by a pure microbial strain has been extensively studied for more than two decades by many researchers (Hill and Robinson, 1975; Yang and Humphrey, 1975; Götz and Reuss, 1997; Banerjee *et al.*, 2001; Kumar *et al.*, 2005). Few important findings reported in the literature are discussed in this section. Kumaran and Paruchuri (1996) studied the kinetics of biotransformation of phenols using pure microbial cultures and mixture of microbial consortium. They estimated the bio-kinetic parameters by fitting the experimental data obtained from a wastewater treatment plant to Monod and Haldane models.

Kennes *et al.* (1997) studied the methanogenic degradation of *p*-cresol in batch and in continuous Up-flow Anaerobic Sludge Blanket (UASB) reactors. They studied growth of two methanogenic cultures in presence of *p*-cresol as sole carbon source or together with a mixture of Volatile Fatty Acids (VFA). Both the cultures produced methane from VFA in the presence of *p*-cresol, up to concentrations of about 200 mg/L without significant inhibition in their activities. After several transfers, one of the cultures could tolerate and remove higher *p*-cresol concentrations. The culture was obtained from an industrial effluent contaminated with phenolic compounds. Further in the process, *p*-cresol was completely degraded to methane and carbon dioxide. The addition of VFA as co carbon sources very slightly delayed *p*-cresol removal in batch assays but allowed, on the contrary, the use of higher *p*-cresol influent concentrations in continuous UASB reactors than in the absence of VFA.

Aerobic batch degradation of phenol using immobilized *Pseudomonas putida* was studied by Hannaford and Kuek (1999). In their study, they changed the alginate concentrations between 2 and 4%, which had little effect on the degradation rate of phenol. They observed that when the initial phenol concentration was increased,

degradation rate was not significantly affected until levels higher than 1200 mg/L. When the ratio of total bead volume to the volume of medium was increased, degradation rate increased too progressively, however the quantum of increase was small. Wang and Loh (1999) studied the kinetics of phenol biodegradation by *Pseudomonas putida* ATCC 49451 in batch operation for various initial phenol concentrations ranging from 25 to 800 mg/L. They mainly studied the phenol degradation profile, especially for cultures containing high initial phenol concentration and they also proposed a new model to describe the same.

Monterio et al. (2000) studied the phenol biodegradation by *Pseudomonas putida* 548 in a batch reactor. They varied the initial phenol concentration from 1 to 100 mg/L. They observed that the length of the lag phase occurring before the exponential growth phase increases linearly with initial phenol concentration. The maximum specific growth rate (μ_m) of *Pseudomonas putida* was higher than that observed in mixed cultures (0.436 h^{-1}). Goudar et al. (2000) studied phenol biodegradation in a batch experiment using an acclimatized inoculum with initial phenol concentrations ranging from 0.1–1.3 g/L. They observed that phenol inhibited biodegradation at high concentrations. The experimental results were fitted to the well-known Andrews model and the biokinetic parameters were estimated.

Banerjee et al. (2001) evaluated phenol degradation using both free and calcium alginate immobilized cells of *Pseudomonas putida* in batch shake flasks. The free cell growth was carried out with an initial phenol concentration of 2.6 – 10.6 mmol/L, while the growth of immobilized cells were carried out with an initial phenol concentration of 2.4 – 20 g/L. They also observed that the cell growth was inhibited at high phenol concentration (above 5.31 mmol/L). Haldane model was employed to

evaluate the biokinetic parameters the value of μ_{\max} was found to be 0.06 h^{-1} , which is very low for a shake flask study.

Kumar et al. (2005) carried out biodegradation experiments with phenol and catechol using *Pseudomonas putida* MTCC 1194. The bacterial strain used for the degradation experiments were acclimatized with phenol and catechol upto a concentration of 1000 mg/L and 500 mg/L respectively. They observed that the initial phenol concentration of 1000 mg/L and the initial catechol concentration of 500 mg/L were fully degraded in 162 h and 94 h, respectively. Both phenol and catechol exhibited inhibitory behavior and the culture growth kinetics were correlated with Haldane's inhibitory growth kinetic model. They also observed that the bacterial culture died when the initial concentration of phenol and catechol were above 1200 mg/L and 600 mg/L, respectively.

Karigar et al. (2006) studied the ability of *Arthrobacter citreus*, isolated from a hydrocarbon contaminated site, to consume phenol as the sole carbon source. The phenol degradation studies in their work showed that complete degradation of the compound occurred within 24 h. The organism metabolized phenol with a maximum initial concentration of 22 mM, whereas higher levels were inhibitory.

Rodriguez et al. (2006) studied the biodegradation of phenol by an acclimatized activated sludge. They found the Haldane model inadequate to describe the microbial growth, and hence adopted a new two-step modeling technique. In the first step, phenol was considered to be degraded by a fraction of the total biomass, having one or several metabolic intermediate products. They also assumed that the intermediates are degraded during the second step, by another portion of biomass. The proposed

model is capable of describing both phenol degradation and biomass growth profiles at various initial conditions with only one set of model parameters.

Mixtures of organic chemicals are highly prevalent in wastewaters from industrial sites. Occurrence of the environmental contaminants in mixtures is a crucial problem because the removal or degradation of one component can be inhibited by other compounds in the mixture. Moreover, different conditions may be required to treat different compounds within the same wastewater sample (Reardon *et al.*, 2000). Currently, quantitative information on the rates and patterns of microbial degradation of substrate mixtures is scarce.

Reardon *et al.* (2000) studied biodegradation kinetics of benzene, toluene and phenol, both in single and mixed substrate systems using *Pseudomonas putida* F1. They reported the kinetics of the growth of the culture and developed mathematical models to describe their results. In the tested concentration range, toluene and benzene biodegradation kinetics were well described by the Monod model. Although a small degree of substrate inhibition was noted, the Monod model was able to characterize phenol biodegradation. Of the models tested, Sum Kinetics with Interaction Parameters (SKIP) model provided the best description of the paired substrate results. This model, with parameters determined from one and two substrate systems, provided an excellent prediction of the biodegradation kinetics for the three substrate system.

Gallego *et al.* (2003) studied degradation and detoxification of a mixture of persistent compounds (2-chlorophenol, phenol and *m*-cresol) by using pure and mixed indigenous cultures in aerobic reactors. Biodegradation assays were performed in batch and continuous flow reactors. In their study, individual compounds were

degraded by pure bacterial cultures within 27 h. The mixture of 2-chlorophenol (100 mg/L), phenol (50 mg/L) and *m*-cresol (50 mg/L) was degraded by mixed bacterial culture under batch conditions within 36 h.

Murialdo et al. (2003) studied the degradation of phenol and chlorophenols using a mixed microbial culture, and found the culture capable of degrading phenol, pentachlorophenol, 2,3,5,6 tetrachlorophenol and 2,4,6 trichlorophenol, but not 2,4,5 trichlorophenol. Their results suggest the feasibility of the use of toxic chemicals such as phenols, hexadecane and other chlorophenols as co-substrates in field decontamination processes. The inhibitory effect of pentachlorophenol (PCP) and the influence of a readily degradable ancillary carbon source on the performance of a pure culture on phenol degradation were reported by the authors. The preliminary characterization and identification of the bacterial species in the mixed culture responsible for higher PCP degradation was also carried out.

Bai et al. (2006) studied biodegradation of phenol and *m*-cresol as mixed substrates using *Alcaligenes faecalis*. They observed strong interaction effect between the two during the culture growth on the degradation of the substrates. Both *m*-cresol and phenol inhibited the degradations of each other. The overall culture growth rate was, however, due to the co-action between phenol and *m*-cresol. In addition, the cell growth and substrate degradation kinetics of phenol and *m*-cresol, both as single and mixed substrates, were investigated over a wide range of their initial concentrations (phenol: 10 – 1400 mg/L and *m*-cresol: 5 – 200 mg/L). The single-substrate kinetics was described well using the Haldane-type kinetic models.

Tsai and Juang (2006) studied the mixture effects on the biodegradation of phenol and sodium salicylate (SA) by *Pseudomonas putida* CCRC 14365. The growth kinetics

results showed that phenol was a better substrate for *P. putida* than SA. They observed that the addition of SA to phenol, and *vice versa*, did not notably alter the maximum cell density. Their results proved that cells adapted with comparatively hard-to-degrade substrate (SA, in this case) enhanced the overall biodegradation efficiency of mixed homologous carbon and energy substrates. More recently, Adav et al. (2007) studied the degradation of phenol by an *Acinetobacter* strain. Degradation tests for the *Acinetobacter* strain at various phenol concentrations suggested that the strain completely degraded phenol with no time lag at an initial phenol concentration 500 mg/L. The phenol-fed aerobic granules were synthesized by merging several smaller granules, each with a core of proteins and nucleic acids, surrounded by an outer layer enriched with polysaccharides. Batch tests revealed that the suspended *Acinetobacter* strain could effectively degrade phenol at an initial phenol concentration of up to 1000 mg/L and the growth ceased at a phenol concentration of 1500 mg/L. They described the inhibitory kinetics with Haldane substrate inhibition model.

Biodegradation of phenolics has also studied by employing mixed culture; nevertheless, the studies are very limited. Pawlowsky and Howell (1973) first reported the degradation of phenol by mixed bacterial cultures. Further study with such mixed culture is limited. Fang and Zhou, (2000) studied the effects of Hydraulic Retention Time (HRT) and phenol concentration on the degradation of phenol and *p*-cresol in wastewater. They carried out investigations in two UASB reactors with effluent recirculation at 37°C for over 440 days. After acclimatization, nearly all the phenol and *p*-cresol at moderate concentrations were degraded. While treating wastewater containing 800 mg/L of phenol and 300 mg/L of *p*-cresol at HRT ranging 2-12 h, the first reactor consistently removed 95% of phenol, 65% of *p*-cresol and

85% of COD at 8-12 h of HRT. The efficiency, however, decreased at lower HRT. On the other hand, the second reactor was able to remove 75-80% of COD at 24 h of HRT when the phenol concentration was between 1200 and 1500 mg/L and *p*-cresol concentration was 400 mg/L. The removal efficiency decreased as phenol concentration was further increased. They also observed that high levels of residual phenol and *p*-cresol in the effluent suppressed the activity of biogranules; however, the suppression of bioactivity was only transient and the biomass was able to regain its full activity after lowering the phenolic concentrations in the wastewater.

Nuhoglu and Yalcin (2005) investigated phenol biodegradation using a mixed culture isolated from a wastewater treatment plant. They found that the culture could degrade the phenol up to a maximum concentration of 1450 mg/L. However, there were gross mismatch between the measured and estimated values of final results for the case of initial phenol concentration greater than 100 mg/L. They adopted and applied a new model, originally developed for representing phenol degradation in pure culture in their study to estimate the same.

Vinod and Reddy (2005) carried out experiments to study the biodegradation of phenolic wastewater using microorganisms in a fluidized-bed bioreactor (FBR). They performed the experiments at various conditions of wastewater flow rate, dissolved oxygen (DO) concentration and inlet phenol concentration. The wastewater with feed phenol concentration as high as 1254 mg/L was found successfully biodegraded to 50 mg/L in the fluidized-bed bioreactor, whereas feed with concentration up to 1034 mg/L could be completely biodegraded to zero mg/L. They also evaluated the biokinetic parameters for the growth of the cells in batch experiments. Maeda et al. (2005) studied the degradation of *o*-cresol by using waste activated sludge in a gas-

liquid–solid three phase slurry bioreactor. The biodegradation kinetics of *o*-cresol was examined in batch experiments at various initial *o*-cresol concentrations (from 30 to 600 mg/L), waste activated sludge concentrations (from 1000 to 11500 mg/L) and aeration rates (from 0.05 to 1.0 L/min). The kinetic parameters of aerobic biodegradation were estimated using Haldane substrate inhibition equation.

2.5. Design of Experiments

Design of experiments is a statistical design technique, which involves changing the levels of influential variables simultaneously, as compared to varying only one variable and its level at a time in conventional experimentation. The statistical interpretation of the results are in the form of analysis of variance (ANOVA), student's *t*-test, P-value, *F*-value etc. which give better understanding of the factor effects and their interaction on a given response. Statistical designs of experiments are necessary for systematic investigations requiring only a low number of experiments, and to interpret results in a meaningful manner (Montgomery, 2004). The factorial experimental design methodology involves changing all variables from one experiment to the next. The reason for this is that variables can influence each other, and the ideal value for one of them can depend on the values of the others. This interaction between variables is a frequent phenomenon.

2.5.1. Factorial Design of Experiments

The 2^k design is particularly useful in the early stages of experimental work, when there are many factors likely to be investigated. It provides the smallest number of runs with which '*k*' factors can be studied in a complete design. Because there are only two levels for each factor, it is assumed that the response is approximately linear

over the range of the factors level chosen. The statistical model for a 2^k design would include k main effects, $\binom{k}{2}$ two factor interactions, $\binom{k}{3}$ three factor interaction and so on and one k -factor interaction. That means, for 2^k design, the complete model would contain $2^k - 1$ effects. The levels of the factors may arbitrarily be called “low” and “high” and denoted by “-” and “+” respectively. For example, in 2^2 design, two factors *viz.* A and B at two levels are chosen. The experimental design consists of treatment combinations denoted by (1) “a”, “b”, “c”, “ab”. A suitable number of runs carried out to replicate the levels of variables at their center point (0) provides an estimate of the residual error associated with the experiments and also the curvature of the response. Three degrees of freedom is associated with the four treatment combination in 2^2 design, which in turn consists of two degrees of freedom associated with main effects of A and B, one degree of freedom associated with interaction effect between A and B (Montgomery, 2004).

2.5.2. Analysis of Variance

Analysis of variance (ANOVA) is a collection of statistical models, and their associated procedures, in which the observed variance is partitioned into components due to different explanatory variables. In general terms, ANOVA explains any variation in the statistically derived model and significance of the model parameters. The model parameters, usually indicated in ANOVA, are the main effects, interaction effects and error terms, and their significance in the model is represented by Fischer ‘ F ’ and associated P values. The other items in ANOVA table are degrees of freedom (df), sum of squares (SS) and mean squares (MS). The MS value of a model term in an ANOVA table is obtained by dividing SS over df and its F value is obtained by dividing MS due to the model term by MS due to error. Normally, larger F and lower

P values of a model term in ANOVA indicate good significance of the term over others.

The fundamental technique is a partitioning of the total sum of squares into components related to the effects used in the model. For example, we show the model for a simplified ANOVA with one type of treatment at different levels.

$$SS_{\text{Total}} = SS_{\text{error}} + SS_{\text{Treatment}} \quad (2.6)$$

The number of degrees of freedom (df) can be partitioned in a similar way and it specifies the chi-square distribution, which describes the associated sums of squares.

$$df_{\text{Total}} = df_{\text{error}} + df_{\text{Treatment}} \quad (2.7)$$

2.5.3. Student 't' Test

A t -test is any statistical hypothesis test in which the test statistic has a Student's t distribution if the null hypothesis is true. It is applied when sample sizes are small enough that using an assumption of normality and the associated z -test leads to incorrect inference. The Student t -distribution in probability and statistics is a probability distribution that arises in the problem of estimating the mean of a normally distributed population when the sample size is small. It is the basis of the popular Student t -tests for the statistical significance of difference between two sample means and for confidence intervals for difference between two population means. The Student t -distribution is a special case of the generalized hyperbolic distribution.

A test of the null hypothesis is that the means of two normally distributed populations are equal. Given two data sets, each characterized by its mean, standard deviation and

number of data points, one can use some kind of 't' test to determine whether the means are distinct, provided that the underlying distributions can be assumed to be normal. All such tests are usually called Student *t* tests, though strictly speaking that name should only be used if the variances of the two populations are also assumed to be equal. There are different versions of the *t* test depending on whether the two samples are;

1. Independent of each other (*e.g.*, individuals randomly assigned into two groups)
2. Paired, so that each member of one sample has a unique relationship with a particular member of the other sample (*e.g.*, the same people measured before and after an intervention).

If the calculated P-value is below the threshold chosen for statistical significance (usually, the 0.05 level), then the null hypothesis, which usually states that the two groups do not differ, is rejected in favor of an alternative hypothesis, which typically states that the groups do differ.

1. A test of whether the mean of a normally distributed population has a value specified in a null hypothesis.
2. A test of whether the slope of a regression line differs significantly from 0.

Once a *t* value is determined, its corresponding P value can also be found using a table of values from Student's *t*-distribution.

Factorial design of experiments has been highly adopted in biosorption studies and medium optimizations (Sen and Swaminathan, (2004); Carmona *et al.*, (2005).

Peternele *et al.* (1999) studied the uptake of cadmium and lead, using a 2³ factorial

design. Three operational factors were analyzed: temperature, ionic strength and pH. Similarly, Barros et al. (2003) studied the effects of pH, heavy metal and biomass concentration on biosorption of cadmium from oil field waters using *Aspergillus niger*. The biosorption process was modeled based on 2^3 factorial design. The authors had chosen biomass concentration, as the most important factor in their study. For degradation studies, Kargi and Eker (2005) studied the continuous mode for removal of 2,4-dichlorophenol (DCP) and toxicity from synthetic wastewater employing a Rotating Perforated Tubes Biofilm Reactor (RTBR). A Box–Wilson statistical experiment design method was used to investigate the effects of major operating parameters such as, type of feed chemical oxygen demand (COD) and feed 2,4-dichlorophenol concentrations on COD, DCP removals.

Niccolai et al. (2003) in their study on medium optimization for the production of constitutive recombinant *Helicobacter pylori* Neutrophil Activating Protein (NAP) in *Escherichia coli* adopted Central Composite Design (CCD) composed from the superimposition of two-level factorial design. Sen and Swaminathan (2004) evaluated the statistical factorial design based response surface modeling and optimization to elucidate and analyze the effects of inoculum age and size on surfactin production. Carmona et al. (2005) studied biosorption of chromium using factorial experimental design. The removal of Cr^{3+} and Cr^{6+} was studied, separately, using the factorial design 2^3 . The three factors considered were pH, temperature, and metal concentration at two markedly different levels. The results were analyzed statistically using the Student's *t*-test, analysis of variance and F-test to define the most important process variables affecting the metal removal efficiency. Recently, many researches have applied statistical experimental designs for medium optimization for the production of

various cultures (Imandi *et al.*, 2008; Reddy *et al.*, 2008; Wang *et al.*, 2008a; Wang *et al.*, 2008b).

In all the above studies, the authors have utilized a factorial design of experiments and observed that the statistical approach yielded a better and meaningful interpretation of the results. The factorial design approach for phenolics biodegradation studies is, however, scant.

2.6. Microbial Growth Kinetics and Substrate Inhibition Models for Single Substrate Biodegradation Systems

For any bacteria to grow appreciably, the amount of substrate must be sufficiently high relative to the number of cells to permit several or many doublings in the initial population. If the bacterial cell density is high relative to the substrate concentration, little or no increase in the cells is possible. Therefore it is apparent that the extent of bacterial growth depends on the initial substrate concentration. In order to describe the kinetics of substrate degradation by microbes, several kinetic models such as growth-associated models (logarithmic, logistic and Monod with growth), non-growth associated models (zero order, first order and Monod based) and three-half order models have been reported in the literature (Schmidt *et al.*, 1985; Brunner and Focht, 1986; Alexander 1999). The mathematical forms of these models are shown below.

Non-growth associated	{	Zero order	$S = S_0 - k_0 t$	$S_0 \gg K_S$	(2.8)
		First order	$S = S_0 \exp(-k_1 t)$	$S_0 \ll K_S$	(2.9)
		Monod with no growth	$K_S \ln \frac{S}{S_0} + S - S_0 = -k_2 t$ ($k_2 = \mu_{\max} X_0$)	$S_0 \sim K_S$	(2.10)

Growth associated	{	Logarithmic	$S = S_0 + X_0 [1 - \exp(\mu_{\max} t)]$	$S_0 \gg K_S$	(2.11)
		Logistic	$S = \frac{S_0 + X_0}{1 + \frac{X_0}{S_0} [\exp(K(S_0 + X_0)t)]}$ ($K = \frac{\mu_{\max}}{K_S}$)	$S_0 \ll K_S$	(2.12)
		Monod with growth	$K_S \ln \frac{S}{S_0} = (S_0 + X_0 + K_S) \ln \frac{X}{X_0} - (S_0 + X_0) \mu_{\max} t$	$S_0 \sim K_S$	(2.13)

Thee-half-order model	$\frac{1}{t} [\ln(S_0 - (S_0 - S + k_0 t) + k_0 t) / S_0] = -k_1 - \frac{k_2 t}{2}$	(2.14)
-----------------------	---	--------

where, μ is the specific growth rate (h^{-1}), μ_{\max} is the maximum specific growth rate (h^{-1}), K_S is the half-saturation constant (mg/L), X and X_0 are the biomass concentrations (mg/L) at times 0 and t (h) respectively; S_0 is the initial substrate concentration (mg/L), S is substrate concentration at time t (mg/L) and k_0, k_1 and k_2 are zero, first (h^{-1}) and second (h^{-2}) order rate constants, respectively. Very

recently, Mahanty et al. (2008) in their study on biodegradation of pyrene by *Mycobacterium frederiksbergense* observed that an three-half-order kinetic model provided the best fit to the entire degradation profiles with coefficient of determination (R^2) value >0.99 .

To establish the effect of substrate concentration on growth of microbial culture, specific growth rates of the culture at different substrate concentrations is calculated as per the following relationship:

$$\mu = \frac{1}{X} \frac{dX}{dt} \quad (2.15)$$

where, μ is the specific growth rate (h^{-1}), X is the biomass concentration (mg/L). The inhibition on the growth of culture can be modeled using suitable substrate inhibition models described in literature (Okpokwasili and Nweke, 2005; Kumar *et al.*, 2005; Nuhoglu and Yalcin, 2005). Usually, the microbial growth can be represented by a simple Monod equation (Monod, 1949):

$$\mu = \frac{\mu_{\max} S}{K_s + S} \quad (2.16)$$

where, S is the limiting substrate concentration (mg/L), μ_{\max} is the maximum specific growth rate (h^{-1}), K_s is the half saturation constant (mg/L). However, Eqn. (2.16) is not capable of explaining growth inhibition of microorganisms at higher substrate concentrations. In such a case, Haldane and Han-Levenspiel models are normally used to represent growth kinetics of a culture. The Haldane model (Kumar *et al.*, 2005) has the following form:

$$\mu = \frac{\mu_{\max} S}{K_s + S + \frac{S^2}{K_i}} \quad (2.17)$$

Where, K_i is the inhibition coefficient (mg/L). An extended Monod type model, originally proposed by Han-Levenspiel, is also efficient in explaining the growth of the microorganism at different concentrations of substrate (Han and Levenspiel, 1988; Okpokwasili and Nweke, 2005). In the said model, specific degradation rate is expressed by the following equation:

$$q = \frac{q_{\max} \left[1 - \frac{S}{S_m} \right]^n}{K_s + S - \left[1 - \frac{S}{S_m} \right]^m} \quad (2.18)$$

where, q is specific substrate degradation/utilization rate, q_{\max} is the maximum specific substrate degradation/utilization rate, S is substrate concentration, S_m is critical inhibitor concentration above which reaction stops, n and m are empirical constants. For fitting the obtained experimental specific growth rates to the model Eqn. (2.1) the terms q and q_{\max} are replaced with μ and μ_{\max} , respectively.

Yano and Koga proposed a model (1969), based on a theoretical study on the dynamic behavior of single vessel continuous bioreactor. In their study, growth inhibition occurred at high concentration of rate limiting substrate *e.g.*, the acetic acid fermentation from ethanol, the gluconic acid fermentation from glucose, the tannase fermentation with tannic acid as the sole carbon source, a bacterium production from pentane, etc. The model form is given in Eqn. 2.19 (Yano and Koga, 1969):

$$\mu = \frac{\mu_m}{(K_s / S) + 1 + \sum_{j=1}^n (S / K_j)^j} \quad (2.19)$$

where, K_j is a positive constant. Similarly, a kinetic model (Edward model) was proposed (Eqn. 2.20), which is the modified form of Haldane model (Mulchandani and Luong, 1989):

$$\mu_i = \mu_m \frac{S}{S + K_s + (S^2 / K_{si})(1 + S / K)} \quad (2.20)$$

where, K_{si} is the substrate inhibition constant (mg/L) and K is a positive constant. The model proposed by Luong (1987) as represented in Eqn. (2.21), appeared to be useful for representing the kinetics of substrate inhibition. Although the proposed model is of generalized Monod type, it accounts for substrate stimulation at both its low and high concentrations. The model has the capability to predict the values of S_m , the maximum substrate concentration, above which the growth is completely inhibited (Luong, 1987).

$$\mu = \frac{\mu_m S}{K_s + S} \left[1 - \frac{S}{S_m} \right]^n \quad (2.21)$$

Several authors, as stated earlier in this chapter, have successfully applied most of these models to adequately describe their single substrate degradation and microbial growth in their systems.

2.7. Treatment of Phenolics in Airlift Bioreactors

The implication of Airlift Bioreactor for treating the phenolics is becoming popular recently due its advantages like it does not need any mechanical agitation and a low energy is sufficient for required aeration in the process (Hannaford and Kuek, 1999; Quan *et al.*, 2004; Loh and Ranganathan, 2005; Maeda *et al.*, 2005; Ryan *et al.*, 2005;

Vinod, Reddy, 2005; Jajuee *et al.*, 2007). Moreover they are simple to operate, attains a high yield and they can be easily scaled up from a laboratory scale up procedure.

Loh and Ranganathan (2005) performed the biotransformation of 4-chlorophenol (4-CP) in presence of phenol in an External-loop Fluidized Bed Airlift Bioreactor (EFBAB). The authors reported the advantages of a 4 L external-loop inversed fluidized bed airlift bioreactor. They tested the bioreactor for batch co-metabolic biotransformation of 4-CP in presence of phenol at various concentration ratios of phenol and 4-CP (ranging from 600 mg/L phenol and 200 mg/L 4-CP to 1600 mg/L phenol and 200 mg/L 4-CP) at 9% expanded polystyrene beads loading and 2.8% (10 g) granulated activated carbon loading. They had successfully achieved 4-CP and phenol biotransformation in their bioreactor system, which ascertained its potential for field applications.

Loh and Liu (2001) tested a 4 L external loop inversed fluidized bed airlift bioreactor (EIFBAB) for treating high strength phenolic wastewater. They used expanded polystyrene beads of specific gravity 0.713 and diameter 1.0 - 1.18 mm as supporting material, for immobilizing *Pseudomonas putida* ATCC11172. The effect of the extent of valve opening, under cell-free condition, on gas holdup and liquid circulation velocity was also investigated for gas velocities ranging from 0.01 to 0.12 m/s.

Biodegradation of 2,4 - dichlorophenol (2, 4 -DCP) and phenol in an internal loop airlift bioreactor immobilized with *Achromobacter* sp. was performed by Quan et al. (2004). The bioreactor was packed with honeycomb-like ceramic as carrier to immobilize microorganism *Achromobacter* sp., capable of degrading 2,4 - DCP. They operated the reactor under continuous mode of operation. Effects of phenol on 2,4 - DCP removal were also investigated under fed-batch and continuous operations. Their

results showed that the pure strain could easily be immobilized on the carrier and proliferated using 2,4 -DCP as the sole carbon source. Moreover, in the process of fed-batch operation, removal rate of 2, 4 - DCP decreased with the increase in run number, while that of phenol was just the contrary. Their results also showed that with the increase of phenol loading rates, the removal efficiency of 2, 4 - DCP declined from 100 to 87.9%, while that of phenol remained at about 99.6%. Presence of phenol inhibited the biodegradation of 2, 4 - DCP and caused the major carbon source shift from 2, 4 -DCP to phenol.

Viggiani et al. (2006) evaluated biodegradation of phenol with *Pseudomonas stutzeri* OX1 in an airlift biofilm reactor of 150 mL capacity. Phenol bioconversion by *P. stutzeri* OX1 using either free or immobilized cells was investigated with an aim of searching for optimal operating conditions of a continuous bioconversion process. The following analysis were done: (a) free-cell growth and products of phenol bioconversion by batch cultures of *P. stutzeri*; (b) growth of *P. stutzeri* cells immobilized on carrier particles; (c) bioconversion of phenol-bearing liquid streams and the establishment and growth of an active bacterial biofilm during continuous operation of an internal-loop airlift bioreactor. Data indicate that bacterial growth was substrate-inhibited, where the limiting phenol concentration was about 600 mg/L. Continuous bioconversion of phenol-bearing liquid streams was successfully obtained in a biofilm reactor operated in the internal-circulation airlift mode. Phenol conversion exceeded 95%. Biofilm formation and growth during continuous operation of the airlift bioreactor were quantitatively and qualitatively assessed. They also observed that the culture took a long period of 7 days for completely degrading phenol with a maximum initial concentration of 450 mg/L.

Modeling of local dynamic behavior of phenol degradation in an internal loop airlift bioreactor by the yeast *Candida tropicalis* was studied by Feng et al. (2007). They developed a Computational Fluid Dynamic (CFD) model, combining hydrodynamics with biochemical reactions, to simulate the local transient flow patterns and the dynamic behaviors of cell growth and phenol biodegradation. To validate their proposed model effectively, the simulated local hydrodynamic characteristics of the gas-mineral salt medium solution (gas liquid) two-phase system was shown.

Jajuee et al. (2007) studied the biodegradation performance and the rate of oxygen transfer in a pilot-scale novel airlift immobilized bioreactor of 10 L working volume. They inoculated the reactor with an acclimatized population of contaminant degrading microorganisms. Immobilizing the microorganisms on a non-woven polyester textile, they developed the active biofilm, thereby obtained biodegradation rates of 81 mg/L/h and 40 mg/L/h for *p*-xylene and naphthalene, respectively. Monod kinetic model was found to be suitable for correlating their experimental data, obtained during the course of batch and continuous operations.

Sahinkaya and Dilek (2007) studied the biodegradation kinetics of 2,4-dichlorophenol (2,4-DCP) by (a) culture (Culture M) acclimatized to mixture of 4-chlorophenol (4-CP) and 2,4-DCP and (b) culture (Culture 4) acclimated to 4-CP only. The study was carried out in aerobic batch reactors. Also, pure strains isolated from mixed cultures were tested for their ability towards the biodegradation of 2,4-DCP. They observed a linear relationship between time required for complete degradation and initial 2,4-DCP concentrations for both mixed cultures. It was also observed that the Haldane equation can be used to predict specific degradation rate with determination

coefficient (R^2) greater than 0.99 as a function of initial 2,4-DCP concentrations; and, it also adequately described 2,4-DCP concentration profiles during its biodegradation.

It is clear that the above researchers focused on treating wastewater in an Internal Loop Air Lift Reactor (ILALR) by employing microbes, they, however, neglected the process involving a mixed bacterial culture, which could yield a complete treatment of phenolics even at higher concentration in shorter time. Free cell culture, instead of immobilizing the culture on a medium, which yields simplicity of operation and better mass transfer between the gas and liquid phase, show comparable performance with the immobilized culture. In addition, it is feasible to adopt such systems for real wastewater treatment. The researchers have also failed to evaluate the reactor stability towards shock organic loading conditions, which helps to study the stability of reactor towards higher pollutant concentration. Also, continuous operation of the reactor, similar to that of real wastewater treatment plant, has not been largely dealt with. Therefore all these unexplored research directions were extensively studied and reported in the present thesis.

Hence, the present thesis is focused to develop and study the effectiveness of an indigenous mixed microbial culture in treating synthetic wastewater containing phenol and *m*-cresol as single and mixture of substrates employing an internal loop airlift bioreactor. It is also intended to compare the results of biodegradation with that of photocatalytic degradation of phenolic compound of similar level of toxicity.

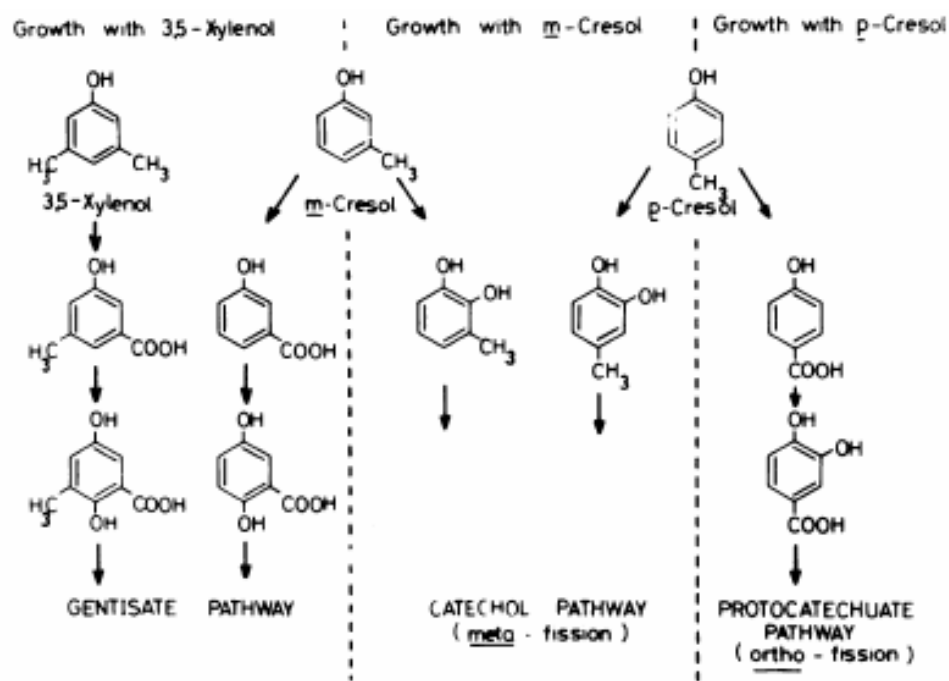


Fig 2.1: Biodegradation pathway for the metabolism of 3,5 xyleneol, *m*-cresol and *p*-cresol by *Pseudomonas putida* (Hopper and Taylor, 1975).

CHAPTER 3

MATERIALS AND METHODS

3.1. Chemicals and Reagents

Phenol and *m*-cresol, used in the study, were of analytical grade; glucose and inorganic salts, used in preparing microbial growth media, were of reagent grade. All the chemicals and reagents were purchased from Merck[®], India. Hi 25[™] Enterobacteriaceae and Hi mobility[™] Biochemical kit used in the characterization of the indigenous mixed microbial consortium was purchased from HIMEDIA[®], India.

3.2. Indigenous Mixed Microbial Culture and Culture Conditions

An indigenous mixed microbial culture, potent to degrade phenolic compounds, was isolated and enriched from a sewage treatment plant located in Guwahati, India. The obtained sample was centrifuged to remove the solid particles present in it. Then the culture was initially grown in 250 mL Erlenmeyer flask containing 100 mL of Mineral Salt Medium (MSM) with glucose 2 g/L and pH 7.0 under agitation (150 rpm) at 27 °C. The composition of the MSM and its amount is shown in Table 3.1.

3.3. Enrichment of the Culture to Degrade Phenolic Compounds

Fresh culture grown in glucose and MSM was used as inoculum in 250 mL Erlenmeyer flasks containing autoclaved 100 mL MSM solution initially containing phenol (50 mg/L) or *m*-cresol (50 mg/L) as the sole carbon and energy source. The flasks were kept in rotary shaker and maintained at 150 rpm and 27°C. Phenol or *m*-cresol degradation was monitored during incubation and after complete exhaustion of the carbon source the culture was now grown in MSM containing a higher concentration of the phenolic compound. The procedure was repeated up to a maximum concentration of 800 mg/L in case of phenol, and in case of *m*-cresol the maximum concentration was 1000 mg/L (Nuhoglu and Yalcin, 2005). The completed enrichment of the indigenous mixed culture was carried out for a period of more than one month in each case. Figs.3.1 and 3.2 shows the complete profile of phenol and *m*-cresol degradation, respectively, obtained during the enrichment period.

3.4. Characterization and Identification of the Indigenous Mixed Microbial Culture

3.4.1. Biochemical Characterization

Biochemical tests for characterizing the indigenous mixed microbial culture was performed using the commercial kits mentioned earlier. Each kit is a standardized colorimetric identification system utilizing thirteen biochemical tests and eleven carbohydrate utilization tests. The tests are based on the principle of pH change and substrate utilization. Upon incubation, organisms undergo metabolic changes, which are indicated by a color change in the media that is either visible spontaneously or after addition of a reagent. Oxidase test was performed separately using oxidase

reagent provided with the kit. The staining tests were performed as per the standard procedure detailed in Benson microbiological applications lab manual (Brown, 2001).

Each well in the kit was inoculated with 50 μ L of fresh culture suspension by the surface inoculation method, and the incubation temperature was maintained at $27\pm 2^\circ\text{C}$ for 18-24 h. Tests were performed as per the standards supplied with the test kit. The test details were furnished in Appendix.

3.4.2. Scanning Electron Microscopy (SEM)

Freshly grown cells in MSM containing phenol were centrifuged, dried and coated with gold film in a sputter coater, and finally, the cell morphology was recorded in LEO 1430VP SEM instrument at a magnification of 4350 at 15 KV.

3.5. Biodegradation Studies in Batch Shake Flasks

3.5.1. Single Substrate System

Batch biodegradation experiments in this study were carried out in 250 mL Erlenmeyer flasks with 100 mL MSM containing phenol or *m*-cresol as the sole carbon source and incubated in orbital shaker maintained at 27°C and 150 rpm. The concentrations of phenol and *m*-cresol were in the range of 100 – 800 mg/L and 100 – 900 mg/L, respectively. 1% v/v of the respective freshly grown enriched culture (phenol or *m*-cresol) was added to the biodegradation flasks as the inoculum. Samples were taken at regular time intervals and analysed for biomass and residual phenol or *m*-cresol concentrations. A sample collected during the middle and end of the experiment were analyzed for the intermediates concentrations. Each experiments

were performed in triplicates and the standard deviation of the results obtained from each set was found to $\pm 0.25 - 4.5$

3.5.2. Mixed Substrate System

Mixed substrate degradation study containing both phenol and *m*-cresol as the substrates were planned as per 2^2 factorial design of experiments. Two different concentration ranges of the substrates – low concentration range (100 – 300 mg/L of phenol, 100 – 200 mg/L of *m*-cresol) and high concentration range (300 – 600 mg/L of phenol, 200 – 600 mg/L of *m*-cresol) – were chosen in this mixed substrate degradation study. Table 3.2 presents various combinations of the initial concentrations of the phenolics, where -1 and +1 indicate respective low and high concentration levels and 0 indicates center point or middle level of the two factors. Three center point replicates were included in the design to check for experimental error; in total, seven combinations (experimental runs) of initial concentrations of *m*-cresol and phenol were investigated in this mixed substrate degradation system. 1% v/v of a freshly grown *m*-cresol acclimatized culture was added to the biodegradation flasks as the inoculum. As before, samples were collected during the experiments and analyzed for the biomass and the phenolics concentrations. The results of biomass growth and substrate degradation in the study were statistically analyzed in the form of analysis of variance (ANOVA) and students 't' test using the statistical software MINITAB (Version 12.2 PA, USA).

3.6. Phenol Biodegradation in a Batch Stirred Tank Reactor

3.6.1. Experimental Set up

The batch stirred tank reactor set up in this study consisted of a 5 L glass vessel fitted with an impeller driven by a DC motor. Ports for sampling, liquid addition and withdrawal through peristaltic pump and thermometer for monitoring the temperature inside the vessel were provided in the set up. A schematic of the setup is shown in Fig. 3.3. Four batches of experiments were conducted with initial phenol concentration varying from 100 to 400 mg/L in 4 L of MSM. These concentration levels were chosen based on the extent of total time taken by the culture for complete degradation of phenol. The experiments were carried out under batch mode at constant temperature of $29^{\circ}\text{C} \pm 2^{\circ}\text{C}$ with continuous stirring at 150 rpm. 10% v/v of a freshly grown enriched culture was added to the reactor as the inoculum. Samples were withdrawn at regular time interval (approximately 6 hours), centrifuged ($10,000 \times g$ for 3 min) and analyzed for residual phenol concentration (Biofuge Pico, Rota No.3328, Heraeus). For each concentration duplicate experiments were performed under the same condition and average values of each experiment are reported. The standard deviation of obtained experimental data was in the range of ± 0.25 to 3.0.

3.7. Feasibility of the Indigenous Mixed Culture to Treat a Refinery Industry Wastewater

After evaluating the potential of the mixed culture for treatment of “synthetic” wastewater containing phenolics, the culture was tested for treatment of a real industrial effluent. The effluent was obtained from a petroleum refinery complex located at Guwahati, India. The general characteristics of effluent, such as Chemical

Oxygen Demand (COD), pH, Dissolved Oxygen (DO) and heavy metals (lead, chromium, nickel) were analyzed and are presented in Table 3.3. The experiments were performed in 250 mL Erlenmeyer flasks with 100 mL refinery wastewater and incubated in orbital shaker maintained at 27 °C and 150 rpm. The experiments were carried out after adjusting the wastewater pH to 7.0. The samples were collected at regular time interval and analyzed for the more acceptable wastewater quality parameter - Chemical Oxygen Demand (COD) concentration.

3.8. Phenol Degradation in a Solar Photoreactor

In order to compare the efficiency of phenol degradation by the indigenous mixed culture with a well established advanced oxidation process, photo catalytic experiments were carried out in a batch reactor (Fig. 3.4) of 1 L capacity made of glass, with continuous stirring using a magnetic stirrer in presence of sunlight as the UV source. The experiments were carried out from morning to evening i.e., 7.00 AM to 5.00 PM. Two different TiO₂ catalysts were used to assess the performance of this process – Anjatox and Degussa P-25. While the loading rate for Anjatox[®] was varied from 3 g/L to 18 g/L and Degussa P-25 was varied from 1 g/L to 4 g/L. The initial phenol concentration was varied from 50 - 200 mg/L. The samples were collected at regular time interval for every one-hour, centrifuged at 10,000 ×g, 10 min to separate the catalyst, and the supernatant was subsequently analyzed for the residual phenol concentration. Intermediates formed at the end of the treatments were also analyzed.

3.8.1. Characterization of the Photocatalysts

3.8.1.1. X-Ray Diffraction (XRD) Analysis

The XRD analysis of the photocatalyst materials was performed with Seifert Model No. 3003TT. From the XRD peaks, the crystallite size of the catalysts was calculated by applying the Scherrers formula. The Scherrers formula is given below:

$$D = k \lambda / \beta \cos\theta \quad (3.1)$$

where, $k = 0.9$, D is the particle size (nm) λ is the X-ray wavelength (1.5406 Å), θ is the contour peak angle (radian) and β is the width of the obtained peak (radian).

3.8.1.2. BET Surface Area Analysis

Surface area of the catalysts was studied with a surface area analyzer (Beckman Coulter Model No. SA 3100). Nitrogen gas was used in the analysis for the determination of adsorption isotherm from which the surface area of the catalyst was calculated.

3.8.1.3. Particle Size Distribution

Laser Particle Size Analyzer (Malvern, Model No. Mastersizer 2000) with wet distribution mode was used in the determination of the particle size distribution. The equipment has broad measuring range *i.e.*, minimum of 0.02 μm and maximum of 2000 μm .

3.9. Biodegradation Studies in an Internal Loop Airlift Bioreactor (ILALR)

3.9.1. Experimental Setup

An ILALR made of perspex acrylic material with a working volume of 2.5-L was specially fabricated to study phenol biodegradation by the indigenous mixed culture. The reactor consisted of two concentric tubes, where the inner tube was a removable draft tube (40×5 cm) and the external tube had dimensions of 60×8 cm. The top and bottom of the reactor was sealed with a flange made of stainless steel. Compressed air from a compressor was fed from the bottom of the reactor *via* a nozzle of diameter 0.8 cm. Sterile air was fed in the reactor by filtering it through an air filter. The nozzle was placed inside the inner tube and the superficial gas flow was measured with a rotameter (0 - 5 L/min) with a needle valve. The schematic of the ILALR is shown in Fig. 3.5 along with its dimensions in Table 3.4. A photograph of the ILALR during its operation is presented in Fig. 3.6.

3.9.2. Hydrodynamic Studies with the ILALR

3.9.2.1. Residential Time Distribution (RTD)

The RTD in the ILALR was performed by tracer analysis using potassium chloride (0.01N) as the tracer. Ten mL of the tracer was injected rapidly through the liquid flow inlet to the reactor. Samples were drawn from a sampling port (indicated in Fig 3.5) at every 5 s and were analyzed for the exiting potassium chloride concentration using a Total Dissolved Solid (TDS) meter (Consort C-863 Multi parameter analyzer, Belgium). The tracer analysis was repeated at various inlet gas flow rates from 1 to

3.0 L/min. All the experiments were carried out at atmospheric pressure and at $26 \pm 1^\circ\text{C}$.

3.2.2.2. Volumetric Mass Transfer Coefficient (k_La) Determination

Volumetric mass transfer coefficient of oxygen in the ILALR was determined for both non-living and living (bacteria) systems using the dynamic gassing out method (Kamp *et al.*, 1987). For determination of k_La in the non-living system, deionized water was utilized, and for living system, the mixed culture growing in MSM containing 100 mg/L of phenol was employed. A digital dissolved oxygen (DO) meter (Consort C-863 Multi parameter analyzer, Belgium) with fast response probe capable of measuring DO at every 5 s interval was used. Two types of inert gases, namely argon and nitrogen of 99.9 % purity, were used for degassing the systems reactor. In all the experiments a superficial gas flow rate of 2 L/min was used at ambient conditions.

3.9.2.3. Bubble Diameter Analysis in the Riser and Downcomer Sections of the ILALR

During the RTD and mass transfer experiments in the ILALR, the size of gas bubbles in its riser and downcomer sections were detected by taking snapshots using a digital camera (Canon, model no A-420, China) and analyzed in j-image software. The mean diameter of the bubbles was calculated and their effects on the RTD and liquid mixing pattern in the reactor were also analyzed.

3.9.3. Batch Biodegradation Studies with the ILALR

3.9.3.1. Single Substrate System

The reactor (2.5 L capacity) was operated in batch to study the scale up effect from shake flask. The batch study was initially done for single substrate system with phenol or *m*-cresol at concentration 100 mg/L. The study was repeated with various concentrations of the substrate upto a maximum feed concentration of 600 mg/L in case of phenol and 400 mg/L in case of *m*-cresol. 10% v/v of the respective freshly grown enriched culture was added to the reactor treating phenol or *m*-cresol in the beginning as the inoculum. Samples were withdrawn from the sampling port and were analyzed for biomass and residual phenol or *m*-cresol concentrations. The standard deviation of obtained experimental datas was in the range of ± 0.3 to 3.5.

3.9.3.2 . Mixed Substrate System

Mixed substrate degradation study at various combinations of phenol and *m*-cresol concentrations were adopted with a maximum of 300 mg/L each. Table 3.5 accounts for the combinations. As before, samples were collected during the experiments and analyzed for the biomass and the phenolics concentrations. The amount of inoculum added was same as that of the single substrate system; however, the seed culture was freshly enriched to grow and degrade *m*-cresol as the sole carbon source in MSM in batch shake flask.

3.9.4. Fed-batch Biodegradation Study with the ILALR

3.9.4.1. Single Substrate System

In order to overcome the observed substrate inhibition on its biodegradation and the culture growth, fed batch operations were evaluated. The reactor was initially started in batch mode with phenol or *m*-cresol of concentration 100 mg/L and then switched to fed-batch mode upto a maximum phenol or *m*-cresol concentration of 600 mg/L. 10% v/v of a freshly grown enriched culture was added to the reactor in the beginning as the inoculum. Samples were withdrawn from the sampling port and were analyzed for biomass and residual phenol or *m*-cresol concentrations. The standard deviation of obtained experimental data was in the range of ± 0.4 to 4.5.

3.9.4.2. Mixed Substrate System

Mixed substrate degradation was also studied for different feed substrate concentration combinations in this fed batch operated system. The reactor was initially started in batch mode with phenol and *m*-cresol of concentration 50 mg/L each and then switched to fed-batch mode upto a maximum phenol and *m*-cresol of concentration 300 mg/L each. As before, 10% v/v of freshly grown enriched culture (using *m*-cresol as the sole carbon source in MSM) was added to the reactor as the inoculum. Samples were withdrawn from the sampling port and were analyzed for biomass and residual phenol or *m*-cresol concentrations. The standard deviation of the obtained experimental results was in the range of ± 0.4 to 4.5. The details of fed batch operation adopted in the study are presented in Table 3.6.

3.9.5. Continuous Degradation Studies with the ILALR

3.9.5.1. Single Substrate System

The reactor was initially operated in batch mode with an initial phenol concentration of 50 mg/L as the substrate in MSM. The reactor contained 10 % v/v of a freshly grown enriched culture (either in phenol or *m*-cresol) as the inoculum. Once the culture growth was established, the reactor was switched to continuous mode. For all the continuous experiments, the medium and the concentrated substrate solutions were fed by a peristaltic pump (Miclins, India; Model no. PP 20). An outlet was made at the top of the reactor to make it an overflow type vessel. The outlet is used to withdraw sample and to maintain a constant culture volume (2.5 L). The continuous degradation of phenol and *m*-cresol in the ILALR was performed at two different HRTs 4.1 h and 8.3 h, respectively by providing feed flow rates 5 mL/min and 10 mL/min with the aid of the peristaltic pump. Samples were collected at regular time interval and analyzed for the residual phenolics concentration. The various stages involving inlet concentration of phenol/*m*-cresol, flow rate and hours of operation, necessary to study the continuous treatment of synthetic wastewater containing phenol /*m*-cresol in single substrate system, is detailed in Table 3.7. Results presented are average of three values obtained from analysis of the samples.

3.9.5.2. Mixed Substrate System

This degradation study was carried using phenol and *m*-cresol as the mixed substrate at both the said HRTs. Based on the results of the single substrate degradation study, following concentration ranges of phenol and *m*-cresol were chosen in this study – 100 to 300 mg/L of both phenol and *m*-cresol. For choosing combination of

concentration levels of these two compounds, a 2^2 factorial design of experiments with two compounds as the factors at two different levels was applied. Tables 3.8 and 3.9 show the design matrix employed in the study along with the operating conditions (HRT, stages and treatment time) in the ILALR. In these tables, '-1' indicates low level (100 mg/L) and '+1' indicates high level (300 mg/L) of the two factors and '0' indicates center point or middle level (200 mg/L) of the 2 factors. The schematic of the continuous operation of the ILALR is illustrated in Fig. 3.7. Samples collected from the outlet of the ILALR were analyzed thrice for residual phenol and *m*-cresol concentrations. The results presented in this continuous study are average of these three values - similar to that of the single substrate system.

3.9.5.3. Stability Studies on the Performance of the ILALR

The key problem of any wastewater treatment involves irregular organic loading due to changes in process conditions. In order to address this problem in our study, experiments were carried out by subjecting the ILALR to operations leading to intermittent and shock loading conditions. Initially the reactor was operated at low substrate (phenol or *m*-cresol) concentration of 100 mg/L (in single substrate system only) and the concentration of the substrate was increased gradually to 200 mg/L and suddenly to 600 mg/L, 800 mg/L (in case of phenol) and 800 mg/L (in case of *m*-cresol) under continuous mode to check the performance stability of the reactor. The Hydraulic Retention Times (HRT) maintained in the reactor were again 4.1 and 8.3 h to follow their effects in this study.

3.10. Analytical Methods

The experimental methods used in the present work include determinations of concentrations of biomass, phenol, *m*-cresol and intermediates. For off-line analytical methods, samples of 1 mL volume were taken from the shake flasks/BSTR/ ILALR.

3.10.1. Determination of Biomass

Cell density in the samples was estimated with Diode Array Spectrophotometer (Spekol 1200, Analytik Jena, Germany) by measuring its absorbance (OD) at 600 nm wavelength. OD₆₀₀ was then converted to dry cell weight by a calibration curve, which was obtained by plotting dry weight of biomass per milliliter vs OD₆₀₀. For determination of biomass concentration as dry weight, samples were centrifuged for 10 min at 10 000 g at room temperature (Biofuge Stratos, Heraeus instruments, Kendro, Hanau, Germany) in ependroff tubes. The pellets were dried at 50°C for 24 h, cooled in an exsiccator at room temperature and weighed. The tubes were washed, dried and re-weighed to determine its empty weight. The difference between the first and second weight was used to determine the dry weight of biomass in mg/L.

3.10.2. HPLC Analysis

About 100 µL of sample was filtered using a syringe sterile filter (PTFE filter media of 13 mm diameter, pore size 0.45 µm, Whatman, USA) to remove the biomass. Concentrations of the substrates in the biomass free sample were quantified by using HPLC (High Performance Liquid Chromatography). According to the nature of the determinate substrate, different parameters were used as shown below. The standard curves for estimating phenol and *m*-cresol in this HPLC analysis are shown in Figs. 3.8 and 3.9.

For determination of phenol, m-cresol, Intermediates (other than organic acid)**Detector:** Perkin – Elmer UV-Detector 200**Detection:** UV-Absorption $\lambda = 275$ nm**HPLC-pump:** Perkin – Elmer HPLC-pump model 200 series**Flow rate:** 1.0 mL/min**Column:** C-18 column (Chromo pack 250mm \times 4.5mm \times 5 μ m)**Mobile-phase:** Acetonitrile: water (60:40)**Temperature:** Room temperature.***For determination of Intermediates (Organic Acids)*****Detector:** Perkin – Elmer UV-Detector 200**Detection:** UV-Absorption $\lambda = 210$ nm**HPLC-pump:** Perkin – Elmer HPLC-pump model 200 series**Flow rate:** 0.6 mL/min**Column:** Acclaim OA column of dionex (150 mm \times 4.0 mm \times 5 μ m)**Mobile-phase:** 100 mM Na₂SO₄, pH 2.65 adjusted by using methanesulfonic acid**Temperature:** Room temperature.**3.10.3. Chemical Oxygen Demand (COD) and Heavy Metal Analysis**

Refinery wastewater was quantified in terms of COD and the test was performed as per the standard methods prescribed by the American Public Health Association (1998) using a COD thermo reactor (Spectroquant TR 420 Merck[®], Germany). The concentrations of the heavy metals, viz. lead and arsenic, in the refinery wastewater were measured using atomic absorption spectrophotometer (Varian, USA, Model No. Spectra AA 240FS) at their respective absorbance maxima.

Table 3.1: Composition of the mineral salt medium used in the study

Sl. No	Inorganic salts	Amount (mg/L)
1.	(NH ₄) ₂ SO ₄	230.00
2.	CaCl ₂	8.00
3.	FeCl ₃	1.00
4.	MnSO ₄ ·H ₂ O	100.00
5.	MgSO ₄ ·7H ₂ O	100.00
6.	K ₂ HPO ₄	500.00
7.	KH ₂ PO ₄	250.00

Table 3.2: 2² full factorial design with three center point replicates adopted in the mixed substrate biodegradation study for both the initial concentration ranges

Expt. run No.	Factors and their levels	
	Phenol	<i>m</i> -Cresol
1.	-1	-1
2.	-1	+1
3.	+1	-1
4.	+1	+1
5.	0	0
6.	0	0
7.	0	0

Table 3.3: Characteristics of the refinery wastewater

Sl. No.	Parameters	Quantity
1.	pH	8.6
2.	Dissolved Oxygen	0.95 mg/L
3.	Arsenic	55 – 60 $\mu\text{g/L}$
4.	Lead	45-50 $\mu\text{g/L}$
5.	COD	10000 mg/L
6.	COD after adjusting the pH to 7	4800 mg/L

Table 3.4: Geometrical details of the internal loop airlift reactor (all units are in cm)

Diameter of external tube (D_R)	8.00
Diameter of internal tube (D_I)	5.00
Top Clearance (T_D)	10.00
Bottom Clearance (B_D)	10.00
Internal tube height (I_H)	40.00
External tube height (E_H)	60.00
Diameter of the nozzle (N_D)	0.8

Table 3.5: Combinations of the phenolics concentrations adopted to study the batch degradation of the mixed substrates in the ILALR

Expt. run no.	Phenol (mg/L)	<i>m</i> -Cresol (mg/L)
1.	100	100
2.	200	100
3.	200	200
4.	100	300
5.	200	300
6.	300	300

Table 3.6: Concentrations of the phenolics in single substrate and mixed substrate system along with volume treated in each step in the ILALR operated under fed batch mode

Step	Phenol concentration (mg/L)		<i>m</i> -Cresol concentration (mg/L)		Volume treated (mL)
	Single substrate system	Mixed substrate system	Single substrate system	Mixed substrate system	
1.	100	50	100	50	2200
2.	200	100	200	100	2275
3.	300	200	300	200	2350
4.	400	300	400	300	2425
5.	600	-	600	-	2500

Table 3.7: Various stages of continuous operation in the ILALR treating synthetic wastewater containing either phenol/*m*-cresol (* Shock loading concentration)

Stage of operation	HRT (h)	Phenol concentration (mg/L)	Hours of operation in each stage (h)	<i>m</i> -Cresol concentration (mg/L)	Hours of operation in each stage (h)
I		100	30	100	25
II		200	48	200	24
III		300	40	300	26
IV	8.3	600*	36	400	30
V		800*	32	500*	28
VI		-	-	800*	7
VII		-	-	100	30
I		100	30	100	24
II		200	38	200	24
III	4.1	300	30	300	26
IV		500*	24	500*	5
V		100	46	100	27

Table 3.8: 2^2 full factorial design matrix along with the stages and time of operation for studying degradation of phenol/*m*-cresol as mixture at 8.3 h HRT

Stage of operation	Factors and their levels		Hours of operation (h)
	Phenol	<i>m</i> -Cresol	
I	-1	-1	26
II	0	0	30
III	-1	+1	24
IV	0	0	26
V	+1	-1	30
VI	0	0	24
VII	+1	+1	28
VIII	-1	-1	28

Table 3.9: 2^2 full factorial design matrix along with the stages and time of operation for studying degradation of phenol/*m*-cresol as mixture at 4.1 h HRT

Stage of operation	Factors and their levels		Hours of operation (h)
	Phenol	<i>m</i> -Cresol	
I	-1	-1	26
II	0	0	16
III	-1	-1	14
IV	-1	+1	16
V	-1	-1	18
VI	0	0	12
VII	-1	-1	16
VIII	+1	-1	14
IX	-1	-1	16
X	+1	+1	4
XI	-1	-1	24

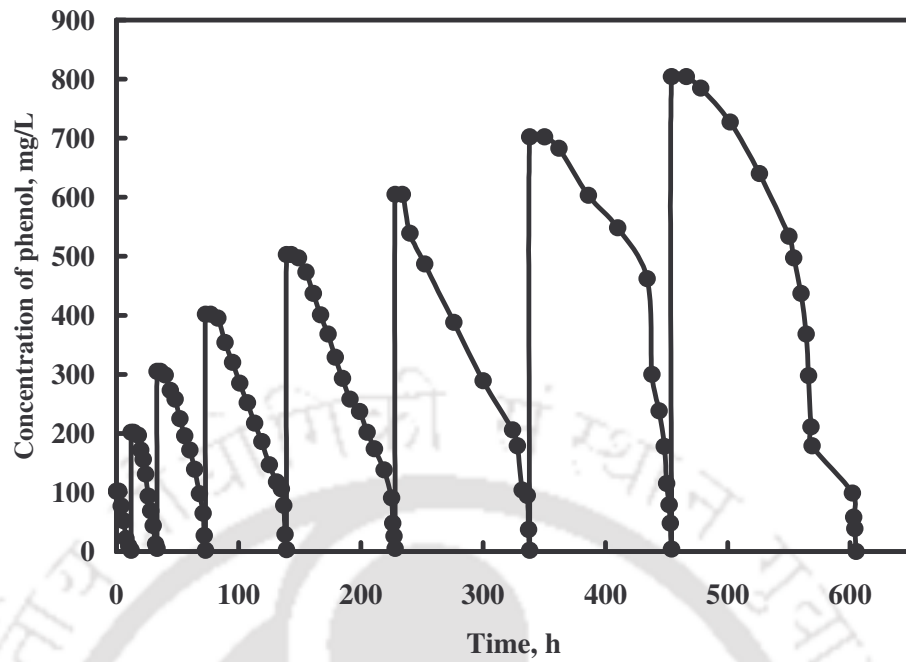


Fig. 3.1: Phenol degradation profile followed during the enrichment period.

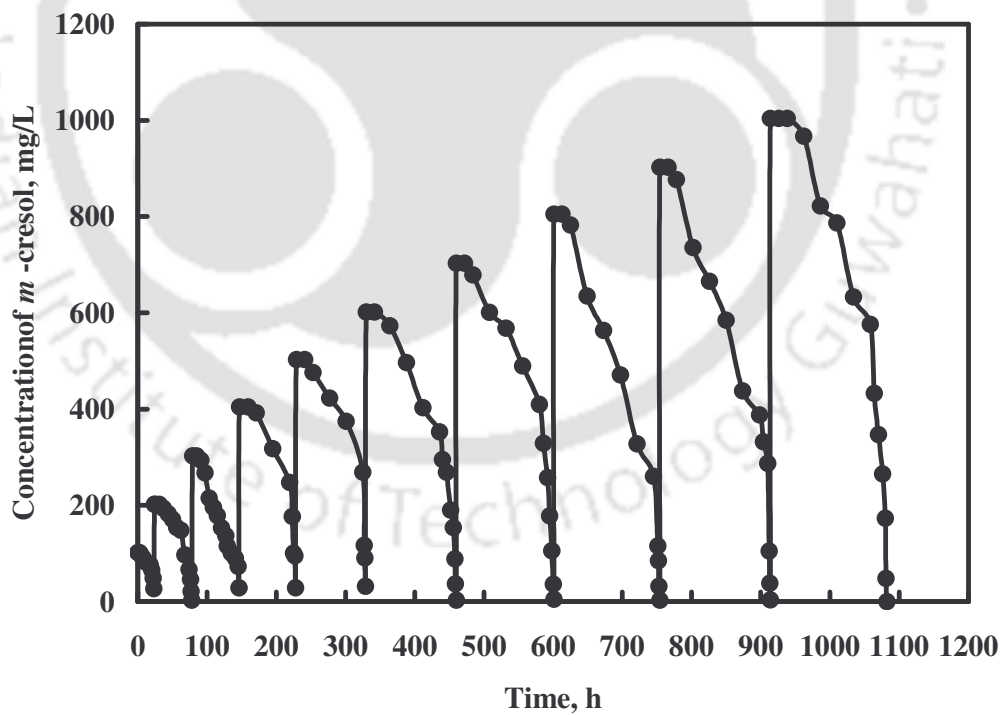


Fig.3.2: *m*-cresol degradation profile followed during the enrichment period.

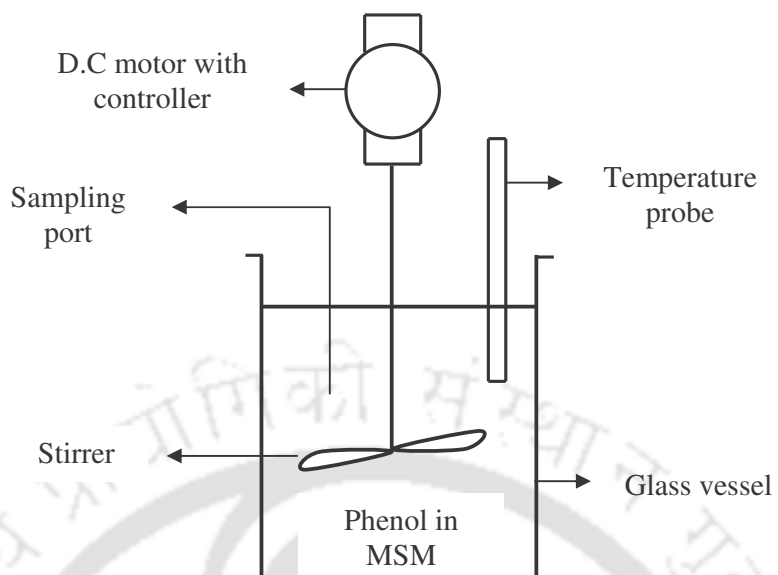


Fig. 3.3: Schematic of the simple batch stirred tank reactor.

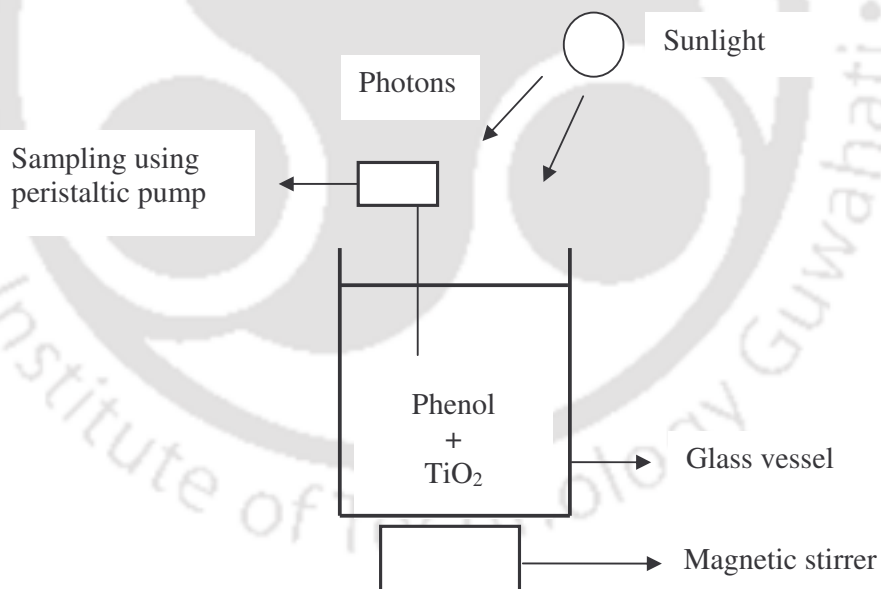


Fig. 3.4: Schematic of the solar photoreactor.

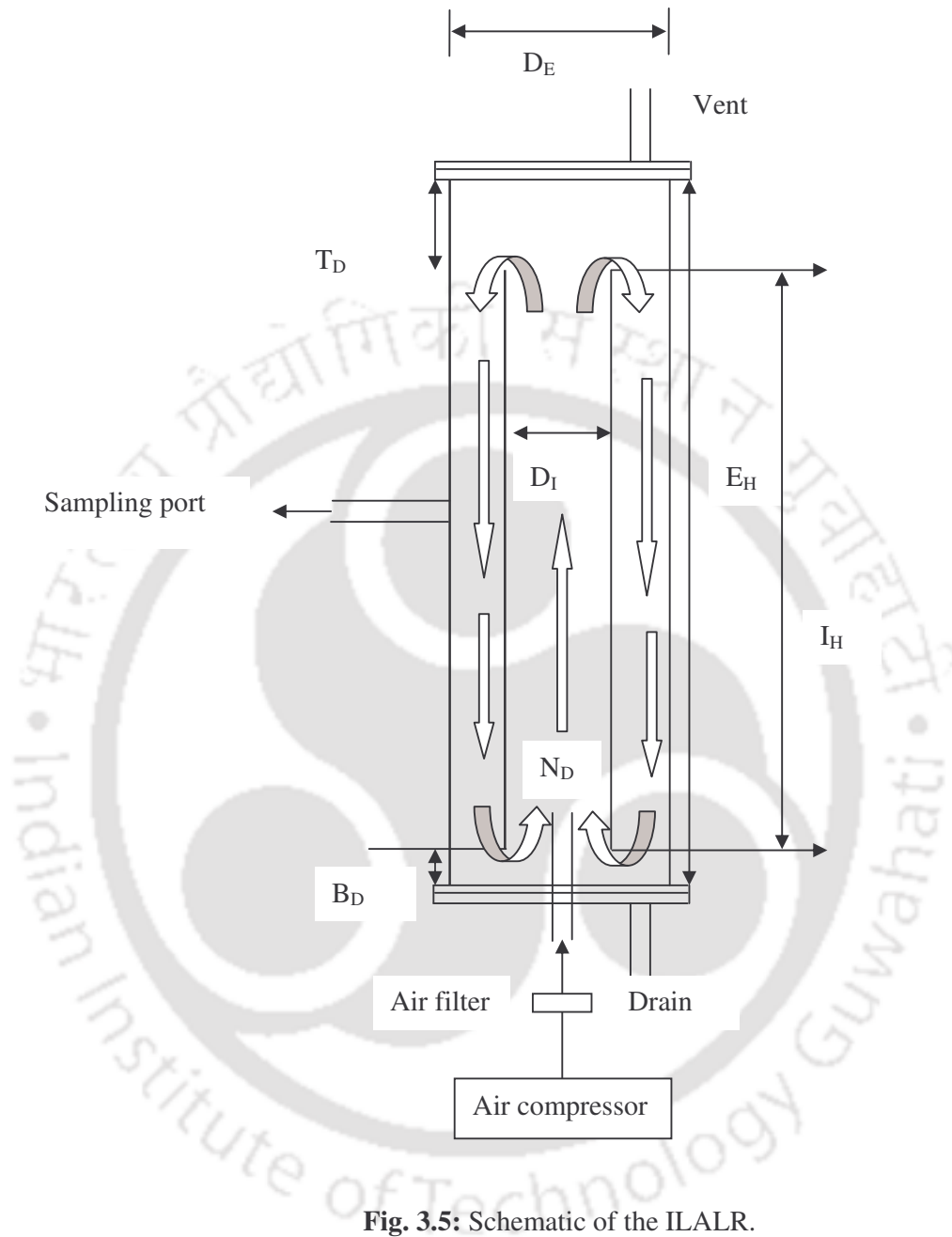


Fig. 3.5: Schematic of the ILALR.



Fig. 3.6: Photograph of the ILALR used in the study.

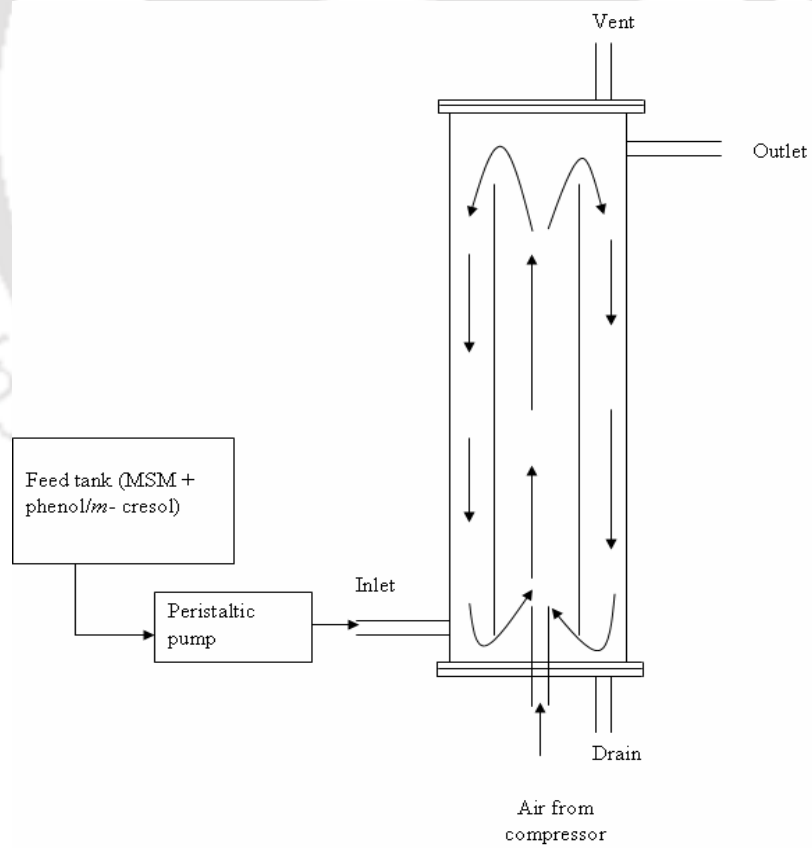


Fig.3.7: Schematic of the ILALR in continuous operation

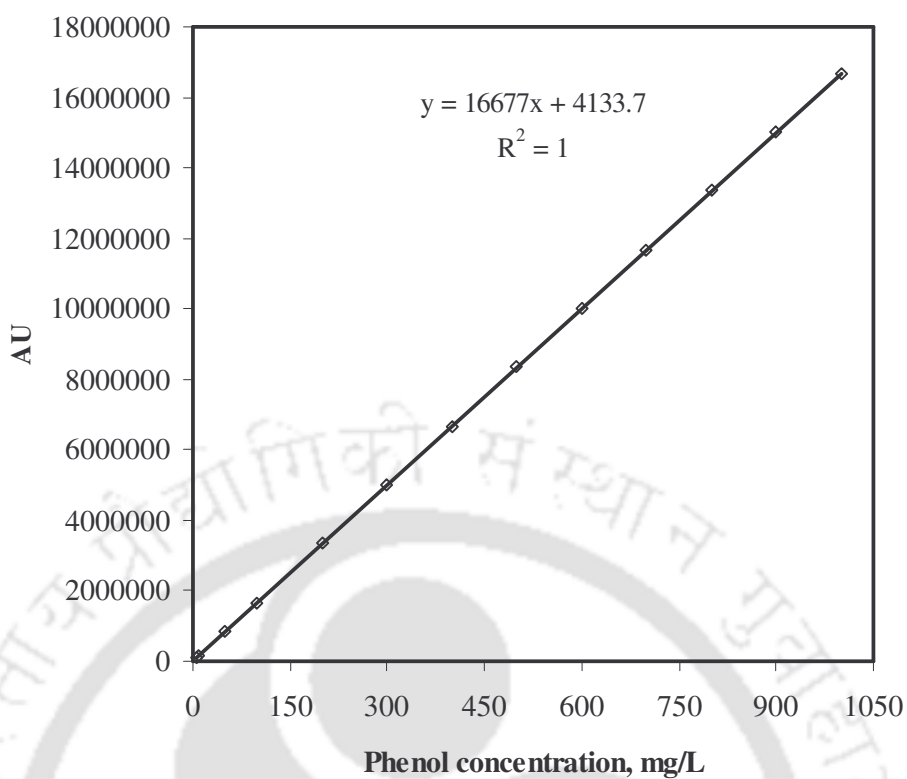


Fig.3.8: Calibration curve obtained for phenol estimation using the HPLC.

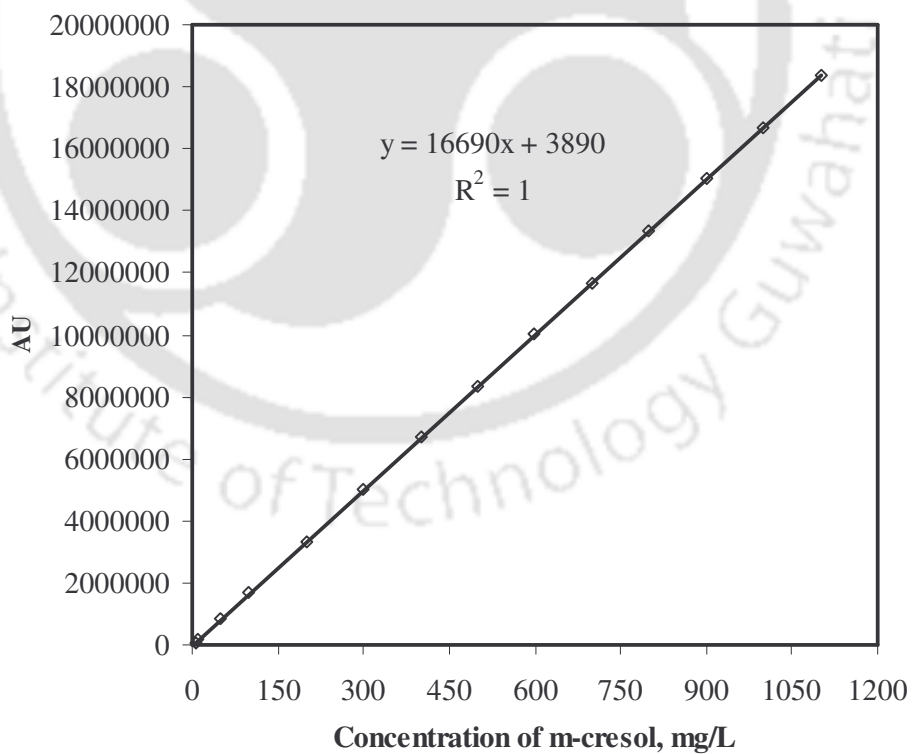


Fig.3.9: Calibration curve obtained for *m*-cresol estimation using the HPLC.

CHAPTER 4

RESULTS AND DISCUSSION

Biological treatment with mixed microbial strains is an attractive alternative for the treatment of contaminated ground, surface, and wastewaters containing phenolics. This research contributes to the study and development of a new degradation technique that employs an indigenous mixed microbial consortium in an internal loop airlift bioreactor for the treatment of recalcitrant organic substances present in industrial wastewater.

4.1. Characterization Results of the Indigenous Mixed Microbial Culture

Upon Gram staining, the enriched mixed microbial culture when examined under light microscope revealed uniformly small Gram-negative shaped bacteria rods of varying lengths (Figs. 4.1). SEM image of the culture also confirmed the above observation that indicated the average size of 1.3 to 1.8 μm (Figs. 4.2). Detailed and routine biochemical characterization tests carried out with the indigenous mixed culture further confirmed the predominant presence of *Pseudomonas* group of species in the mixed consortium. This revealed that the enriched culture capable of degrading phenolic compounds in our work was mainly due to *Pseudomonas* spp. All these tests, including tests for urease, catalase, oxidase, IMViC (Indole production; Methyl – red; Voges Proskauer's; Citrate utilization) and gram-staining confirmed the same.

(Radehaus and Schmidt, 1992). Table 4.1 presents the detailed results of the above mentioned tests.

4.2. Batch Biodegradation of the Phenolics in Shake Flasks

4.2.1. Culture Growth and Phenol Degradation Kinetics – Single Substrate System

Enrichment of the mixed culture was carried out by allowing it to grow in presence of phenol or *m*-cresol up to a maximum initial phenol concentration of 800 mg/L or 1000 mg/L initial concentration of *m*-cresol in MSM. However, in both the cases, glucose was used as a feed substrate during the initial stage of acclimatization to enhance its rate of growth. Nevertheless, the culture was grown only in presence of phenol or *m*-cresol in the later stages of acclimatization. It can be argued that the species of microorganism, enriched to grow and degrade such high concentration levels of phenolics, would certainly be able to treat phenolics in real industrial wastewater, which usually contains a lesser concentration level of the pollutants

4.2.1.1. Effect of Initial Concentration of Phenol

Fig. 4.3 shows the time profile of phenol degradation by the culture. It could be observed from the figure that the culture was able to completely degrade phenol up to a maximum concentration of 800 mg/L, for which it took about 69 h. The total time taken by the culture to degrade phenol at all its initial concentrations may be divided into two phases: initial lag phase and active degradation phase. As illustrated in Fig 4.3, the extent of these two phases, in turn, depended on initial phenol concentration. The degradation and growth profile of the culture for phenol at an initial concentration of 800 mg/L could be well explained by normalizing it with respect to

the biomass, which yield specific growth and degradation rates. In order to study the effect of initial phenol concentration on its degradation rate, slopes of the respective degradation curves in Fig. 4.3 were calculated at each concentration. From the variation in phenol degradation rate with respect to its initial concentration as depicted in Fig. 4.4, a maximum degradation rate was obtained at a phenol concentration of 400 mg/L. On the growth of the culture, phenol had a significant inhibitory effect, particularly at higher concentrations (Kumar *et al.*, 2005; Stoilova *et al.*, 2006). The profile of biomass concentration of the culture (as OD₆₀₀) at different initial concentrations of phenol is shown in Fig. 4.5. It is clear that phenol did not show any inhibitory effect on the microorganism when its concentration was within the range of 100 to 500 mg/L, as almost no lag phase was observed during the growth of the culture. Moreover, final biomass output of the culture was found to be proportionate with the phenol concentration in this range. However, when the culture was grown in MSM containing phenol concentrations more than 500 mg/L a stationary phase, in terms of the culture growth, was prominent in each of these concentrations and the extent of the stationary phase, depended upon the initial concentration of phenol in the media. For example, time taken by the culture to reach stationary growth phase at phenol concentration of 500 mg/L was higher than that at a lower phenol concentration. Similarly, inhibition effect was distinct at phenol concentrations more than 500 mg/L and the microbial culture took longer time for its maximum growth (*e.g.* maximum 69 h at 800 mg/L). Also, Dapaals and Hill (1992) in their study with *Pseudomonas putida* observed that the length of lag phase increased with increase in phenol concentration, in the range 60 mg/L to 600 mg/L. Despite the above, absorbance of the culture at higher concentration of phenol was more, which could be an indication of capability of the culture for effective degradation of phenol.

4.2.1.2. Kinetics of Phenol Biodegradation

In order to describe the kinetic behavior of phenol degradation, several kinetic models, such as growth-associated models (logarithmic, logistic and Monod with growth), non-growth associated models (zero order, first order and Monod based) and three-half order model (Schmidt *et al.*, 1985; Alexander 1999) were tested. The mathematical forms and description of these models were already given in Chapter 2. Among these kinetic models, only the three-half order kinetic model (Brunner and Focht, 1986) could fit all the experimental data obtained at different initial phenol concentrations. Table 4.2 presents the results of fitting these models to the experimental data, which gave high coefficient of determination (R^2) values between the model predicted and experimental degradation profile at all initial phenol concentrations

It could be explained clearly with this three-half order kinetic model that the reaction undergoes zero order in the initial lag phase and then to first and or second order in the active degradation phase. Similarly, Mahanty *et al.* (2008) in their study on biodegradation of pyrene by *Mycobacterium frederiksbergense* observed that an three-half-order kinetic model provided the best fit to the entire degradation profiles with coefficient of determination (R^2) value greater than 0.99 at all initial pyrene concentrations in the medium.

4.2.1.3. Modeling the Kinetics of Growth of the Culture

The variation in ' μ ' with respect to initial phenol concentrations were then modelled using different microbial growth kinetic models found in the literature (Monod, 1949; Yano and Koga, 1969; Luong, 1987; Han and Levenspiel, 1988; Mulchandani and

Luong, 1989; Kumar *et al.*, 2005). Detailed descriptions about the growth kinetic model were already given in Chapter 2.

The best fitting models were also evaluated for estimating the bio-kinetic parameters of growth in models. The model equations were solved using nonlinear regression method of MATLAB 7.0. Also, constraints for positive integer values the biokinetic parameters estimated were implemented while solving the model equations. Fig. 4.6 shows the specific growth rate computed from experimental data along with those predicted by the various models. In all the cases, a reduction in specific growth rate of the culture was observed above phenol concentration of 300 mg/L, which clearly indicates a substrate inhibition pattern on the culture growth.

Among the models, Han-Levenspiel model fitted the data well with the least Root Mean Square (RMS) error, which was followed by the Luong model. All the other substrate inhibition models did not yield accurate results, as observed from their RMS values. Table 4.3 shows the kinetic parameters obtained from these models along with a measurement of model precision in terms of RMS error. Table 4.3 also compares the values of the parameters K_s and μ_{max} estimated using the linearized form of Monod's model with those of the substrate inhibition models. The modeling results of Han-Levenspiel and Monod kinetics were comparable and the RMS error of Han-Levenspiel model is quite small. On the other hand, estimation of half saturation constant from Haldane model is not comparable with those from the other models and the RMS error value is also on the higher side. It is clear that Monod's model, which was used to describe the specific growth rate region only upto a maximum point, could predict μ_{max} and K_s values quite high compared to those predicted by the non similar models.

However, the model fitting in this study proved that the culture is capable of growing well even with quite high predicted μ_{\max} value due to phenol in the medium. These values of the bio kinetic parameters were also compared with those reported in the literature on phenol degradation using different microbial culture and were found to be in good agreement with each other.

Table 4.4 makes a comparison of the growth kinetics of the culture during phenol degradation in batch shake flasks with the literature. From the estimated biokinetic values, the inhibition constant K_i estimated by Haldane model was higher than those reported in literature (Kumar *et al.*, 2005; Rodriguez *et al.*, 2006). This vary fact reveals a good potential of the culture in utilizing phenol as a substrate for its growth. Similarly, the maximum substrate concentration at which the culture ceases to grow was estimated to be 790 mg/L and 800 mg/L according to the Han-Levenspiel and Luong model, respectively, values which were very close to the experimentally observed value of 800 mg/L. It could be well said from this high value of the biokinetic constant that the culture is capable of sustaining and growing at a high concentration level thereby proving that culture is highly efficient for complete degradation of similar concentration levels of phenol in wastewater. However, there seem to be some difference in the biokinetic constants values predicted by the various models, which could be reasoned based on the fact that these models were originally developed for systems containing pure microorganism and different substrates. This could also be due to the fact all these substrate inhibition models could not predict the entire specific growth rate profile with very high accuracy. Nevertheless, a general substrate inhibition profile on par with the experimental observation was predicted by the models.

4.2.1.4. Modeling the Kinetics of Phenol Degradation

The kinetic profile at each phenol concentration was further used to calculate the specific phenol degradation rate, given by:

$$q = -\frac{1}{X} \frac{dS}{dt} \quad (4.1)$$

where, q is the specific substrate degradation rate (h^{-1}), q_{\max} is the maximum specific substrate degradation rate (h^{-1}), S is substrate concentration (mg/L), X is the biomass concentration (mg/L) and t is the time taken by the culture for completely degrading the substrate (h). The variation in specific degradation rate with initial phenol concentration is shown in Fig. 4.7.

It is evident from the figure that the rate of specific degradation rate declined at higher concentrations of phenol indicating substrate inhibition on rate similar to the culture specific growth rate inhibition by phenol at its same higher concentrations (Okpokwasili and Nweke, 2005). Although the original models (described in Chapter 2) were initially developed for explaining substrate inhibition on the growth rate of microorganisms, by changing some of the terms in these models, they could be applied for modeling the variation of specific substrate degradation rate with various initial concentrations of phenol in this study. The terms, μ and μ_{\max} in the original model equations, are replaced with q and q_{\max} , respectively to give the following the set of Eqns. (4.2) - (4.6).

$$q = \frac{q_{\max} S}{K_s + S} \quad (4.2)$$

$$q = \frac{q_{\max} S}{K_s + S + \frac{S^2}{K_i}} \quad (4.3)$$

$$q = \frac{q_{\max}}{(K_s / S) + 1 + \sum_{j=1}^n (S / K_j)^j} \quad (4.4)$$

$$q_i = q_{\max} \frac{S}{S + K_s + (S^2 / K_{si})(1 + S / K)} \quad (4.5)$$

$$q = \frac{q_{\max} S}{K_s + S} \left[1 - \frac{S}{S_m} \right]^n \quad (4.6)$$

Thus, the newly replaced terms in these model equations represent specific substrate utilization rate (q) and maximum specific substrate utilization rate (q_{\max}), respectively. These model equations were also solved using nonlinear regression method and similar procedure, as before in MATLAB[®] 7.0. From Fig. 4.7 it is observed that almost all the adopted models fit the experimental data reasonably well. Table 4.5 shows the degradation kinetic parameters obtained from these models along with a measurement of model precision in terms of RMS error. The results of this model fitting and the estimated kinetic parameter values clearly indicate the effectiveness of the mixed culture in degrading phenol.

4.2.1.5. Analysis of Probable Intermediates during Phenol Degradation

In order to understand whether the phenol has been completely degraded by the culture with no intermediates at the end of each biodegradation experiments, samples were collected during (middle) and end of the biodegradation experiments and analyzed for various intermediates using High Performance Liquid Chromatography (HPLC). At the middle of the biodegradation experiments some considerable amount of hydroquinone, benzoquinone, catechol and organic acids such as oxalic acid,

maleic acid, acetic acid, formic acid and tartaric acid in very low concentrations of less than 5 mg/L, in all the flasks. However, no such intermediates could be detected at the end of the each experiment ensuring complete degradation of phenol by the culture. Fig. 4.8 is a typical illustration of the concentrations levels of the various intermediates obtained during biodegradation of phenol at 100 mg/L initial concentration.

4.2.2. Culture Growth and *m*-Cresol Degradation Kinetics

In the previous section, the potential of the culture to degrade phenol was studied. Further studies were aimed at investigating its potential to degrade more toxic phenolics such as *m*-cresol, and the present section reports the results obtained on the culture growth and *m*-cresol degradation as a single substrate.

4.2.2.1. Effect of Initial Concentration of *m*-Cresol

Similar to the phenol degradation profile, Fig. 4.9 shows the time profile of *m*-cresol degradation by the culture. It is evident from the profile that the time taken by the culture to degrade *m*-cresol was dependent upon its initial concentration. For example, while the culture took only about 14 h for completely degrading *m*-cresol when its initial concentration was 100 mg/L, it, however, needed about 136 h for degrading an initial concentration of 900 mg/L. The time profile of *m*-cresol degradation revealed that the whole degradation process could be divided into two-phases: an initial lag phase and an active degradation phase (Fig. 4.9). The degradation rates were thus calculated from the corresponding slopes of curves obtained during active *m*-cresol biodegradation, which normally followed a lag phase in its degradation (Fig. 4.9). A maximum degradation rate could be achieved at an initial concentration of 300 mg/L;

concentrations either below or above 300 mg/L yielded lesser degradation rates indicating a strong influence of *m*-cresol initial concentration on its degradation rate. Similar observation was reported by Yan et al. (2006) in their study involving biodegradation of *m*-cresol by *Candida tropicalis*, where a maximum *m*-cresol biodegradation occurred at an initial *m*-cresol concentration of 280 mg/L. But contrary to the effect of initial concentrations of phenol on its degradation rate, the maximum degradation rate of *m*-cresol was affected even at its lesser concentrations.

Growth of the culture also followed a similar pattern with that of the degradation of *m*-cresol. This fact is illustrated in Fig. 4.10, where biomass growth (OD_{600}) of the culture is plotted against time for various initial concentrations of *m*-cresol in the media. It is observed that there was no lag phase during the culture growth for *m*-cresol concentrations between 100 mg/L and 300 mg/L; however, a lag phase was evident at its concentration greater than 500 mg/L. Such lag in the culture growth above certain concentration may be highly attributed due to *m*-cresol being more toxic compared to other compounds like glucose and phenol used in the study. Moreover, as the *m*-cresol concentration was increased in the media, the culture took more time (14 h at 100 mg/L vs. 136 h at 900 mg/L) to exhibit a complete growth. The specific growth rates (μ) at various initial concentrations of *m*-cresol were calculated as per the Eqn. (2.15).

When μ was plotted versus initial *m*-cresol concentrations, there was an increase in μ value of the culture for *m*-cresol concentrations below 200 mg/L and above this concentration, the μ value declined progressively. This behavior, synonymous with that of the phenol effect, clearly indicated substrate inhibition on the growth of culture. The same has been reported by other authors, as well (Kumar *et al.*, 2005;

Rodriguez *et al.*, 2006; Yan *et al.*, 2006). Further, on line with phenol degradation study, specific substrate degradation rate due to *m*-cresol, was calculated using the Eqn. (4.1). Fig. 4.11 illustrates the two rates *viz.*, specific growth and degradation rates correlate well with each other at different initial *m*-cresol concentrations. In order to formulate the patterns of *m*-cresol degradation and culture growth and to estimate necessary biokinetic parameters in the system, kinetics of these two phenomena was analyzed by fitting the data to various substrate inhibition models.

4.2.2.2. Modeling the Kinetics of *m*-Cresol Biodegradation

The time profile of *m*-cresol biodegradation, at its different initial concentrations, was fitted to growth associated and non-growth associated kinetic models, as before for phenol. This procedure has been used by Schmidt *et al.* (1985) and Alexander (1999) to describe degradation of organics by microorganisms.

Out of these seven different models tested, only the non-deterministic three- half-order kinetic model fitted the data well with coefficient of determination (R^2) values greater than 0.97. It is to be noted that phenol degradation was also fitted best with three-half order kinetic model as described in the previous section. As both phenol and *m*-cresol are phenolic compounds, their degradation kinetics seem to follow similar pathways. The above observations further substantiate the fact that a three-half-order model containing zero, first and second order rate would be an ideal candidate to fit such two-phase kinetics (Brunner and Focht, 1986).

4.2.2.3. Modeling the Kinetics of the Culture Growth

As both the rates of specific growth (μ) and *m*-cresol degradation (q) were observed to follow substrate inhibition phenomenon at higher concentrations of the substrate,

attempts were made to formulate the kinetic behavior using deterministic models, described in Chapter 2. The model equations were solved using nonlinear regression method in MATLAB[®] 7.0. Fig. 4.12 shows the specific growth rate computed from experimentally obtained data as well those predicted by the different models. Similarly, Fig. 4.13 compares the specific degradation rate obtained from the experiments and model predictions. Table 4.6 and 4.7 present the biokinetic constants estimated from the models along with RMS error between the experimental and model predicted rates. All these modeling results clearly depict the performance of the models in predicting the experimental data quite closely. The table also shows the parameters K_s and μ_{\max} obtained using the linearized form of Monod's model. While the estimated K_s value due to this model was slightly higher than those estimated by the substrate inhibition models; however, μ_{\max} value was comparable. This observation is quite obvious owing to the fact that the Monod's is a growth model whereas Haldane's and Han-Levenspiel models are substrate inhibition models. It appears from the Figs. 4.12 and 4.13 that the predicted specific growth rates by the models are only approximate, and from the RMS error values (Table 4.6), it is apparent that the models due to Haldane, Luong, Edward and Han-Levenspiel were the best fit to the experimental data. Haldane model accurately predicted the substrate inhibition constant (K_i), above which the specific growth and substrate degradation rates decline. In general, a high value of inhibitory constant in any microbial system means that the microbes are capable of sustaining and growing at a high substrate concentration level, and hence, the value obtained in the present study reveals that the culture is highly efficient to grow and degrade a high concentration of *m*-cresol in wastewaters. Han-Levenspiel and Luong models predict yet another biokinetic constant value of important significance - critical substrate concentration (S_m) value -

at which critical growth rate falls to zero. In the present study, the value for *m*-cresol was estimated to be ~ 900 mg/L, however this value was observed to be different from that obtained in the experiments. It is to be mentioned here that while attempting to compare the model parameter values in the study, no other relevant studies were found in the literature that used *m*-cresol as the sole carbon source and a mixed culture for its degradations.

From figures 4.3 and 4.9 referring to degradation profiles of phenol and *m*-cresol by the individually acclimatized mixed culture to degrade the phenolic compounds, it could be observed that the time taken by the culture to degrade low concentrations (100 - 300 mg/L) of the two phenolics in the respective media were almost comparable. And the culture took more time to degrade *m*-cresol than phenol only when it was presented at concentrations particularly above 400 mg/L. But both the models have predicted a higher maximum specific degradation rate for *m*-cresol than phenol, which should have, however, been similar to both the compounds. This could be attributed mainly due to a slightly poorer fit of the model in case of *m*-cresol compared to that of phenol, as also revealed from figures 4.7 and 4.13, respectively. It is worth mentioning here that the models for explaining specific degradation of the compounds in the study were derived from models that were originally developed for describing specific growth kinetics of microorganisms growing on a substrate by simply replacing the terms representing growth parameters in the original model with terms representing degradation of the substrate(s). Therefore, it also appears that the models used in the study to describe specific degradation of the individual compounds need more refinement in terms of the estimable kinetic coefficients which could be explored as a future research prospect.

4.2.3. Culture Growth and Mixed Substrates Degradation Kinetics

4.2.3.1. Simultaneous Degradation Profiles of Phenol and *m*-Cresol

From the results of the previous sections on single substrate systems, it is evident that the culture took longer time to degrade *m*-cresol in comparison to phenol. The single substrate system revealed some comparative performance of the microbial culture to degrade two different phenolics, where affinity of the culture towards degrading a high phenol concentration was shown. However, it is quite likely that in a mixed substrate system the culture may exhibit various other phenomena such as preferential utilization of a substrate, interaction between substrates, effects of concentration ranges of one substrate on the degradation of the other etc. Hence, a series of biodegradation experiments with the mixed substrate media, containing both phenol and *m*-cresol at different concentrations, were performed. The biodegradation patterns of the two substrates, in two different concentration ranges (low and high), are presented in Figs. 4.14 and 4.15. It is observed that in all the cases of biodegradation the microbial culture took longer duration to degrade *m*-cresol completely as compared to phenol. Further, while phenol did not show any lag phase during its degradation, in either low or high initial concentration ranges, a lag phase is observed during *m*-cresol degradation. The lag phase was significant particularly in the high concentration range of *m*-cresol.

Moreover, the degradation patterns of individual substrates in the mixed substrate system differed considerably with those obtained in the single substrate systems (Pakshirajan *et al.*, 2008). Irrespective of the concentration levels of the two substrates, phenol was preferentially degraded over *m*-cresol. This could be attributed to the fact that phenol being a simpler carbon source than *m*-cresol. However, this

preferential uptake of phenol was observed only at its higher concentrations. At lower concentration ranges of the substrates, the total time taken by the microbial culture for simultaneous degradation of the substrates was nearly the same.

Bai et al. (2006) studied the biodegradation of phenol and *m*-cresol as mixed substrate using *Alcaligenes faecalis* and observed that both phenol and *m*-cresol, in the range of 50 mg/L to 150 mg/L, were consumed simultaneously and a rapid degradation of *m*-cresol took place towards the depletion of the phenol in the medium - a phenomenon very similar to that observed in the present study. Yan et al. (2006) studied mixed substrate biodegradation with the yeast *C. tropicalis* and reported that the presence of phenol at low concentrations (60 – 100 mg/L) enhanced the rate of *m*-cresol biodegradation. A similar effect was observed in the present study, however, at a phenol concentration of 100 mg/L and *m*-cresol concentration of 200 mg/L.

4.2.3.2. Growth of the Culture in the Mixed Substrate System

Biomass profiles obtained at all combinations of initial concentrations of the phenolics are presented in Fig. 4.16 in the form of OD₆₀₀ of the culture. It is clear from the figure that the culture took more time to grow when *m*-cresol was present in the media (together with phenol) at high concentrations (> 600 mg/L); nevertheless, the cell mass output was also high in such cases (Bai *et al.*, 2006). The observation on the biomass profile of the culture in the mixed substrate system differed considerably with the patterns observed in the single substrate system. This phenomenon is, however, quite obvious due to more availability of carbon source in the medium. These observations were in agreement with those of Bai et al. (2006), who studied similar mixed substrate effect on the growth of *Alcaligenes faecalis*. Moreover a lag phase was observed beyond certain concentrations of *m*-cresol (200 mg/L) and phenol

(300 mg/L) probably due to more toxicity of the medium when these compounds were present together compared to their individual presence.

4.2.3.3. Statistical Analysis of the Specific Growth Rate of the Culture

The experimental data on the culture growth at various combinations of initial concentrations of the substrates were used for calculating the specific growth rate of the culture, and Table 4.8 presents the data obtained at low and high initial concentration ranges of phenol and *m*-cresol. The table shows that the specific growth rate was high in the low concentration ranges, whereas these values were very low when the concentration ranges of the substrates were high. This finding confirms the fact that substrate inhibition on the culture growth occurs only in the high concentration ranges of the substrates. Statistical analyses in the form of analysis of variance (ANOVA) and Student's 't' test were performed based on the above results. This analysis was done mainly to interpret the individual roles played by the two substrates, and to model the variation in specific growth rate due to these factors. This was felt necessary because although literature is replete with mechanistic models that deduce the interaction effects between any two substrates on growth rate of microorganisms, there exists hardly any study, which deals with such type of statistical analysis that is proving useful for clear understanding of the main and interaction effects between the substrates in such type of mixed substrate degradation systems.

Analysis of Variance (ANOVA)

ANOVA of the culture specific growth rate, at low and high initial concentration ranges of the substrates, are presented in Tables 4.9 and 4.10 respectively. In general

terms, ANOVA explains any variation in the statistically derived model and significance of the model parameters. The model parameters are the main effects, interaction effects and error term. The significance of these model terms is represented by Fischer F and associated P values. The other items in ANOVA table are degrees of freedom (df), sum of squares (SS) and mean squares (MS). Normally, large F and low P values of a model term indicate good significance of the term over others. In this study, both the models were able to explain the experimental results on specific growth rate accurately with a very less probability of only 5% variation in the results (*i.e.*, at 95% confidence level).

From Table 4.9, it is observed that, when the variation in specific growth rate of the culture at low concentration ranges of the substrates is considered, the interaction effects between substrates in the model are more significant than their main effects. However, at high concentration ranges of the substrates, neither the interaction effect between the substrates nor the main effects seem to play a major role on the specific growth rate of the culture (Table 4.10). Also, low F values of the error term in both the models, presented in these tables, indicate that the significance of error in the experiments is almost negligible.

Regression Analysis and Student 't' Test

The experimental data on specific growth rate as a function of concentrations of substrates were subjected to statistical regression analysis. As a result, the following regression equations were obtained for each of the two concentration ranges adopted in the study:

$$\mu_{low} = 0.5858 + 0.0539C_{m-cresol} + 0.0668C_{phenol} - 0.1219C_{m-cresol}C_{phenol} \quad (4.7)$$

$$\mu_{high} = 0.1240 - 0.1357C_{m-cresol} - 0.1342C_{phenol} + 0.1213C_{m-cresol}C_{phenol} \quad (4.8)$$

The above equations are second order polynomial equations with concentrations of phenol (C_{phenol}) and *m*-cresol ($C_{m-cresol}$) as the independent variables and the culture specific growth rate as the dependent variable. The substrate levels are in coded units *viz.* -1, +1. Results of Student 't' test on the specific growth rates, at low and high initial concentration ranges of the substrates, are presented in Tables 4.11 and 4.12, respectively. From the Student 't' test results, it was observed that the coefficient of interaction between the substrates in low concentration range is highly significant at 95% confidence level (P value = 0.05), but negative (*i.e.* inhibitory to specific growth rate), with a *t*-value of -5.07. On the other hand, the coefficient of interaction effect between the substrates at high initial concentration range was found to have a positive *t* value of 1.99; however, the significance of this interaction effect was not high (P value = 0.185) which was in agreement with the ANOVA analysis.

Student 't' test on the main effects of the substrates at low initial concentration range revealed that the coefficient of main effect for phenol is more significant than that of *m*-cresol (P values = 0.109 and 0.154, respectively). However, in high concentration ranges of the substrates, the significance of coefficients of their main effects was low (P value = 0.156 each).

Figs. 4.17 and 4.18 illustrate the interaction effect plots between the substrates at low and high concentration ranges, respectively. In general, these plots are obtained by joining the responses at -1 and +1 levels of the factors and tries to signify any interaction between two factors involved in a study. It involves dependent variable

represented on the ordinate and one of the factors on the abscissa. Hence, two lines are obtained whose deviation from being parallel is related to the degree of interaction between the factors (Montgomery, 2004). Fig. 4.17 shows highly significant interaction between phenol and m-cresol on specific growth rate of the culture, where the 2 lines are completely non-parallel and cross each other well. In other words, the effect of one factor depends on the level of the other. Whereas in the high concentrations range of the substrates, the two lines in Fig 4.18 are relatively parallel to each other, which confirms that there exist least interaction between the substrates. These observations were also consistent with the findings of the student 't' test on interaction effects between the substrates.

4.2.3.4. Biomass Yield and Specific Degradation Rate of the Substrates

The experimental data on the substrate degradation at various combinations of initial concentrations of the substrates were further used for calculating the biomass yield and their specific degradation rates. The following equation was employed to calculate the biomass yield.

$$Y_{X/S} = \frac{X_M - X_0}{S_0 - S_M} \quad (4.9)$$

where, X_M and X_0 are the respective maximum and initial dry cell concentrations (mg/L) at time 0 and t (h), $Y_{X/S}$ is the biomass yield, S_0 and S_M are the total substrate (phenol + *m*-cresol) concentrations (mg/L) corresponding to time 0 and t (h) respectively in the medium. The total biomass yield values obtained in both the concentrations ranges of the substrates are presented in Tables 4.13 and 4.14.

It could be observed that the yield values are higher in low concentration ranges of the substrates than in higher concentration ranges. However, in both the concentrations ranges of the phenolics, the biomass yield value decreased with an increase in *m*-cresol concentration. Abuhamed et al. (2004) observed a maximum biomass yield value of 0.75 when benzene was used as one of the substrates in their mixed substrate media at its initial concentration of 700 mg/L; the culture used in their study was a *Pseudomonas putida* strain. In the present study, a highest yield value of 2.17 was obtained at a combination of 100 mg/L phenol and 100 mg/L *m*-cresol; a lowest value of 1.44 was obtained at a combination of 300 mg/L phenol and 400 mg/L *m*-cresol. Such high values of biomass yield, obtained in the present study, may be attributed to two factors: (1) mixed microbial culture was used for biodegradation rather than a single microbial strain and (2) phenol and *m*-cresol are relatively simpler carbon sources compared to volatile hydrocarbon substrate benzene. The values of biomass yield further confirm that the substrate inhibition of the culture occurred in their high concentrations ranges. Moreover, irrespective of the concentration levels of the substrates, the yield values saturated at high concentration ranges - the yield remained almost the same above 300 mg/L concentration of both the substrates.

Table 4.15 presents the individual values of substrate degradation rate (q) for both phenol and *m*-cresol obtained in this mixed substrate degradation study. The results show that in high concentration ranges of the substrates, phenol specific degradation rates were always higher than those of *m*-cresol, except when both the substrates were present in their low levels (-1). It is also observed that in the low concentration ranges relatively high specific degradation rates of the compounds were obtained.

However, within a given concentration range, particularly in their low ranges, a wide variation in the q values of both phenol and m -cresol was observed, which depended upon the combination levels of concentrations in each experimental run. The error in the study proved almost negligible as the three runs at their center point (0) levels yielded similar results for the q values of phenol and m -cresol in both the concentration ranges.

4.2.3.5. Sum Kinetics Model Fitting of Experimental Specific Degradation Rate

In order to identify the effect of interaction between the two substrates on their individual specific uptake rates, the experimental data was fitted to a sum kinetics model proposed by Yoon et al. (1977). However, the sum kinetics model was slightly modified, wherein the specific growth rate μ in the original equation was replaced with specific degradation rate q , as represented by Eqn. (4.10).

$$q = \frac{q_{\max,1}S_{1L}}{K_{S,1} + S_{1L} + \frac{S_{1L}^2}{K_{I1}} + I_{2,1}S_{2L}} + \frac{q_{\max,2}S_{2L}}{K_{S,2} + S_{2L} + \frac{S_{2L}^2}{K_{I2}} + I_{1,2}S_{1L}} \quad (4.10)$$

The interaction parameter $I_{i,j}$ indicates the degree to which substrate i affects the biodegradation of substrate j ; a large value of the parameter indicates a strong inhibition on the substrate uptake by microorganisms (Yoon *et al.*, 1977). The other kinetic parameters $q_{\max,j}$, $K_{S,j}$, K_{Ij} in the equation are the same as those for any single substrate system, *i.e.*, maximum specific degradation rate, half-saturation and inhibition constants due to substrate j in the medium. A non-linear regression technique was employed in solving the model equation in MATLAB 7.0. Appropriate constraints were set during the parameter estimation so that they are estimated as positive values. The results of model fitting yielded very high determination

coefficient (R^2) (0.99 for phenol and 0.98 for *m*-cresol) when different combinations of the two substrates were tried in their low concentration ranges. The following values of interaction parameters (I_{ij}) were thus obtained by solving the model equations:

$$I_{phenol(100\text{ mg/L})/m-cresol(100\text{ mg/L})} = -1.37$$

$$I_{phenol(100\text{ mg/L})/m-cresol(200\text{ mg/L})} = 1.322$$

$$I_{m-cresol(100\text{ mg/L})/phenol(100\text{ mg/L})} = 0.103$$

$$I_{m-cresol(100\text{ mg/L})/phenol(200\text{ mg/L})} = -0.36$$

While the interaction parameter $I_{phenol:m-cresol}$ represents the effect of phenol on *m*-cresol degradation, the other interaction parameter ($I_{m-cresol:phenol}$) represents the effect of *m*-cresol on phenol degradation. In general, a negative value of the interaction parameter denotes strong intensity of inhibition. Hence, it is inferred that 100 mg/L *m*-cresol was inhibitory to phenol degradation, when phenol initial concentration was 200 mg/L than when present low at 100 mg/L. Similarly the effect due to phenol on *m*-cresol degradation was also tend to be true. In literature, a maximum interaction parameter value of 5.16 has been reported for the effect of toluene on benzene degradation by a *Pseudomonas putida* strain (Abuhamed *et al.*, 2004). Again considering the fact that phenol being a relatively simpler and easily assimilable substrate than toluene and benzene, a large value of its inhibitory effect on *m*-cresol degradation is not unlikely. It was observed that the sum kinetics model failed to describe the degradation kinetics of the substrates in their high concentration ranges. Nevertheless, the observation that the mechanistic model failed to explain the mixed substrate degradation system by the culture could however, be substantiated from the interaction effect plots between the two substrates on specific phenol degradation rates, in their low and high concentration ranges (Figs. 4.19 and 4.20).

Fig. 4.19 shows high and significant interactions, where the lines are completely non-parallel and cross each other well. In other words, the effect of concentration of one substrate depends on the concentration of the other. On the other hand, the two lines in Fig. 4.20 are relatively parallel to each other, which confirm that there exists least interaction between the substrates at higher concentration ranges on phenol specific degradation rate. Similar observations were found for the interaction between the two substrates on *m*-cresol specific degradation rates as well.

4.2.4. Evaluation of the Culture to Treat a Refinery Effluent

After establishing the potential of the mixed culture in treating synthetic wastewater containing the phenolics, both in single and mixed substrate systems, in batch shake flasks, its capability to treat a real industry effluent was evaluated. The effluent was obtained from a petroleum refinery complex located at Guwahati, India. The general characteristics of the effluent, such as Chemical Oxygen Demand (COD), pH, Dissolved Oxygen (DO) and heavy metals (lead, chromium, nickel) were analyzed and are presented in Table 4.16. From the table, it is observed that heavy metals were less than 60 µg/L in concentrations, which could be quite acceptable to biological treatment systems, and therefore any further pre-treatment to remove the heavy metals was not felt necessary. However, pH was found to be 8.6, which denotes an alkaline nature of the effluent – unsuitable for bacteria like *Pseudomonas* spp. to grow. Hence, pH of the effluent was neutralized by adding 0.01N sulfuric acid to suit the growth and activity of the culture in the study. In general total solid content of any wastewater is sum total of dissolved and suspended solids. A major portion of the refinery wastewater contains suspended organics that constitutes the suspended solids portion which is nearly 5000 mg/L with a range varying anywhere between 1956 and

14448 mg/L (Punima and Jain, 1998). In the present work, no attempt was made to remove these total suspended solids before measuring the initial COD of the raw wastewater. For that matter, no pre-treatment of the raw wastewater was performed, which could have resulted in a very high COD value 10000 mg/L. However, some pretreatment of raw wastewater was performed after adjusting the pH but before measuring the COD for biological treatment using the mixed culture. That has resulted in drastic reduction in the COD. It has occurred mainly due to the above mentioned pre-treatment step where suspended solids were filtered out after performing pH adjustment. The updated COD following pre-treatment was thus measured to be 4800 mg/L, is value that is still typical of influent wastewater in any biological treatment systems. Fig. 4.21 shows the COD removal profile by the culture as a function of time, which shows that the culture took only maximum of almost 4 days to completely detoxify the wastewater. Hence, it could be surmised that the culture is highly potent to treat real industrial wastewaters, as well.

It is a well known fact that microorganism capable of degrading a toxic/recalcitrant compound can degrade another less toxic compound relatively easily. In this feasibility study to reduce COD of the pH adjusted wastewater, the mixed culture used was initially acclimatized to grow and degrade *m*-cresol up to a maximum concentration of 1000 mg/L, which is so far known to be the most recalcitrant among the phenolic compounds. Hence, for the *m*-cresol acclimatized culture to degrade any other organics - less toxic than *m*-cresol and normally present in such refinery wastewaters – may not require further acclimatization. This phenomenon could well be used to explain the relative easiness with which the mixed culture could reduce the initial COD of the pH adjusted wastewater within 90 h in batch shake flasks although the wastewater may contain organics, other than phenol and/or *m*-cresol. However,

more investigations on the exact nature of organics present in the wastewater may further help substantiate this observation.

In order to further extend the scope of this mixed culture in treating phenolics, studies were aimed at scaling up the degradation process from a simple batch shake flasks to laboratory scale reactor. The result of the reactor studies on degradation of phenolics by the culture is discussed further. Also to compare the efficiency of the culture to degrade phenol with that of an emerging advanced oxidation process, results obtained using a solar photo catalytic reactor are also presented and discussed in the following sections.

4.3. Performance of Batch Stirred Tank Reactor in Degrading Phenol

In our previous section, phenol degradation by the culture revealed 100% degradation efficiency of phenol upto a maximum initial concentration of 800 mg/L within 69 h of culture. However, experiments in that study were performed in batch shake flasks of 250 mL capacity with a working volume of only 100 mL. To establish the potential of the culture in higher scale phenol degradation, further study was undertaken with an objective of investigating the kinetics of phenol degradation and growth of the culture in a simple Batch Stirred Tank Reactor (BSTR) of higher volume.

4.3.1. Effect of Initial Phenol Concentration on the Culture Growth and its Degradation

Figs. 4.22 and 4.23 show time profiles of phenol degradation and biomass growth during the batch reactor experiments. As observed earlier in case of batch shake flasks study, the amount of time taken by the culture to degrade phenol was dependent on its initial concentration in the reactor.

It is observed that concentration of phenol, between 100 and 300 mg/L, did not show any lag phase in the culture growth, but the amount of biomass was found to be less as compared to when grown at phenol concentration of 400 mg/L. Further in this concentration range (100 - 300 mg/L), a stationary phase in the culture growth was evident, which depended on the initial concentration of phenol. For example, at 300 mg/L of initial phenol concentration, the time taken by the culture to reach stationary growth phase was higher than that at lower initial concentrations of phenol. A striking feature in this BSTR was that the inhibition to the culture growth was distinct at 400 mg/L of phenol concentration and the culture took much longer time (~ 194 h) for its growth and complete phenol degradation. In comparison to the results of the biodegradation study in shake flasks, this time taken by the culture is found to be much higher. Moreover, the amount of biomass produced in the BSTR was also less compared to that in the shake flask study. It should be mentioned here that for a fair comparison between the two studies, *i.e.* shake flasks and BSTR, agitation was ensured in the systems (in the case of BSTR, agitation was provided by mechanical stirring as mentioned in materials and methods). Despite maintaining the stirring rate and other controlling parameters such as the amount of inoculum (%) and temperature in this reactor study, the time taken in this scale up study was considerably longer than in the previous shake flasks study. This large difference in degradation time could probably be attributed to the fact that aeration demand by a relatively large-scale system is much higher than by a small shake flask. An optimum stirring in shake flasks not only improves the contact between substrates and the microbes but also provides proper aeration in the system. This particular aspect of proper aeration in the BSTR could have therefore, limited the performance of the culture, which lead to

further investigation on estimating the biokinetic constants to confirm the poor performance in this reactor system.

4.3.2. Modeling the Culture Growth and Phenol Degradation Kinetics

As before for single substrate system study in batch shake flasks, growth associated and non-growth associated kinetic models (Schmidt *et al.*, 1985) were employed to describe the degradation of phenol in the BSTR. The forms of these models and their validity, in relation to initial substrate concentration, S_0 , and half-saturation constant, K_s , are given in Chapter 2. Among the six different models tested, only the non-deterministic zero order kinetic model could fit the data well with coefficient of determination (R^2) values greater than 0.97 at and above 200 mg/L initial phenol concentration, whereas the other growth associated model yielded low coefficient of determination (R^2) (*i.e.* < 0.75). However, for the initial phenol concentration of 100 mg/L, the zero order model fit was only slightly accurate, as determined by R^2 value ($= 0.79$). This poor fit is due to the fact that the zero order kinetic model is best valid for values of $S_0 \gg K_s$; however, K_s in this study, as presented later, was found to be ~ 40 mg/L. All the other non-growth associated models resulted in poor fits with R^2 values less than 0.5 at all the initial concentrations of phenol.

In order to further relate the pattern of phenol degradation with the culture growth in the system, kinetics of these two phenomena were analyzed. This was achieved by calculating the specific growth rate (μ) and specific substrate degradation rate (q) from the biomass output and phenol degradation profiles, respectively, and using the equations described in chapter 2. Fig. 4.24 illustrates a plot of the specific rates of culture growth and phenol degradation calculated at various initial phenol concentrations in the media. Both these rates declined after an initial rise, hence

revealing substrate inhibition characteristics due to higher phenol concentration in the system (Wang and Loh, 1999).

The previously tested Haldane and Han-Levenspiel model equations were applied to the data to describe the substrate inhibition pattern by using nonlinear regression method using MATLAB[®] 7.0. However, for applying the models to estimate the specific substrate degradation rates, the term μ was replaced with q and then solved. The fitness of these models is depicted in Figs. 4.25 and 4.26 respectively. The biokinetic constants of growth of the culture along with Root Mean Square RMS error between experimental and model values are presented in Table 4.17.

Between the two models, Haldane model seemed to fit the data quite accurately than the Han –Levenspiel model (Fig. 4.26 and Table 4.17). Nevertheless, both the models indicated, by their estimated biokinetic constants values, that the phenol degradation as well as biomass growth in the system were not appreciable enough relative to the those in the batch shake flasks.

Overall, it could be said that though the culture had a good potential to degrade phenol, the geometry of the BSTR probably affected the degradation potential of the culture during scale up. This shortcoming was envisaged to be overcome by adopting an appropriately designed bioreactor, which will ensure proper but non-vigorous mixing as well as sufficient aeration in the system. Airlift reactor (ALR) was chosen as an ideal reactor to satisfy this criteria apart from being simple in construction, easy in operation, perfect geometry for mixing thus aiding in good mass transfer between gas and liquid phase. An Internal Loop ALR was therefore fabricated for further evaluation of the culture in degrading phenolic compounds. Prior to biodegradation experiments in the ILALR, hydrodynamic studies such as residential time distribution

(RTD), liquid circulation, bubble diameter and mass transfer studies were carried out and their results are given in section 4.5. Because, it is also intended to do a comparative study on the performance of the present biological method in phenol degradation with some other emerging non-biological method - solar photocatalysis - was chosen, which is one of such popular methods for degrading phenolic compounds. The next section of this chapter briefly deals with a study on solar photocatalysis treatment of phenol containing synthetic wastewater and its comparison with phenol biodegradation by the mixed culture.

4.4. Solar Photocatalytic Degradation of Phenol by TiO₂-Based Heterogeneous Catalyst

The study aims at investigating the merits of phenol degradation by means of solar photocatalysis and compares its performance with that of biodegradation by the culture. Photocatalytic experiments in this study were carried out using titanium dioxide (TiO₂) as the photocatalyst. Among the available photocatalyst, TiO₂ has been proven to be the most suitable for widespread environmental applications. Also TiO₂ is biologically and chemically inert, stable to photo and chemical corrosion and inexpensive too. Furthermore, TiO₂ is of special interest since it can use natural (solar) UV radiation. This is because TiO₂ has an appropriate energetic separation between its valence band (VB) and conduction band (CB), which can be surpassed by the energy of a solar photon. The VB and CB energies of the TiO₂ are estimated to be +3.1 and -0.1 volts, respectively, which means that its band gap energy is 3.2 eV and therefore absorbs in the near UV light situation ($\lambda < 387$ nm). Although ZnO seems to be a suitable alternative to TiO₂, it dissolves in acidic solutions and hence cannot be used for technical applications (Bahnemann *et al.*, 1991). Other semiconductor particles

(e.g. CdS or GaP) absorb larger fractions of the solar spectrum than TiO_2 and can form chemically activated surface-bond intermediates, but unfortunately, such catalysts are degraded during the repeated catalytic cycles usually involved in heterogeneous photocatalysis.

Degussa[®] P-25 is one of the well-known and widely used TiO_2 available worldwide for various commercial applications. However, it is expensive and needs to be imported for regular use in Indian industries. Hence, the present study utilized yet another TiO_2 that is inexpensive and easily available in local market in India, whose photocatalytic efficiency and other physical parameters such as crystallite grain size, particle size distribution and BET surface area could be comparable with those of Degussa P-25 catalyst. Anjatox[®] TiO_2 is such indigenous brand manufactured by Travancore Titanium Products, India and is commonly used in textile and pharmaceutical industries in India. The main advantage of Anjatox[®] TiO_2 is its easy availability and lower cost than Degussa P-25[®]. This section presents lab scale treatment of phenol with the said TiO_2 products viz. Degussa P-25[®] and the Anjatox[®] (anatase grade), and compares their performance in terms of phenol degradation activity.

4.4.1. Characterization Results of the Photocatalysts

X-Ray Diffraction Analysis

The results of X-ray diffraction (XRD) analysis of Anjatox[®] and Degussa P-25[®] TiO_2 are shown in Figs. 4.27 and 4.28 respectively. The results were well comparable with each other. The width of the peak obtained for Degussa P-25[®] TiO_2 is narrower than that of the Anjatox[®] TiO_2 . Implying that the crystalline structure of Degussa P-25[®]

TiO₂ is less than that of Anjatox[®] TiO₂. The crystalline grain size of the catalysts was determined by using the Scherrer's formula, given in Chapter 3.

The crystallite size of Anjatox[®] TiO₂ was found in the range of 55-60 nm. On the other hand, Degussa P-25[®] TiO₂ had smaller crystalline structure of only 21 nm (Vione *et al.*, 2005). The intensity of the X-ray was much higher for Anjatox[®] TiO₂ than that of Degussa P-25[®] TiO₂, which further confirms the fact that Anjatox[®] TiO₂ is highly crystalline in nature whereas the Degussa P-25[®] TiO₂ is relatively amorphous in nature.

Particle Size Distribution

Figs. 4.29 and 4.30 show the particle size distribution of the catalysts. It is observed that the size distribution is almost uniform for Degussa P-25[®] TiO₂ compared to that of the Anjatox[®]. Vione *et al.* (2005) studied the particle size distribution of Degussa P-25[®] TiO₂ and reported that the particle size was in the range of 0 – 0.2 μm, whereas in the present study it is observed that the particle size distribution lies between 0.2 and 89 μm and had a uniform distribution. The reason for this difference in particle size distribution for the same photocatalyst material is largely unknown. For Anjatox[®], the particle size distribution was found to be uniform, but had a bimodal nature of distribution. Most of the particles were in the range of 0.1 to 101 μm i.e. almost similar to that of Degussa P-25[®] TiO₂.

Catalysts Surface Area

Analysis of the catalysts surface area using the BET surface area analyzer revealed that Anjatox[®] had a larger surface area than Degussa P-25[®]. The surface area of the

catalysts was determined by adsorbing liquid nitrogen on its surface. The values of surface area for Degussa P-25[®] TiO₂ was found to be 65 m²/g, whereas that of Anjatox[®] was 10.6 m²/g.

4.4.2. Effect of Photocatalyst Concentration on Phenol Degradation

Fig. 4.31 shows the effect of catalyst loading of Anjatox[®] and Degussa P-25[®], respectively on phenol degradation at 100 mg/L initial concentration. The catalyst loading for Anjatox[®] was varied from 3 to 18 g/L and it was observed that the maximum phenol degradation efficiency was 50 % at 9 g/L of the catalyst, which was found to be optimum for phenol degradation. Similarly, for Degussa P-25[®] the catalyst loading was varied from 1 to 4 g/L. It was observed that the maximum degradation is 90% with 3 g/L of the catalyst. All these experiments were carried out simultaneously for a period of 10 h so as to provide identical environmental conditions, particularly intensity of solar radiation. Only the catalyst loading was in these runs and the phenol concentration was held constant at 100 mg/L. While Degussa P-25[®] was found slightly more active at its low concentration, Anjatox[®] resulted in high phenol degradation at its high concentrations. This behavior can be attributed to lower scattering of radiation by Anjatox[®] when compared with Degussa P-25[®]. Differences in substrate degradation rates under photocatalytic conditions can also be due to different charge-carrier dynamics (Vione *et al.*, 2005).

4.4.3. Effect of Initial Concentration of Phenol

Using the above found optimum catalyst loading of 9 g/L of Anjatox and 3 g/L of Degussa P-25 catalysts, effect of initial phenol concentration on its degradation by the respective photocatalytic reactor systems was investigated. Figs. 4.32 and 4.33

illustrates this effect on the photocatalytic reactor performance employing either Degussa P-25 or Anjatox. It was observed that the photoreactor employing Anjatox is capable of degrading only very low initial phenol concentration of 50 mg/L, but within 7 h. On the other hand, the reactor with Degussa P-25 catalyst indicated a slightly better result in degrading this concentration, where only 5 h was required. It has been studied by many researchers that the Degussa P-25[®] (Zhang *et al.*, 2001; Vione *et al.*, 2005) has a higher photocatalytic activity than that of any other catalyst of the similar grade. Nevertheless, concentrations above 50 mg/L were not completely degraded at all by using either of these two photocatalyst even after 10 h.

4.4.4. Analysis of Intermediates during Phenol Degradation

Photocatalytic oxidation is known to yield certain intermediates when phenol is oxidized by solar UV rays (Alnaizy and Akgerman, 2000). The samples collected at regular intervals were analyzed for the intermediates in HPLC. Considerable amount of hydroquinone, benzoquinone, catechol and organic acids such as oxalic acid, maleic acid, acetic acid, formic acid, citric acid and tartaric acid were found in the analysis. The various intermediates analyzed are shown in the Fig. 4.34 along with their concentrations. It was also observed from the this analysis that phenol undergoes transformation through these intermediates and finally converted to CO₂ and H₂O (Alnaizy and Akgerman., 2000; Kubo *et al.*, 2005). The concentration of the obtained intermediates were less than 10 mg/L, which were slightly higher than those quantified in the middle of the biodegradation experiments in batch shake flasks. It is to be emphasized here that no such intermediates could be, however, detected at the end of the biodegradation experiments.

In this photocatalytic study, phenol degradation by the catalyst showed poor degradation efficiency in contrast with the biodegradation by the mixed culture. Moreover, a complete degradation of phenol could not be achieved even at concentrations less than 200 mg/L. Overall, solar photocatalytic degradation may be considered as a poor alternative to biological degradation using the mixed microbial culture.

4.5. Biodegradation of Phenolics in Internal Loop Airlift Reactor

This section aims at exploring the capability of the Internal Loop Airlift Reactor (ILALR) in biodegradation of phenolics and finding the merits and demerits of such operation in comparison to the batch shake flasks and BSTR studies. The goal of this study was also to evaluate the scale-up option between BSTR and ILALR. With the help of such scale-up study, it is possible to analyze the scenario where one can avoid the demerits of one reactor and retain the merits of the other to achieve successful treatment objective.

4.5.1. Hydrodynamics and Mass Transfer Studies

In general, the biodegradation process occurring in a bioreactor depends on the mass transfer rates of substrate(s), oxygen etc., and in turn the transport of mass depends on the hydrodynamic conditions in the reactor. These hydrodynamic conditions largely rely on several factors like reactor geometry, residence time, mixing, bubble diameter, aeration etc. Hence, basic understating of such hydrodynamics becomes necessary for any reactor system to be operated successfully. This section describes the results of hydrodynamics and mass transfer studies with the ILALR.

4.5.1.1. Residence Time Distribution (RTD)

As detailed earlier, the RTD experiments were carried out by passing distilled water in a continuous loop fashion through the riser and downcomer section of the reactor. Compressed air was introduced at the bottom of the riser section. Thereafter, a pulse of tracer 0.01N KCl was injected along the liquid flow at the reactor entrance, and within a short period of time the tracer became evenly distributed throughout the reactor. The concentration of tracer at the reactor outlet was regarded as a measure of the hydrodynamic conditions in analyzing the pattern of liquid flow within the ILALR (Jamshidi *et al.*, 2001)

Fig. 4.35 shows the results of the RTD experiments in the ILALR for various airflow rates. The figure indicates that the overall patterns of RTD in the reactor at all the airflow rates are similar. Mixing time within the ILALR was also calculated from these RTD results, and it is evident that any increase in gas flow rate promoted mixing, thereby decreasing the over all mixing time in the reactor (Fig. 4.35). The RTD profiles also ascertained that the tracer concentration in the ILALR attained uniformity within 5-10 s in all the experiments. And an airflow rate of 2 L/min was found to be optimum in the reactor providing good mixing and aeration. This flow rate was therefore chosen as an ideal setting for further hydrodynamics characterization of the reactor and in biodegradation experiments with the reactor.

In the literature, few relevant RTD studies with ILALR have been reported. Gowthaman *et al.* (1991) performed RTD behaviors in cylindrical and tapered reactors by varying the superficial gas flow rates between 1.7 to 6.8 dm³/min. In order to study whether the flow is either bypassed or remains stagnant or both inside the reactor, the authors analyzed the tracer concentration by converting it into

dimensionless age distribution (rather than using directly). They also observed that the cylindrical and the tapered reactors have some dead space and therefore allowed bypass of the feed. Korpijarvi et al. (1999) studied hydrodynamics in an airlift reactor using NaOH as the tracer. They performed the tracer analysis in both riser and downcomer section at a superficial gas flow rate of 220 L/h and observed that the riser section took 150 s for attaining uniform concentration; whereas, the downcomer section took a maximum time of 250 s. Jamshidi et al. (2001) studied the RTD of liquid in a jet loop bioreactor by varying the superficial gas flow rate between 3000 and 50000 cm³/min, and attained a uniform distribution of the liquid with in 2-6 s. Kelvin et al (2004) investigated the mixing characteristics of an airlift reactor and its individual sections were assessed from the pecllet's number and dispersion coefficient.

During this RTD study, diameter of air bubbles in both riser and downcomer sections of the ILALR was analyzed by taking snapshots (Fig.4.36) of the reactor during its operation. Average diameter of the bubbles was 1.6 cm in the riser section and 0.35 cm in the downcomer section. It is understood that bigger the diameter of the bubble in the riser section, lower is the mass transfer rate inside the reactor. This fact is also reflected in the $k_L a$ value for the non-living system, which is discussed further

4.5.1.2. Volumetric Oxygen Mass Transfer Coefficient ($k_L a$) in the ILALR

.Transfer of oxygen is a major concern in any microbial process requiring oxygen for its growth. Aeration in any biological process is directly related to the oxygen transport from gas phase to liquid phase followed by oxygen uptake by the microbes. The activities of microbes are very often monitored by utilization of oxygen from supplied air. Hence, evaluating the volumetric oxygen mass transfer in any bioreactor is of great importance.

In this study, volumetric oxygen mass transfer coefficient in the reactor was estimated by the dynamic gassing out method and by measuring the dissolved oxygen (DO) concentration in the reactor. A step change in the DO concentration is provided in the inlet gas and the DO is measured periodically. Following equation gives a mass balance on the DO concentration in the system (Kamp *et al.*, 1987):

$$\frac{dC_L}{dt} = k_L a (C_e - C_L) \quad (4.11)$$

where, C_e is the liquid phase oxygen concentration in equilibrium with the gas phase (mg/L), C_L is the concentration of DO in the liquid (mg/L). When $\{-\ln(C_e - C_L)\}$ is plotted against time, $k_L a$ per unit volume corresponds to slope of the plot. Compared to changes in C_e , which is a function of bubbles in the ILALR, the variations in C_L can, however, be followed more accurately with a rapid response DO probe. Because the oxygen transfer rate (OTR) is usually negligible in comparison with the gas flow rate and also that diffusion in gas phase is much faster than in liquid phase, C_e is generally taken as 100% saturation for air (Kamp *et al.*, 1987). In this dynamic gassing out method for $k_L a$ evaluation, two different inert gases *viz.* argon and nitrogen were used to flush out the initial DO content in the reactor. Also the $k_L a$ was determined without the use of any inert gas.

$k_L a$ Estimation Involving a Non-living System in the ILALR

The $k_L a$ in the ILALR was first determined by using distilled water as the non-living system. A plot of C_L as a function of time using the inert gas is depicted in Fig. 4.37. The obtained profile is well comparable with the literatures (Kamp *et al.* 1987; Vandu *et al.*, 2005). The calculated $k_L a$ almost had similar value for both the cases of inert

gases, which was 0.004 s^{-1} . Jin et al. (2006) also showed that irrespective of the nature of inert gas utilized, the value of k_{La} remains largely unaffected. However, in comparison with the literature, the obtained k_{La} value is found to be low (Kamp *et al.*, 1987; Jamshidi *et al.*, 2001; Vandu *et al.*, 2005). This could be due to deployment of a single nozzle for air inlet into the ILALR, where else other researchers have studied k_{La} in their ILALR using diffuser type arrangement for air inlet. Moreover, the adopted inlet airflow rate was quite low. Fig. 4.38 presents k_{La} plot for the nonliving system at various superficial airflow rates. It is clear from the figure that increase in the gas flow rate caused an increase in the k_{La} value. This observation was also found to be valid by Jamshaidi et al (2001), where they evaluated the k_{La} for a jet loop bioreactor by varying the inlet flow rate between 50 and 350 mL/s. Due to the geometrical constraints of the designed ILALR in the present study, the superficial gas flow rate could not be increased beyond 3 L/min as it resulted in high turbulence leading to overflow of the contents from the reactor.

Estimation of k_{La} in the ILALR with a Living System

For a reactor with a living system such as microbes in liquid medium, when a step change is introduced, inlet gas concentration, *viz.* DO concentration depends on the Oxygen Transfer Rate (OTR) and the Oxygen Uptake Rate (OUR) by the microbes. This phenomenon is represented by the following mass balance equation (Kamp *et al.*, 1987):

$$\frac{dC_L}{dt} = k_L a (C_e - C_L) - (OUR) \quad (4.12)$$

Where terms in the equation are same as in the previous equation. A technique for determining both k_{La} and OUR, using a fast response oxygen probe, has been

developed by Bandyopadhyay et al. (1967). It contains two steps. Firstly, aeration is stopped and the OUR is determined from the rate of decrease of the DO concentration.

The second step is resumption of the aeration and the rate of increase of C_L is measured. Finally, the k_La value is calculated by rearranging the eqn. (4.11). Fig. 4.39 is the DO profile obtained in the reactor with the living system, which illustrates this two-step phenomenon. The k_La value calculated from the response curve by eqn. (4.26) was 0.017 s^{-1} . This k_La value closely matched with that of the literature (Kamp et al., 1987; Jin et al., 2006). Kamp et al. (1987) studied k_La values for an External Loop Airlift Reactor (ELALR) during fermentation of *Aspergillus fumigatus* and found it to be 0.016 s^{-1} . Jin et al. (2006) estimated k_La for an activated sludge system in an ILALR, and found it to vary from 0.005 to 0.065 s^{-1} for a superficial airflow velocity of 0.01 to 0.15 m/s .

4.5.2. Batch Biodegradation of Phenol and *m*-Cresol in the ILALR

4.5.2.1. Phenol Biodegradation and the Culture Growth

Fig. 4.40 shows the biodegradation profile of phenol at its different initial concentrations. It is observed from the figure that phenol at concentrations 100 , 200 , 300 , 400 and 600 mg/L were completely and quickly degraded by the culture within 10 , 15.3 , 17 , 27.3 and 47 h , respectively. The results clearly shows a very high ability of the bioreactor system in degrading phenol even at fairly high concentrations using the mixed culture. In literature Viggiani et al. (2006) reported that nearly seven days is required to degrade phenol at a maximum feed concentration of 450 mg/L in an ILALR using *pseudomonas stutzeri* OX1. Compared to this degradation time and

phenol concentration, the present system could be well said to be highly efficient for the purpose.

In addition to the phenol degradation profile, biomass growth in the reactor was also obtained during its operation; Fig. 4.41 shows the biomass profile in the ILALR. Both the biomass and phenol degradation profile at each initial phenol concentration could be found to correlate well with each other; an observation already noticed in the batch shake flask experiments. More importantly, the time required to degrade even a high phenol concentration of 600 mg/L by the culture in the ILALR was quite less in comparison to that in the batch shake flasks.

To better understand the pattern of the culture growth and phenol degradation as a function of initial phenol concentrations, specific growth and degradation rates were calculated. When these two rates were plotted against initial phenol concentration (Fig. 4.42), it revealed substrate inhibition due to phenol on the rates at feed concentrations above 300 mg/L. This observation is also very well similar to that of the batch shake flasks study. Viggiani et al. (2006) in their study observed that substrate inhibition commenced at phenol concentration 200 mg/L. Furthermore, biokinetic constants in the process were estimated by fitting the calculated specific growth rate (μ) data to the previously tested and more successful Haldane's substrate inhibition model by employing non-linear regression technique in MATLAB[®] 7.0. It was observed from the estimated biokinetic parameters that the value of maximum specific growth rate (μ_{max}) was 0.48 h^{-1} and the other parameters like K_s and K_i were found to be 171.2 mg/L and 294.7 mg/L, respectively. Needless to mention here that the Haldane's model indeed provided a good fit to the experimental data with a RMS error value of 0.025. In comparison to the batch shake flask study, these estimates are

found to be high, except that of K_i . Among these three parameters, μ_{\max} is known to have a higher significance since it represents the maximum culture growth for a given substrate. In other words, it could also refer to the potential of the microbial system in degrading the substrate effectively for its growth. Very often, it is also true that high growth of microbial culture in biological treatment process indicate its good potential in the process.

4.5.2.2. *m*-Cresol Biodegradation and the Culture Growth

Using *m*-cresol as the phenolic substrate, batch biodegradation experiments were also carried out in the ILALR at its various initial concentrations ranging from 100-400 mg/L. Fig. 4.43 shows the biodegradation profile of *m*-cresol as a function of time. The figure that the culture could degrade a maximum *m*-cresol feed concentration of 400 mg/L with in 36 h itself. However, at this concentration a lag phase in its degradation was evident probably due to the toxic effect of *m*-cresol at such high concentration, as also reasoned previously. Similarly, the culture biomass output, shown in Fig. 4.44, also exhibited the same effect at 400 mg/L *m*-cresol. Moreover, it was observed that the bioreactor system failed to degrade *m*-cresol at concentrations above 400 mg/L of *m*-cresol, which was contrary to that obtained in the batch shake flask study. In the batch shake flask study, the culture could degrade a maximum *m*-cresol concentration of upto 900 mg/L. Nevertheless, both the shake flask and ILALR studies show similar substrate inhibition pattern due to *m*-cresol on the culture growth. The substrate inhibition of *m*-cresol in the present study is depicted in Fig. 4.45. The reason for the failure of the system to degrade *m*-cresol above 400 mg/L was sought to be explained by estimating the biokinetic parameters. Hence, the

parameters were estimated in a similar way as before by fitting the data to the well-tested Haldane's substrate inhibition model.

Following estimated biokinetic constant values were obtained from this model fitting: $\mu_{\max} = 0.185 \text{ h}^{-1}$; $K_s = 65.1 \text{ mg/L}$ and $K_i = 243.56 \text{ mg/L}$. The ILALR study although agreed with the batch shake flask in terms of the estimated K_s and K_i values, the μ_{\max} value was found to be very low. The μ_{\max} estimated from the Haldane model, thus indeed showed that this scale up from simple batch to the ILALR has affected the growth of the culture. Although the system could be said to have a reasonably good geometry for mixing and oxygen transfer, toxicity of *m*-cresol seem to have a serious effect on the system scale up performance.

4.5.2.3. Biodegradation of Phenol and *m*Cresol in Mixed Substrate System

The concentration range of both phenol and *m*-cresol in this mixed substrate system was set between 100 and 300 mg/L, which were based on the results of the previous single substrate system study. Table 4.18 presents the result obtained in terms of the culture specific growth rate at various concentration combinations of the two substrates.

Fig. 4.46 shows the degradation profile of these two substrates in the mixed substrate system. As observed from the figure, irrespective of the concentration levels of the compounds, phenol was preferentially degraded over *m* cresol, again implied by the fact that phenol is a much simpler carbon source than *m*-cresol. On the effect of phenol initial concentrations on *m*-cresol degradation by the culture, it was observed that at low phenol concentrations (100 and 200 mg/L), rate of *m*-cresol biodegradation is enhanced, whereas at phenol concentration of 300 mg/L the culture failed to

degrade either of the substrates. This may be due to the combined concentration effect due to phenol and *m*-cresol in the medium (Bai *et al.*, 2006). A total loss in activity (degradation as well as growth) in this batch study confirmed the toxic effect of these phenolics at 300 mg/L of each.

Growth pattern of the culture in presence of both phenol and *m*-cresol in the media differed quite largely from that of the single substrate study. This is quite obvious due to availability of more carbon source in this mixed substrate system. The biomass concentration profiles at all concentrations of phenol and *m*-cresol feed concentrations are presented in Fig. 4.47. It is observed from the figure that the culture took more time to grow when *m*-cresol was present in the media (together with phenol); on the other hand, the biomass output was high in such cases.

Table 4.18 also shows the estimated specific growth rate for various combinations of phenol and *m*-cresol in this mixed substrate degradation study. The results show that only for either 100 or 200 mg/L each of phenol and *m*-cresol in the media, the culture growth rate was appreciable. At unequal concentrations of the two substrates, the rate decreased even though the sum of the phenolics concentrations was slightly lesser. Quite similarly, *m*-cresol at concentration 300 mg/L together with phenol, irrespective of its concentration level, had highly inhibitory effect on the culture growth.

To better reveal the interaction effect between phenol and *m*-cresol concentration on the culture growth rate, a sum kinetics model was used. The model was initially tested to predict the variation of experimental specific growth due to various combinations of phenol and *m*-cresol. This model was also used to estimate the relative effects of the two substrates on their individual uptakes (degradation of phenol and *m*-cresol). The form of this model is already shown in Eqn. (4.10).

The model equation was solved using MATLAB[®] 7.0, and the model fitting yielded very high determination coefficient (R^2) value of 0.98. The interaction parameter (I_{ij}) values were found to be 9.9 for $I_{phenol:m-cresol}$ and 3.9 for $I_{m-cresol:phenol}$, respectively. From these interaction parameter values it could be inferred that phenol at 100 mg/L exhibits stronger inhibition on *m*-cresol degradation than vice versa. The interaction parameter values obtained from the model render a fair knowledge on the inhibitory effects in such mixed substrate degradation systems.

Even though the batch operation of the ILALR in degrading phenolics yielded good results upto certain initial concentrations, it however failed to satisfactorily perform at higher concentrations of the substrate(s). To overcome this shortcoming in the reactor, further experiments were performed by operating the reactor under fed batch mode.

4.5.3. Fed-batch Biodegradation of Phenolics

Fed-batch operations are widely used in industries because they combine the advantages from both batch and continuous processes. The main advantages with a fed batch operation are better possibilities of controlling both reaction rate and metabolic reaction by regulated substrate feeding. In some cases, there however might be some limitations caused due to less oxygen transfer in the system. The process can be described by the following set of equations from the standpoint of reactor equilibrium.

$$\frac{dX}{dt} = \mu X - \frac{F}{V} X \quad (4.13)$$

$$\frac{dS}{dt} = (S_0 - S) \frac{F}{V} - \frac{1}{Y_{x/s}} \mu X \quad (4.14)$$

$$\frac{dV}{dt} = F \quad (4.15)$$

where, X is the biomass concentration (mg/L), S_0 is the initial substrate concentration (mg/L), S is the substrate concentration (mg/L) at the end of a batch operation, V is the volume of the reactor (ml), F is the input rate of the substrate (ml/h) and $Y_{x/s}$ is the biomass yield obtained from batch operation (g/g). Using the above governing equations, fed batch operation on of the ILALR was performed, which was aimed at overcoming the substrate inhibition due to phenol/*m*-cresol on their effective degradation by the culture in batch operation of the reactor.

4.5.3.1. Single Substrate System

Fig. 4.48 shows the degradation of phenol and *m*-cresol as single substrates in the fed batch operated ILALR. It is observed that both the substrates were completely degraded by the culture within 26 h and 36 h, respectively. Initially the reactor was operated with a lower substrate concentration of 100 mg/L each, which was very quickly degraded with in 6 h (for both the cases of phenol and *m*-cresol) and later the substrate concentration was increased in step wise manner from 100 to 200, 300, 400 mg/L and finally to 600 mg/L. Hence, operating the reactor under fed batch mode actually took only about 26 and 36 h for complete degradation of phenol and *m*-cresol, respectively at the said concentrations. Thus when compared with simple batch degradation of the phenolics in the ILALR, the degradation time taken by the culture in the fed batch mode was very less, even at their very high concentrations (600

mg/L). The amount of biomass obtained during the fed-batch operation also high confirming the effective uptake of the phenolics by the culture (Fig. 4.49).

4.5.3.2 Mixed Substrate System

The biodegradation pattern of phenol and *m*-cresol in the mixed substrate system is presented in Fig. 4.50. It is observed that the first experimental run with phenol and *m*-cresol at initial concentrations 50 mg/L each were completely degraded within 7 h. In the second step, for a concentration of 100 mg/L each of the substrates, phenol was degraded relatively faster *i.e.* within 4 h while *m*-cresol was degraded relatively slower *i.e.* within 5 h. More strikingly, in both these cases, no lag phase was observed in their degradation profiles. In the third step, the reactor was operated with concentrations of 200 mg/L each, and it was observed that phenol was again preferentially degraded first within 6.3 h while *m*-cresol took 7.3 h. In the final step with the substrate concentrations at 300 mg/L each, after a very brief lag period of 3 h, in case of *m*-cresol only, both the substrates were completely degraded rapidly with in 10.3 h. It is observed that, unlike a simple batch operation in ILALR, such high concentrations of the phenolics could be completely degraded in this fed batch operation of reactor. The degradation rates of phenol and *m*-cresol in the fed batch operation were determined by calculating slope of the biodegradation curves, but neglecting the lag period; and for both phenol and *m*-cresol, the rates increased monotonically. The degradation rates of both the substrates in the various steps are presented in Table 4.19, which were very high compared to those obtained from batch operation of the reactor.

In literature it is reported that Quan et al. (2004) studied biodegradation of 2,4-dichlorophenol and phenol in an internal loop airlift bioreactor immobilized with

Achromobacter sp. In their study, they performed the biodegradation of mixed substrate in fed batch and continuous modes, but the study was mainly aimed at investigating the phenolics degradation in single substrate systems. Apart from this investigation, there are no other studies in the literature pertaining to fed-batch operation of ILALR to treat phenolics.

Thus, the failures observed in the batch operation were highly overcome in the fed-batch mode of operation. Complete degradation of the phenolics is achieved in a much shorter period with almost negligible lag in phenolics degradation time. In line with the degradation profile of the phenolics, biomass output in the system was also high and consistent (Fig. 4.51).

Overall results obtained in the present study showed improved performance of the ILALR in fed-batch mode operation. But on a realistic note, a treatment plant operated under continuous mode would be more desirable, and hence continuous treatment of phenolics in the ILALR was evaluated. The results of continuously operated ILALR in degrading phenolics, in single and mixed substrate systems are reported in the next section.

4.5.4. Biodegradation of Phenol and *m*-Cresol in the Continuously Operated ILALR

The previous section dealing with degradation of phenol and *m*-cresol in the ILALR under batch operation revealed 100% degradation efficiency of both upto a maximum initial concentration of 600 and 400 mg/L, respectively. The time taken in the process was also not high - 47 h for phenol and 36 h for *m*-cresol degradation. However, mixed substrate system in the batch operated IALAR resulted in a poor performance -

no growth of the culture and therefore no degradation of phenol and *m*-cresol at initial concentration of 300 mg/L each. This short coming was greatly over come by operating the reactor under fed batch mode, where better degradation efficiency of the phenolics was obtained within shorter duration of time together with considerable growth of the culture. To further establish the system in treating phenolics from an industrial perspective, the reactor was operated under continuous mode with synthetic wastewater containing the phenolic compounds, both individually and in mixture.

4.5.4.1. Single Substrate System

The various stages involving inlet concentration of phenol/*m*-cresol, flow rate (HRT) and hours of operation in the continuously operated ILALR in treating the phenolic compounds in single substrate system has been detailed in Chapter 3.

The continuous operation was performed under two different HRTs, viz., 4.1 and 8.3 h. Figs. 4.52 – 4.55 shows the reactor performances towards treating phenol and *m*-cresol, respectively, operated at the corresponding HRTs. It could be observed from Fig. 4.52 that 100% degradation efficiency of phenol could be achieved at HRT of 8.3 h at all concentrations. However, in case of *m*-cresol, 100% degradation efficiency in the reactor at the same HRT could be attained only up to 500 mg/L initial concentration, above which the efficiency was found to decrease (Fig. 4.54). Due to this fall in efficiency, initial concentration of *m*-cresol was lowered to 100 mg/L to get a stable performance thereafter. The profile obtained for phenol/*m*-cresol degradation in the reactor when operated at HRT of 4.1 h (Figs. 4.53 and 4.55) showed that complete degradation of the compounds could be achieved only up to a maximum initial concentration of 300 mg/L, above which the reactor failed to perform at 100% degradation efficiency. Operation of the reactor at phenolic concentrations, above

which reduction in its performance was observed were considered to be shock loading conditions in the system and its results are discussed further.

4.5.4.2. Performance of the ILALR under Shock Loading Conditions of Phenol/*m*-Cresol

Any industrial wastewater treatment plant undergoes intermittent organic loading conditions when concentrations of its pollutants change abruptly. In order to evaluate the potential of the ILALR due to such aspects, experiments were carried out by subjecting the ILALR to intermittent and shock loading conditions during the degradation study. Initially, the reactor was operated at low phenol/*m*-cresol concentration of 100 mg/L for a specific period of time as seen earlier, and in the reactor treating phenol as the single pollutant its concentration was increased suddenly to 600 mg/L and then to 800 mg/L at 8.3 HRT. In case of the *m*-cresol degradation system, at the same HRT, its concentration was increased from an initial value of 100 to 500 mg/L and then to 800 mg/L. On the other hand, at 4.1h HRT, the shock loading conditions of either phenol or *m*-cresol were set at a maximum value of 500 mg/L. Figs. 4.52 - 4.55 show the performance profile of the ILALR operated at 8.3 and 4.1 h HRT respectively, under these shock loading conditions in the reactor.

From Fig. 4.52, it is clear that for phenol at 8.3 HRT and a maximum shock loading concentration of 800 mg/L, the degradation efficiency of the reactor fell down only below 87%. The reactor system could, however, regain its maximum efficiency (*i.e.* 100% efficiency) within 12 h time even under this shock loading condition, and after a prolonged operation, no trace of residue of phenol was observed in the outlet. Similarly, for *m*-cresol, the reactor efficiency although decreased slightly when the concentration was increased to 500 mg/L, the full efficiency was restored in due

course of time (Fig.4.54). Nevertheless, in this case of *m*-cresol treating reactor, its efficiency was highly affected at its maximum shock loading concentration of 800 mg/L (*m*-cresol), where the degradation efficiency fell quite drastically to 70%. This fall in degradation efficiency could be reasoned mainly due to high toxicity of *m*-cresol. However, the reactor could regain its stability of treatment immediately when the inlet concentration of *m*-cresol was lowered to 100 mg/L.

Similar shock loading studies were carried out at 4.1 h HRT in the reactor by increasing phenol/*m*-cresol concentration to 500 mg/L. The results are presented in Figs. 4.53 and 4.55 for the two substrates, which indicates that the degradation efficiency of the reactor decreased to almost 70% in both the cases. However, the system showed a complete degradation (100%) only up to a phenol/*m*-cresol concentration of 300 mg/L. Hence, it is evident that lower HRT (4.1 h) with higher pollutant concentration largely affected the operational stability of the reactor in treating the pollutants. It was also made clear that the culture had a high potential to degrade the phenolic compounds even at shock loading concentrations as high as 800 mg/L, of either phenol or *m*-cresol, but at a slightly higher HRT value (8.3 h).

Quan et al (2006) studied biodegradation of 2,4 dichlorophenol (DCP) as single substrate in the continuously operated ILALR using *Achromobacter* sp. The authors observed that 2,4-DCP with an initial concentration of 12.8 mg/L was completely degraded in 28.5 h, and increasing the inlet concentration of 2,4-DCP to 28.5 mg/L resulted in a slight fluctuation in its degradation efficiency, but the reactor quickly reached steady state again. The degradation efficiency of 2,4-DCP in the study ranged from 96.5 – 99%. Compared to this study by Quan et al. (2006), the present study had a maximum concentration of 800 mg/L and a minimum of 100 mg/L of phenol and *m*-

cresol in single substrate systems. Moreover 100% degradation efficiency was achieved at an initial phenol and *m*-cresol concentrations of 800 and 500 mg/L, respectively.

4.5.4.3. Mixed Substrate System

Figs. 4.56 and 4.57 show the degradation profile of phenol and *m*-cresol in the mixed substrate system in the continuously operated ILALR at the two different HRT values 8.3 and 4.1 h. As before, it is evident from Fig 4.57 that the reactor manifests a high performance in removing the pollutants completely at an HRT of 8.3 h; however not for all the concentration combinations (except 300 mg/L each of phenol and *m*-cresol). For most of the concentration combinations of the substrates, the reactor could achieve 100% efficiency, but when the inlet concentrations of phenol and *m*-cresol were increased to 300 mg/L each, the efficiency fell down to 91% for phenol and 75% in case of *m*-cresol. As observed in the single substrate system, a decline in the degradation efficiency, particularly at higher concentration of *m*-cresol (300 mg/L), was noted due to its higher toxicity. Quan et al. (2004) studied the biodegradation of 2,4-dichlorophenol (DCP) and phenol in an internal loop airlift bioreactor immobilized with *Achromobacter* sp. In their continuous operation study they maintained an HRT of 8 h in the reactor. Their results showed that for a maximum initial concentration of 200 mg/L of phenol and 10 mg/L of 2,4 dichlorophenol the removal efficiency of 2,4- DCP declined from 100% to 87.9% with increased phenol loading rate, while the removal efficiency of phenol remained at about 99.6 %. Compared to the present study, the concentration combination of 2,4- DCP and phenol chosen by Quan et al. could be considered too low. Hence, it is quiet straight forward that the present study show good potential of the ILALR system in

handling wastewater containing phenolic compounds, even at their high concentrations.

Similarly, the results of reactor performance in degrading the phenolics in their mixed substrate study at HRT 4.1 h reveal that a complete degradation could be achieved only when phenol/*m*-cresol concentrations were 100 mg/L each. When the reactor was operated above this concentration combinations, complete degradation (100%) was never attained. In all the adopted combinations, when the treatment efficiency fell to 75%, the inlet concentrations of the compounds were decreased to 100 mg/L in order to retain the stability of the system (Fig. 4.57). Hence it is clear from the experiments that an HRT of 8.3 h yielded a higher treatment efficiency of 100% for most of the pollutant combinations.

Jajuee et al. (2007) studied the simultaneous degradation of *p*-xylene and naphthalene as mixture in a novel airlift immobilized bioreactor. In their study, they operated the reactor at low HRT of 0.8 h and obtained a treatment efficiency of only slightly more than 59% at all concentration combinations of the two compounds. However they employed concentration ranges of merely 22 to 101 mg/L in case of *p*-xylene and 6 to 32 mg/L in case of naphthalene. The present study had a maximum concentration of 300 mg/L and a minimum of 100 mg/L each of phenol and *m*-cresol in mixture. Complete degradation (100 % efficiency) was achieved at 100 mg/L each of phenol and *m*-cresol in the mixed substrate system.

Overall, the preceding comprehensive biodegradation study revealed a very high potential of the indigenous mixed microbial culture, viz., *Pseudomonas* spp., isolated from a sewage treatment plant in completely degrading the phenolics compounds, even at their higher concentrations in both single and mixed substrate systems. The

study also revealed the feasibility of an ILALR for treating high strength phenolics wastewater using the indigenous mixed culture by sufficiently meeting the requirements of an industrial wastewater treatment plant



Table 4.1: Results of the various biochemical characterization tests to identify the predominant microbial species in the enriched mixed culture (^a - denotes test result is negative and + denotes test result is positive for *Pseudomonas* spp)

Sl. no.	Tests	Results ^a
1.	ONPG	+
2.	H ₂ S	-
3.	Citrate Utilization	-
4.	Indole	-
5.	Esculin	+
6.	Motility	+
7.	Catalase	+
8.	Voges-Proskauer	-
9.	Urea	-
10.	Methyl Red	-
11.	Nitrate	-

Table 4.2: Determination coefficient (R^2) and rate constant values obtained by fitting three-half order kinetic model to the experimental phenol degradation profile

Initial phenol concentration (S)	Determination coefficient (R^2)	k_0	$k_1 \times 10^{-5}$ (h^{-1})	k_2 (h^{-2})
100	0.9721	-9.1608	65	-0.016
200	0.9741	-13.141	15	-0.0054
300	0.9625	-13.848	10	-0.0042
400	0.9529	-12.436	4	-0.0024
500	0.9701	-12.314	2	-0.0014
600	0.9703	-11.986	0.5	-0.0008
700	0.9721	-11.033	0.4	-0.0006
800	0.9803	-9.3999	0.5	-0.0006

Table 4.3: Estimated growth kinetic parameters during phenol degradation using various models

Model	μ_{max} (h^{-1})	K_s (mg/L)	K_{si}/K_i (mg/L)	S_m (mg/L)	n	m	K	RMS error
Monod	0.37	144.68	-	-	-	-	-	-
Edward	0.35	83.25	500.00	-	-	-	20.00	0.650
Haldane	0.3085	44.92	525.00	-	-	-	-	0.202
Han - Levenspiel	0.4029	110.93	-	790.00	1.00	0.7	-	0.021
Luong	0.412	128.25	-	800.00	1.75	-	-	0.026
Yano-Koga	0.431	103.5	-	-	1.00	-	300.00	0.970

Table 4.4: Comparison of the estimated kinetics parameter of the culture during phenol degradation in batch shake flasks with those found in the literature

Sl.No.	Bacterial culture	Concentration range (mg/L)	Monod's model		Haldane's Model			Temp./pH
			μ_{\max} (h ⁻¹)	K _s (mg/L)	μ_{\max} (h ⁻¹)	K _s (mg/L)	K _i (mg/L)	
1.	Mixed culture I (Pawlowsky and Howell,1973)	0-900	-	-	0.260	25.4	173.0	28 ± 0.5 / 6.6
2.	Mixed culture II filamentous organism (Pawlowsky and Howell,1973)	0-1000	-	-	0.223	5.586	934.5	28 ± 0.5 / 6.6
3.	<i>P.putidia</i> F1 ATCC 17484 (Hutchinson and Robinson,1990)	< 200	-	-	0.388	1.06	903.0	30 / 6.5-6.8
4.	<i>P.putia</i> Q5 (Kotturi <i>et al.</i> ,1991)	≤ 200	-	-	0.119	5.27	377.0	10 / 7.0
5.	NCIB8250 <i>Actino bacter</i> sp.+NCIB10535 <i>Pseudomonas</i> sp.+NCIB1015 <i>Pseudomonas</i> sp. (Livingston and Chase,1989)	0-500	-	-	0.418	2.9	370	30 / 6.7-6.9
6.	<i>Pseudomonas</i> sp. (Okaygun <i>et al.</i> ,1992)	0-170	-	-	0.325	8.2	170.0	21/ 6.7

Table 4.4 continued in the next page ...

Table 4.4 continued ...

7.	<i>A.calcoacetius</i> (phenol only)- <i>P.fluoroscens</i> 2218(phenols only)-Pooled culture (phenols) (<i>P.fluoroscens</i> , <i>P.Pputida</i> , <i>P.cepacia</i> , <i>A.calcoacetius</i> , <i>C.tropicalis</i> (Kumaran and Paruchuri,1996)	60-500	0.465	30.96	0.542	36.2	145	Not mentioned
8.	<i>P.putida</i> DSM 548 (Monterio <i>et al.</i> , 2000)	0-100	-	-	0.436	6.19	54.1	26 / 6.8
9.	<i>P.putida</i> F1 ATCC 700007 (Abuhmed <i>et al.</i> ,2005)	750-1750	-	-	0.051	18.0	430	30 / 7.0
10.	<i>P.putida</i> MTCC 1194 (Kumar <i>et al.</i> ,2005)	0-1000	0.216	20.59	0.305	36.33	129.79	29.9 ± 0.5 / 7.1
11.	Mixed culture (Present study)	0-800	0.37	144.68	0.3085	44.92	525.00	27 ± 1/ 7.0

Table 4.5: Estimated biokinetic parameters obtained from different models during biodegradation of phenol by the culture

Model	q_{\max} (h^{-1})	K_s (mg/L)	K_i (mg/L)	S_m (mg/L)	n	m	K	RMS error
Monod	0.4132	156.46	-	-	-	-	-	-
Edward	0.4321	121.49	210.00	-	-	-	20.00	0.0039
Haldane	0.4643	113.54	376.65	-	-	-	-	0.0074
Luong	0.4142	138.71	-	800	2.05	-	-	0.0173
Han - Levenspiel	0.451	135	-	800	0.6	1.00	-	0.0333
Yano - Koga	0.4510	110.17	-	-	1.00	-	400.00	0.0076

Table 4.6: Culture growth kinetic parameters obtained from different models during biodegradation of *m*-cresol.

Model	μ_{\max} (h^{-1})	K_s (mg/L)	K_{si}/K_i (mg/L)	S_m (mg/L)	n	m	K	RMS error
Monod	0.5155	117.71	-	-	-	-	-	-
Edward	0.5180	71.40	200.00	-	-	-	10.00	0.0168
Haldane	0.6819	79.14	204.42	-	-	-	-	0.0352
Luong	0.6430	94.50	-	900.00	0.85	-	-	0.0159
Han - Levenspiel	0.5561	77.75	-	900.00	1.00	1.00	-	0.0167
Yano - Koga	0.5961	63.42	-	-	1.00	-	250.00	0.0375

Table 4.7: Estimated substrate degradation kinetic parameters obtained from different models during biodegradation of *m*-cresol

Model	q_{\max} (h^{-1})	K_s (mg/L)	K_i (mg/L)	S_m (mg/L)	n	m	K	RMS error
Monod	0.5587	129.49	-	-	-	-	-	-
Edward	0.6001	109.64	500.00	-	-	-	20.00	0.6629
Haldane	0.8377	147.76	525.00	-	-	-	-	0.2298
Luong	0.6543	122.28	-	790	1	-	-	0.0196
Han - levenspiel	0.5951	84.5	-	800	1.75	0.7	-	0.0094
Yano - Koga	0.6161	70.09	-	-	1.00	-	300.00	0.9999

Table 4.8: Calculated specific growth rate of the culture obtained for high and low initial concentration ranges of phenol and *m*-cresol.

Experimental run no.	Initial concentration level of:		Culture specific growth rate (h^{-1}) in:	
	Phenol	<i>m</i> -Cresol	Low range	High range
	1.	-1	-1	0.324
2.	+1	-1	0.701	0.054
3.	-1	+1	0.675	0.051
4.	+1	+1	0.565	0.025
5.	0	0	0.625	0.033
6.	0	0	0.623	0.0335
7.	0	0	0.627	0.0332

Table 4.9: ANOVA of the culture specific growth rate in low concentration ranges of the substrates

Factor	Degrees of freedom	Sum of squares	Mean squares	F value	P value
Main Effects	2	0.029475	0.014737	6.38	0.135
2-Way Interactions	1	0.059390	0.059390	25.72	0.037
Residual error	2	0.004618	0.002309	-	-
Total	5	0.093482	-	-	-

Table 4.10: ANOVA of the culture specific growth rate in high concentration ranges of the substrates

Factor	Degrees of freedom	Sum of squares	Mean squares	F value	P value
Main Effects	2	0.145751	0.014737	4.9	0.170
2-Way Interactions	1	0.058831	0.059390	3.95	0.185
Residual error	2	0.029772	0.002309	-	-
Total	5	0.234353	-	-	-

Table 4.11: Students '*t*' test of the culture specific growth rate in the low concentration ranges of the substrates

Factors	Coefficient	<i>t</i>	P
<i>m</i> -Cresol	0.0539	2.24	0.156
Phenol	0.0668	2.78	0.109
<i>m</i> -Cresol*Phenol	-0.1219	-5.07	0.037
Constant	0.5858	29.86	0.001

Table 4.12: Students '*t*' test of the culture specific growth rate in high concentration ranges of the substrates

Factors	Coefficient	<i>t</i>	P
<i>m</i> -Cresol	-0.1357	-2.22	0.156
Phenol	-0.1342	-2.20	0.159
<i>m</i> -Cresol*Phenol	0.1213	1.99	0.185
Constant	0.1240	2.49	0.131

Table 4.13: Total biomass yield (g/g) values in low concentration ranges of the substrates

Phenol (mg/L)	<i>m</i> -Cresol concentration (mg/L)		
	100	150	200
100	2.17	2.16	2.05
200	2.16	1.76	1.89
300	1.7	1.8	1.9

Table 4.14: Total biomass yield (g/g) values in high concentration ranges of the substrates

Phenol (mg/L)	<i>m</i> -Cresol concentration (mg/L)		
	200	400	600
300	1.9	1.44	1.6
450	1.5	1.6	1.6
600	1.6	1.58	1.6

Table 4.15: Specific degradation rates of phenol and *m*-cresol obtained in low and high initial concentration ranges of the substrates.

Experimental run no.	Initial concentration of:		Phenol specific degradation rate in (h ⁻¹):		<i>m</i> -Cresol specific degradation rate in (h ⁻¹):	
	Phenol	<i>m</i> - Cresol	Low range	High range	Low range	High range
1.	-1	-1	0.114	0.0786	0.099	0.095
2.	+1	-1	0.208	0.0093	0.194	0.0057
3.	-1	+1	0.342	0.043	0.218	0.0087
4.	+1	+1	0.079	0.0085	0.095	0.0081
5.	0	0	0.09	0.0776	0.27	0.0082
6.	0	0	0.0908	0.077	0.273	0.00821
7.	0	0	0.091	0.0777	0.275	0.00823

Table 4.16: Typical characteristics of the refinery wastewater

Sl. No.	Parameters	Quantity
1.	pH	8.6
2.	Dissolved Oxygen	0.95 mg/L
3.	Arsenic	55 – 60 µg/L
4.	Lead	45-50 µg/L
5.	COD (raw wastewater)	10000 mg/L
6.	COD after adjusting the pH to 7	4800 mg/L

Table 4.17: Biokinetic constants estimated by fitting Haldane and Han-Levenspiel substrate inhibition models on the experimental data on growth of the culture

Model	μ_{\max} (h ⁻¹)	K_s (mg/L)	K_i (mg/L)	S_m (mg/L)	n	m	RMS error ($\times 10^{-5}$)
Haldane	0.0324	40.57	140.65	-	-	-	1.86
Han - Levenspiel	0.0257	40.55	-	400	0.6	1.00	5.62

Table 4.18: Specific growth rate of the culture obtained at different combinations of phenol and *m*-cresol concentrations in the ILALR

Experimental Run no.	Phenol (mg/L)	<i>m</i> -Cresol (mg/L)	Culture specific growth rate (h ⁻¹)
1.	100	100	0.25
2.	200	100	0.14
3.	200	200	0.24
4.	100	300	0.09
5.	200	300	0.07
6.	300	300	0.00

Table 4.19: Observed degradation rates of phenol and *m*-cresol in the mixed substrate system in the fed-batch operated ILALR

Step	Initial phenol concentration (mg/L)	Initial <i>m</i> -cresol concentration (mg/L)	Degradation rate (mg/L/h)	
			Phenol	<i>m</i> -Cresol
1.	50	50	7.18	6.77
2.	100	100	19.12	17.67
3.	200	200	29.48	27.72
4.	300	300	34.90	31.88



Fig. 4.1: Photograph of the Gram stained culture taken under light microscope clearly showing the predominant presence of distinct rod shaped Gram-negative bacteria of *Pseudomonas* spp.

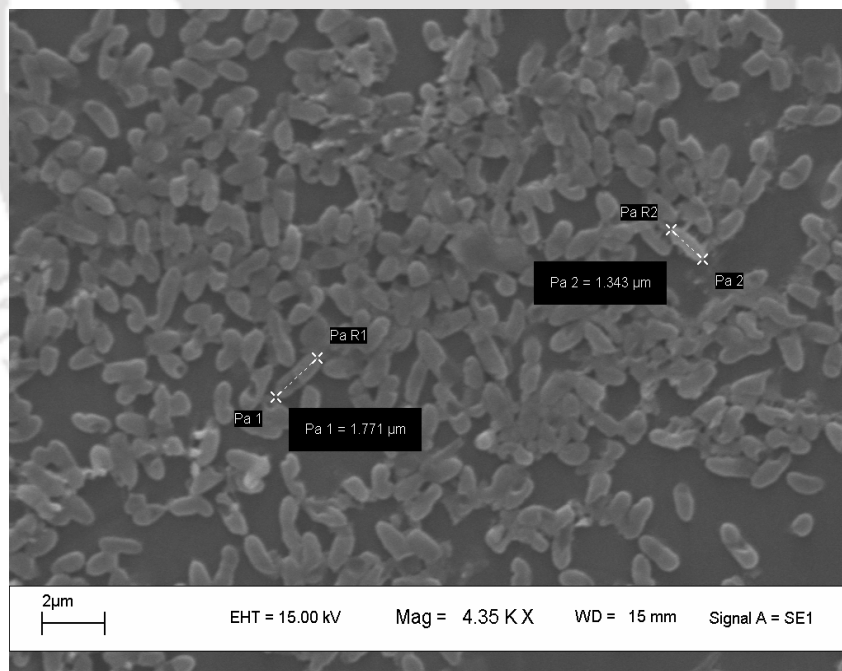


Fig. 4.2: SEM image of the enriched mixed microbial culture confirming the presence of rod shaped *Pseudomonas* spp. bacteria along with its typical sizes.

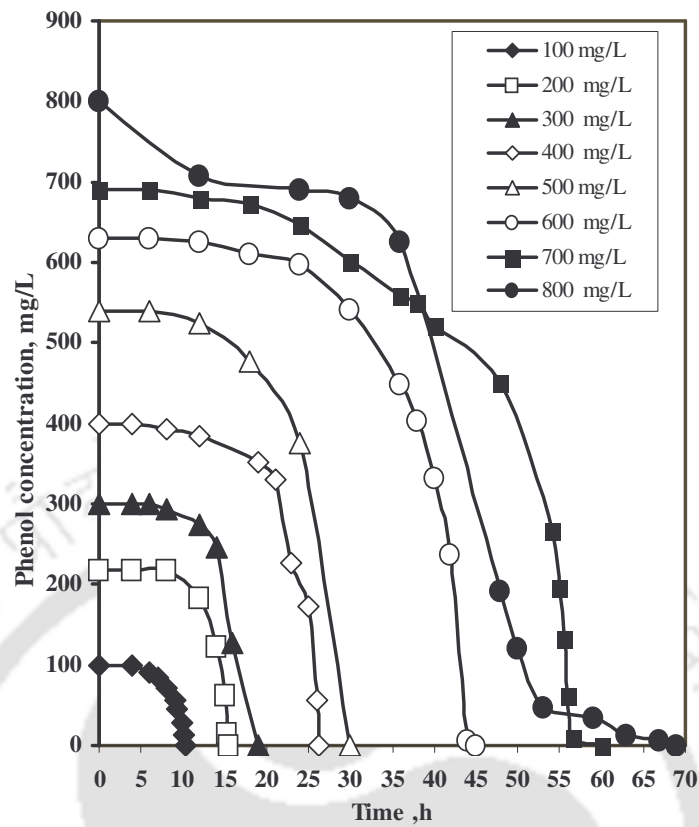


Fig.4.3: Time profile of phenol biodegradation by the culture in the batch shake flasks

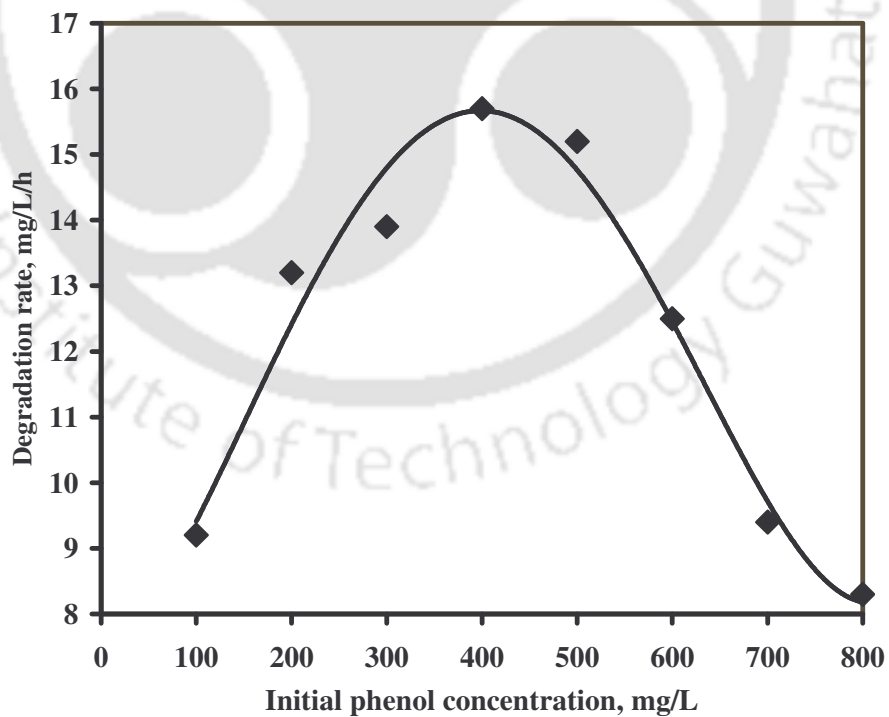


Fig. 4.4: Variation of phenol degradation rate with initial phenol concentrations.

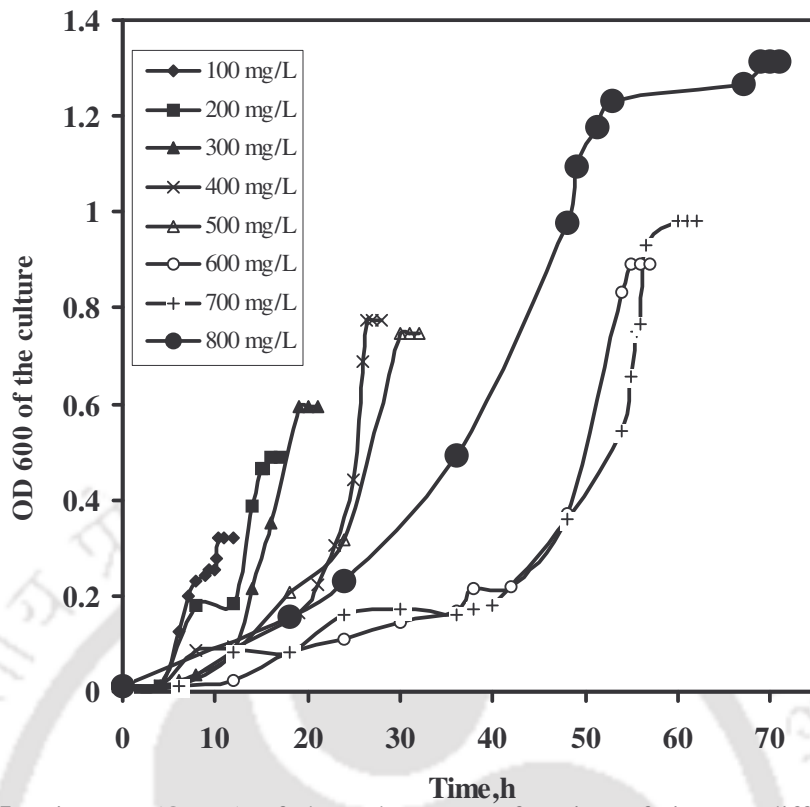


Fig. 4.5: Biomass (OD_{600}) of the culture as a function of time at different initial phenol concentrations.

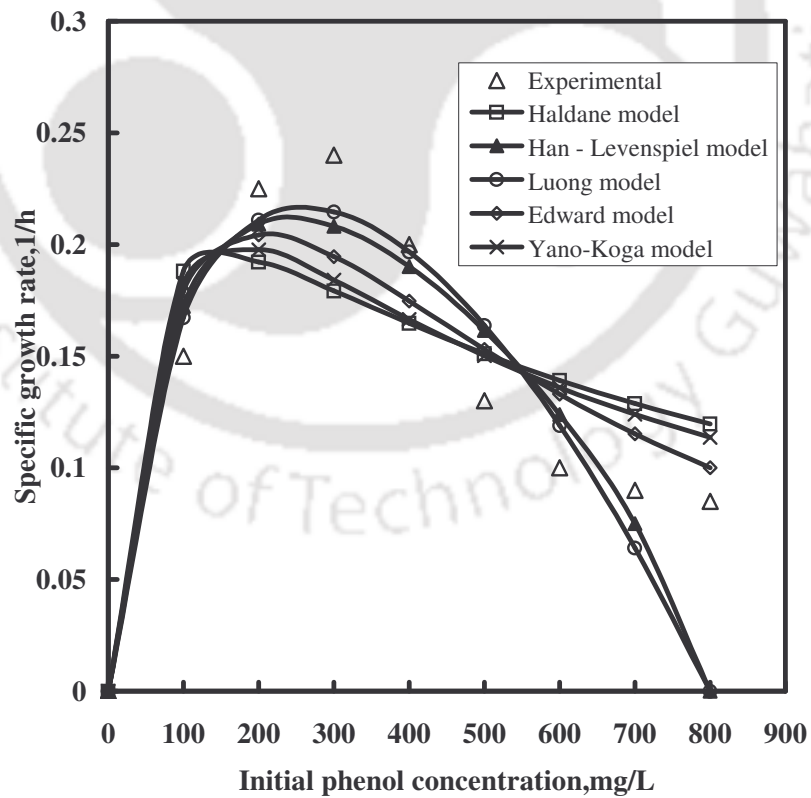


Fig. 4.6: Experimental and model predicted specific growth rate of the culture at different initial phenol concentrations.

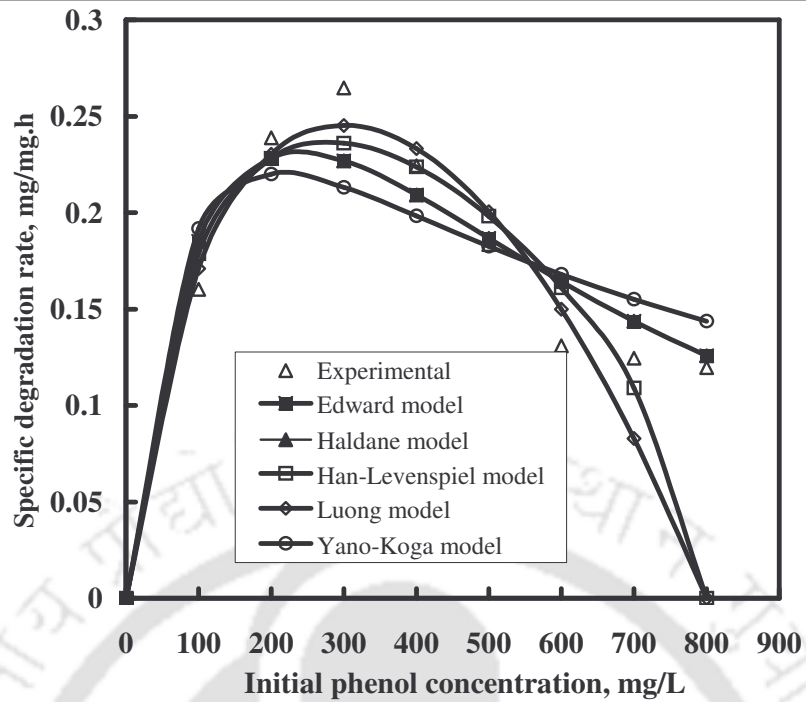


Fig.4.7: Experimental and predicted phenol degradation rate of the culture due to the various models.

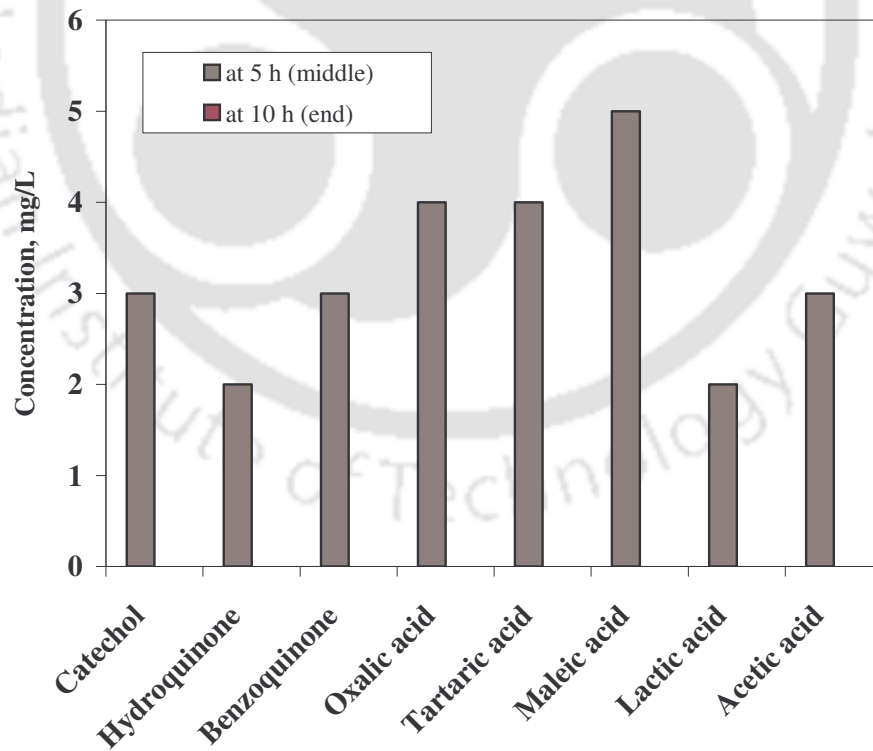


Fig 4.8: Intermediates formed and their concentrations during (middle) and end of batch biodegradation of phenol.

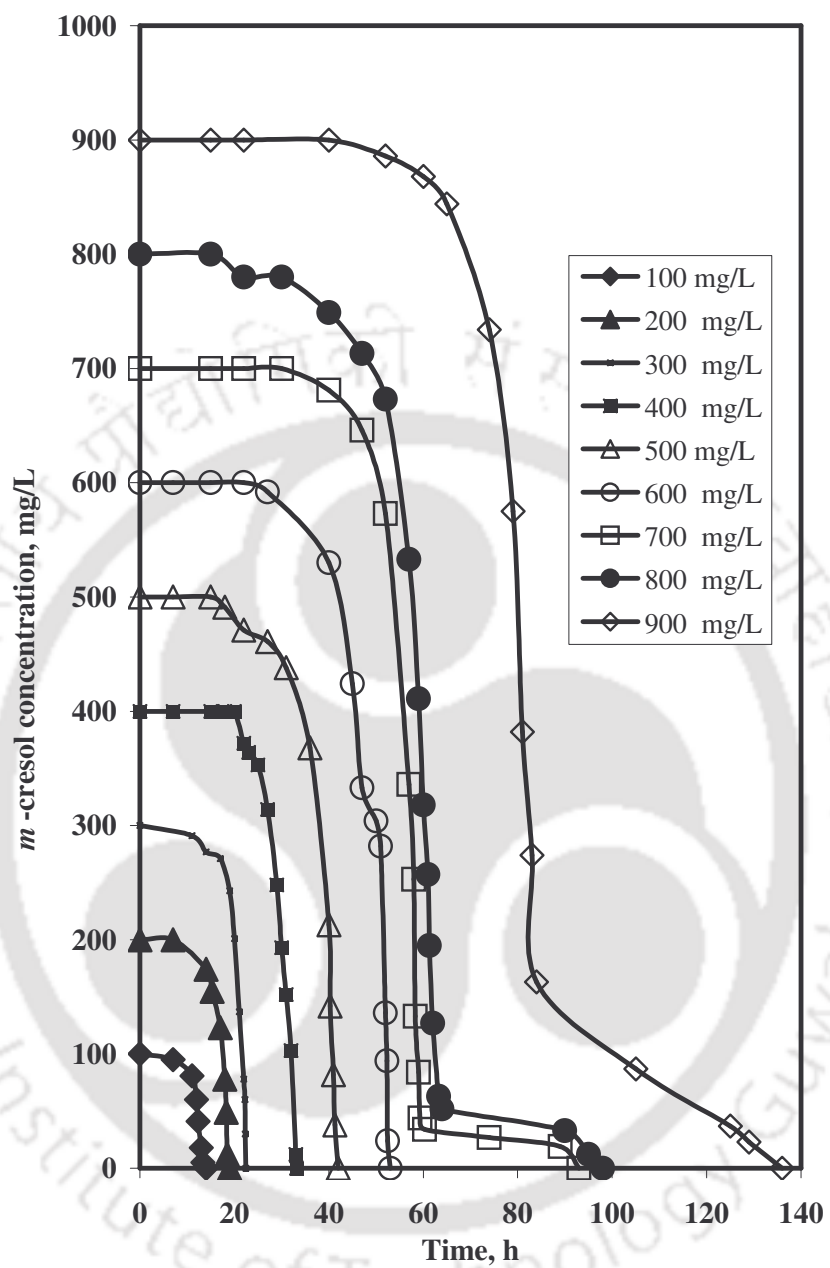


Fig. 4.9: Time profile of *m*-cresol degradation by the culture in batch shake flasks.

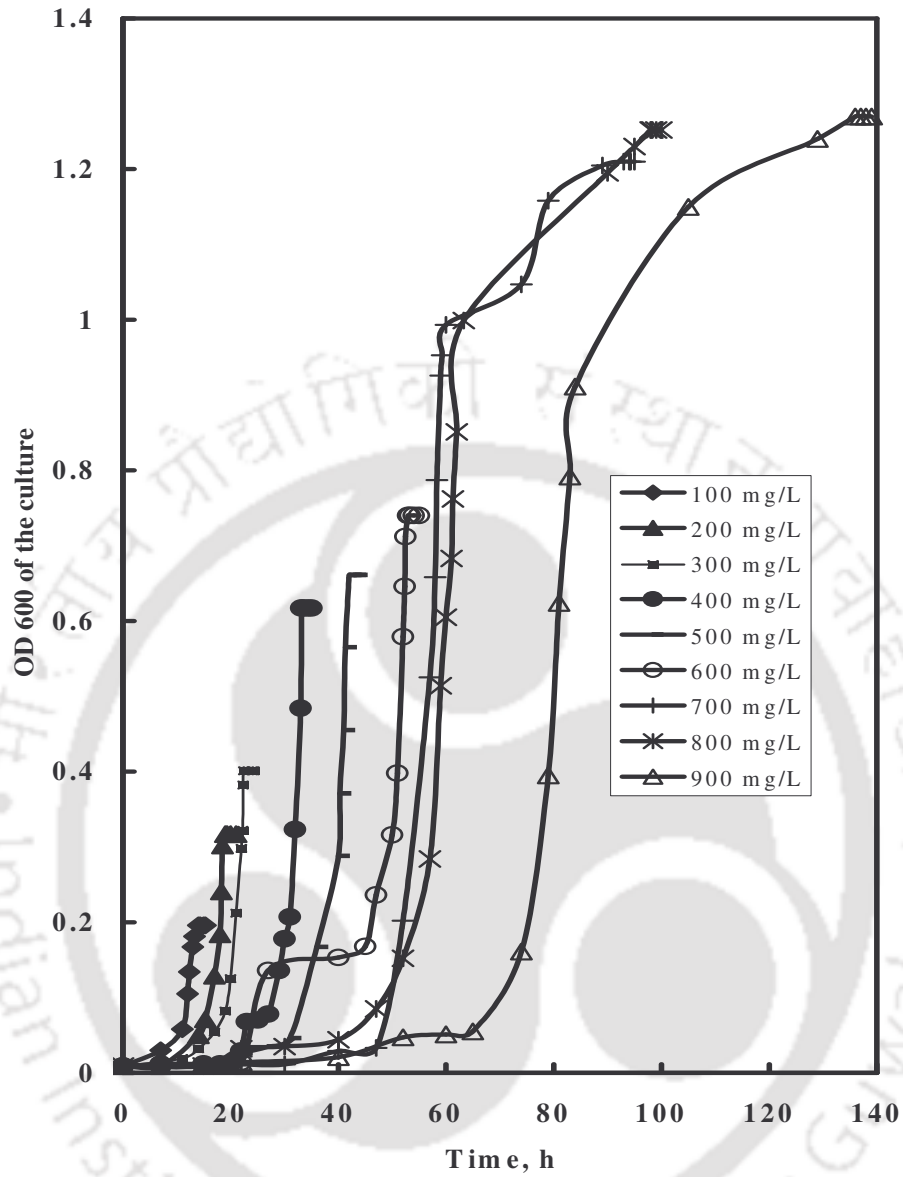


Fig. 4.10: Biomass (OD_{600}) of the culture as a function of time at different initial *m*-cresol concentrations

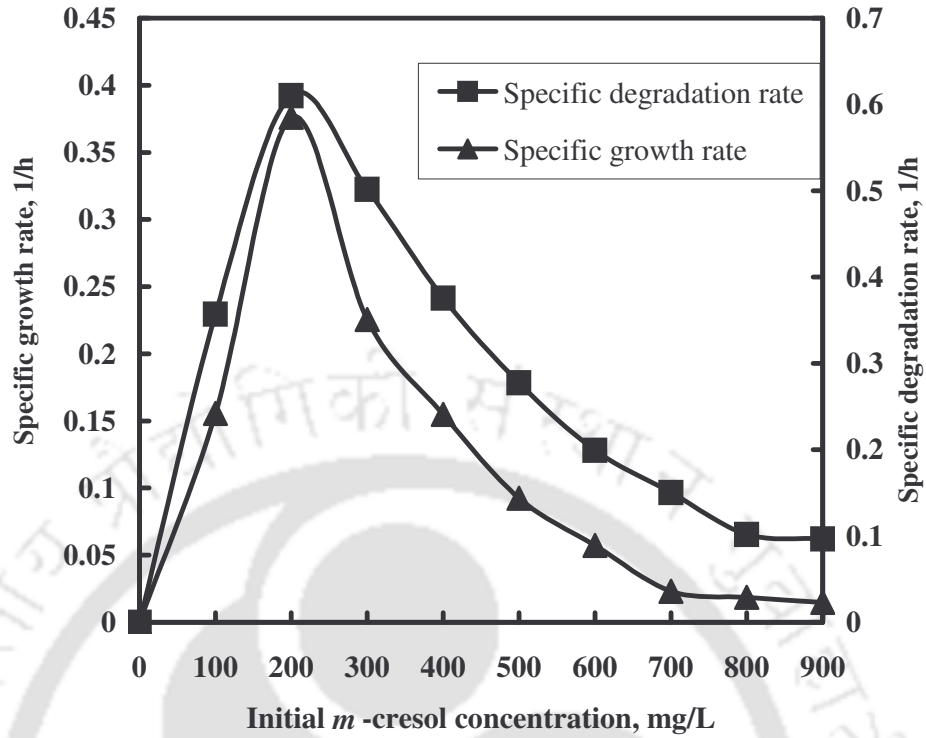


Fig. 4.11: Comparison of specific growth and degradation rates at different initial *m*-cresol concentrations.

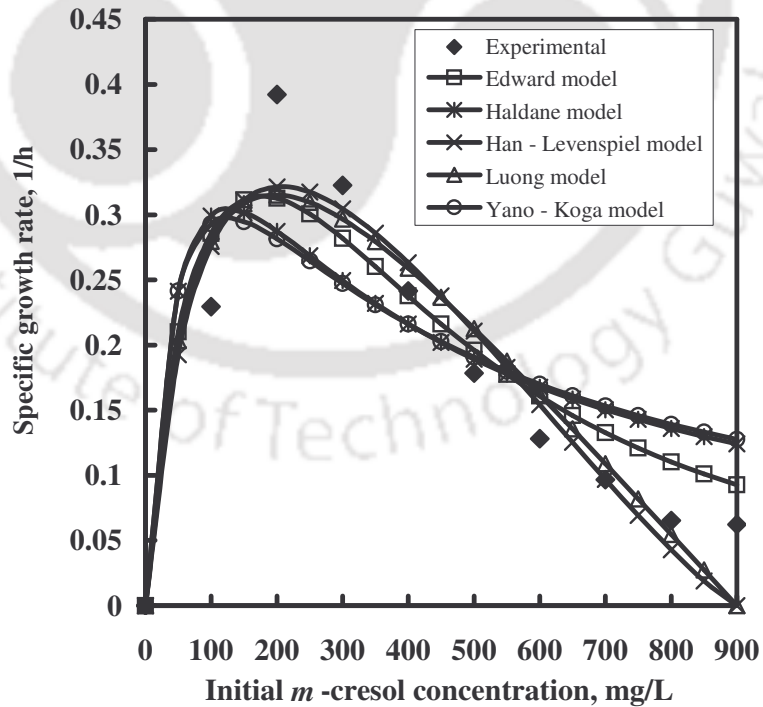


Fig. 4.12: Experimental and model predicted specific growth rate of the culture at different initial *m*-cresol concentrations.

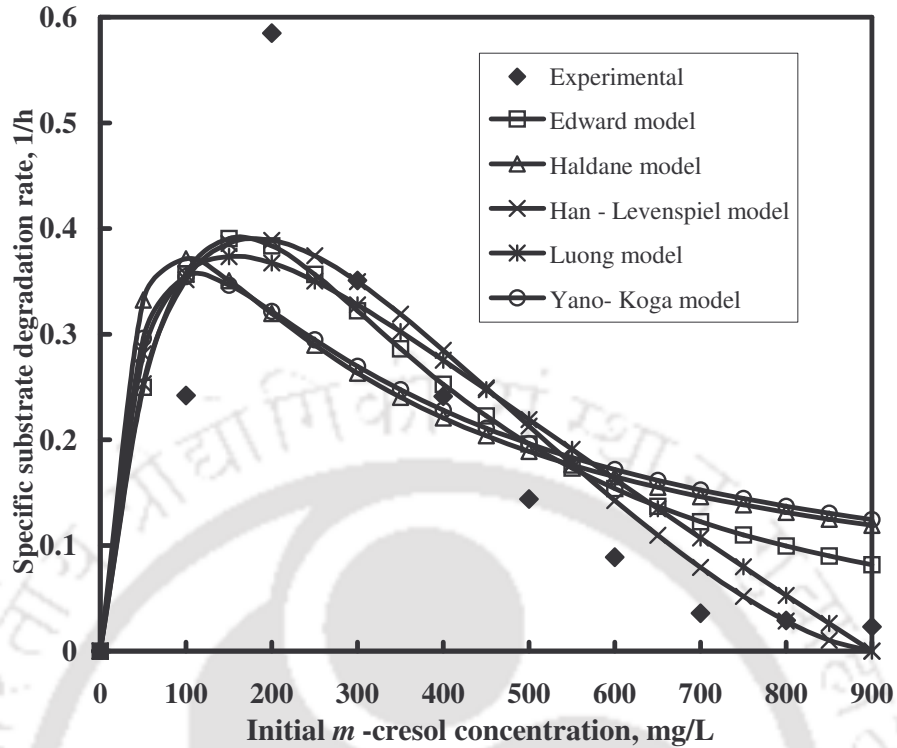


Fig. 4.13: Experimental and various model predicted specific degradation rate of the culture at different *m*-cresol concentrations.

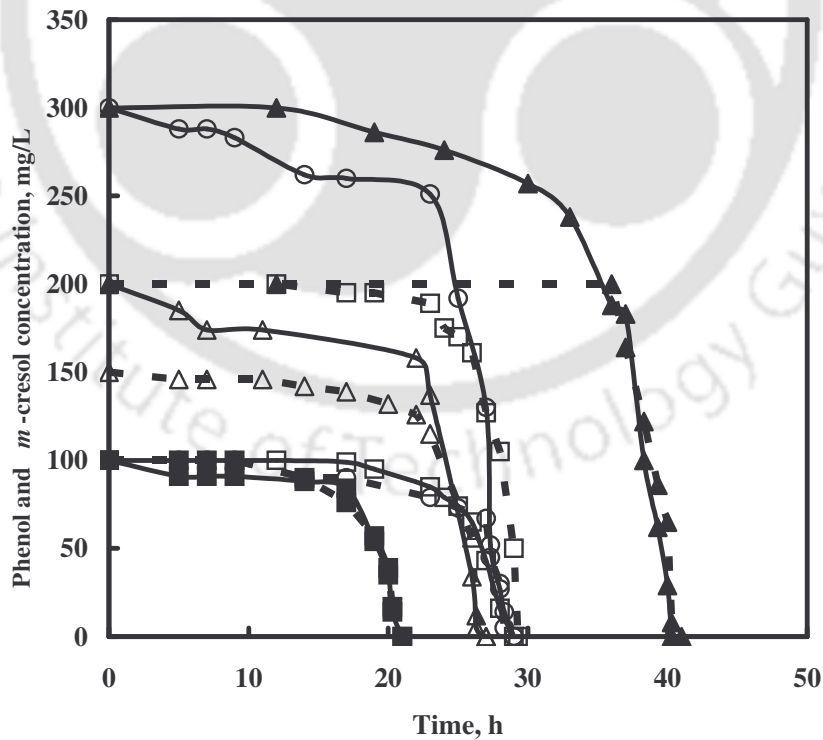


Fig. 4.14: Phenol and *m*-cresol biodegradation patterns shown by the culture at low initial concentration ranges of the substrates [(—) Phenol; (-----) *m*-cresol; Symbols used: Run 1(▪), Run 2(□), Run 3(○), Run 4(▲), Run 5(Δ)].

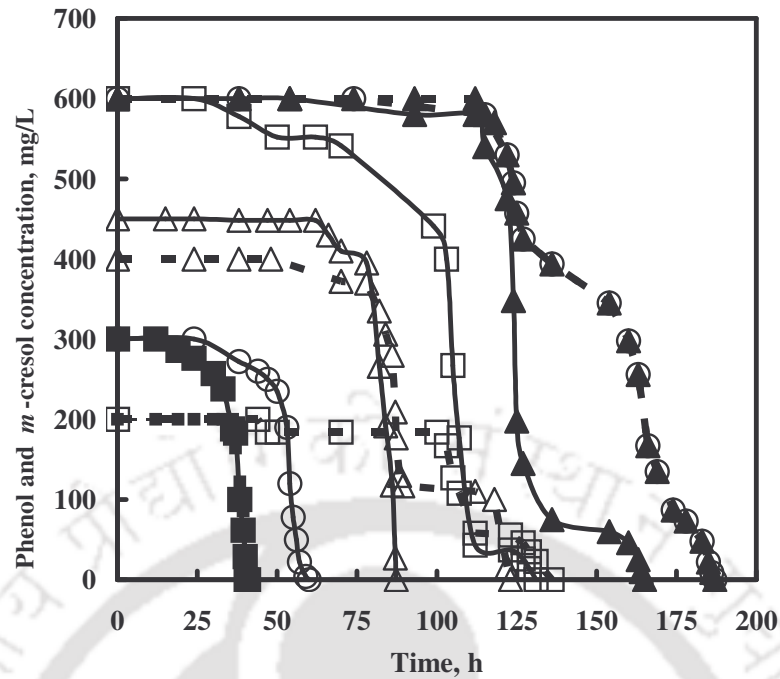


Fig.4.15: Phenol and *m*-cresol biodegradation patterns shown by the culture at high initial concentration ranges of the substrates [(—) Phenol; (-----) *m*-cresol; Symbols used: Run 1(▪), Run 2(□), Run 3(○), Run 4(▲), Run 5(Δ)].

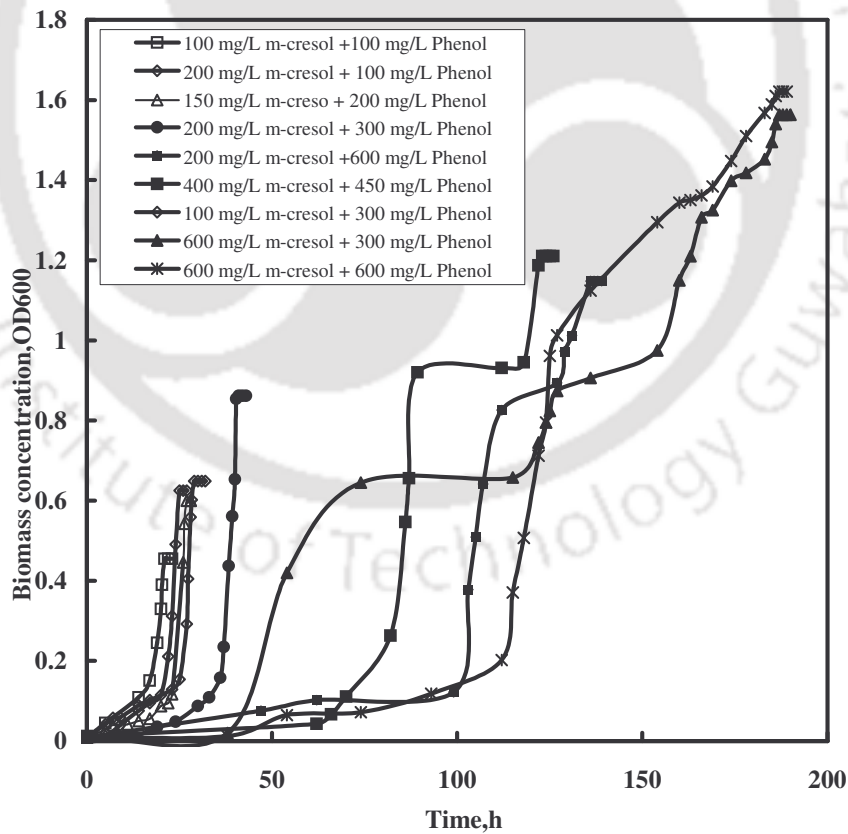


Fig. 4.16: Biomass profile of the culture when grown in medium containing both phenol and *m*-cresol.

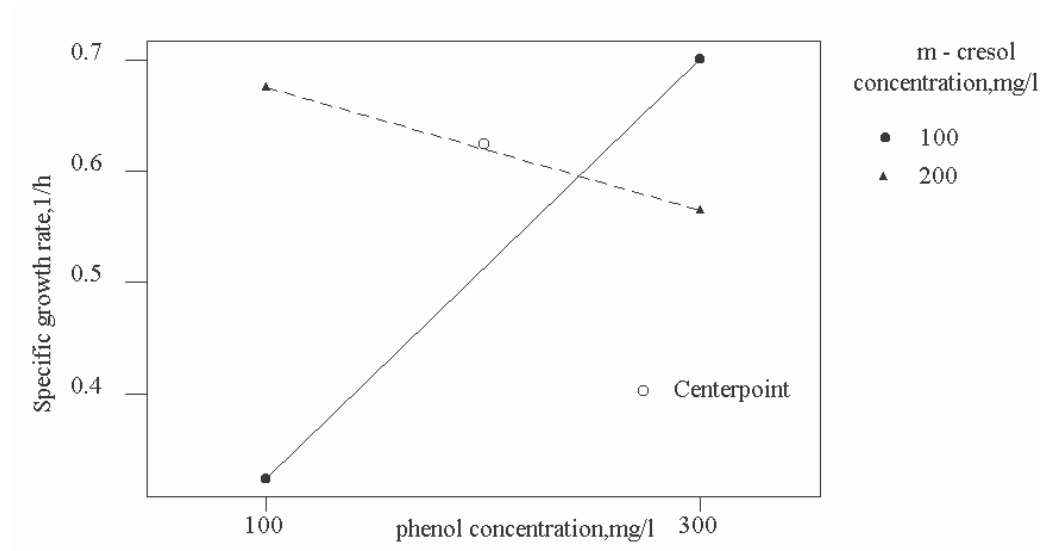


Fig. 4.17: Interaction effect between phenol and *m*-cresol on the culture specific growth rate in their low concentration ranges.

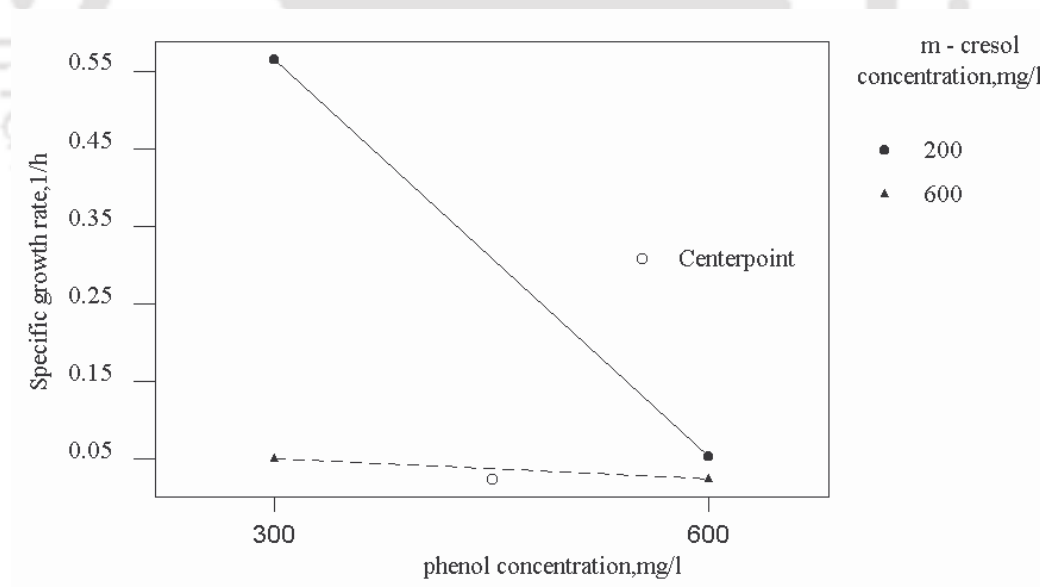


Fig. 4.18: Interaction effect between phenol and *m*-cresol on the culture specific growth rate in their high concentration ranges.

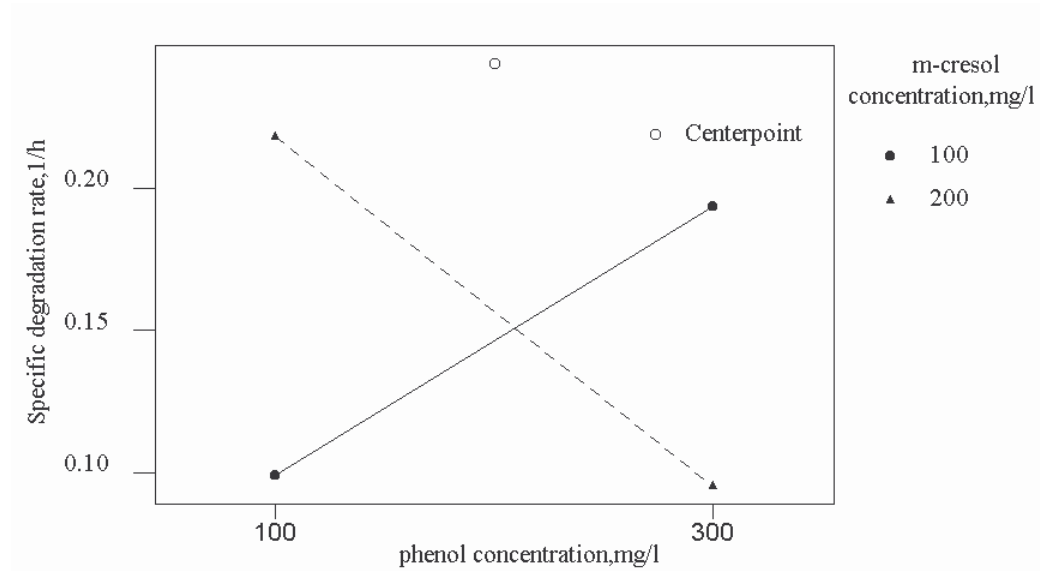


Fig. 4.19: Interaction effect between phenol and *m*-cresol in their low concentration ranges on specific phenol degradation rate.

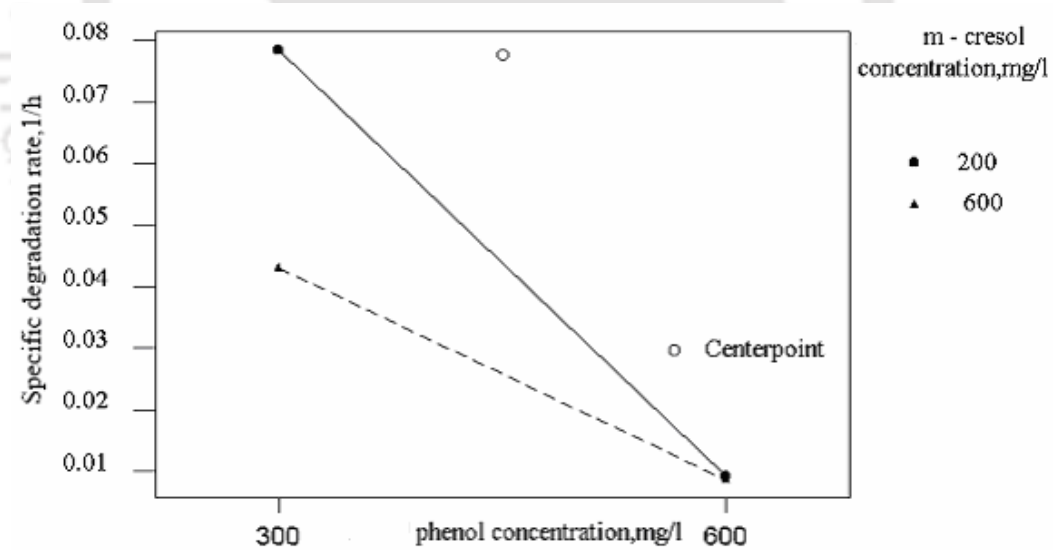


Fig. 4.20: Interaction effect between phenol and *m*-cresol in their high concentration ranges on specific phenol degradation rate.

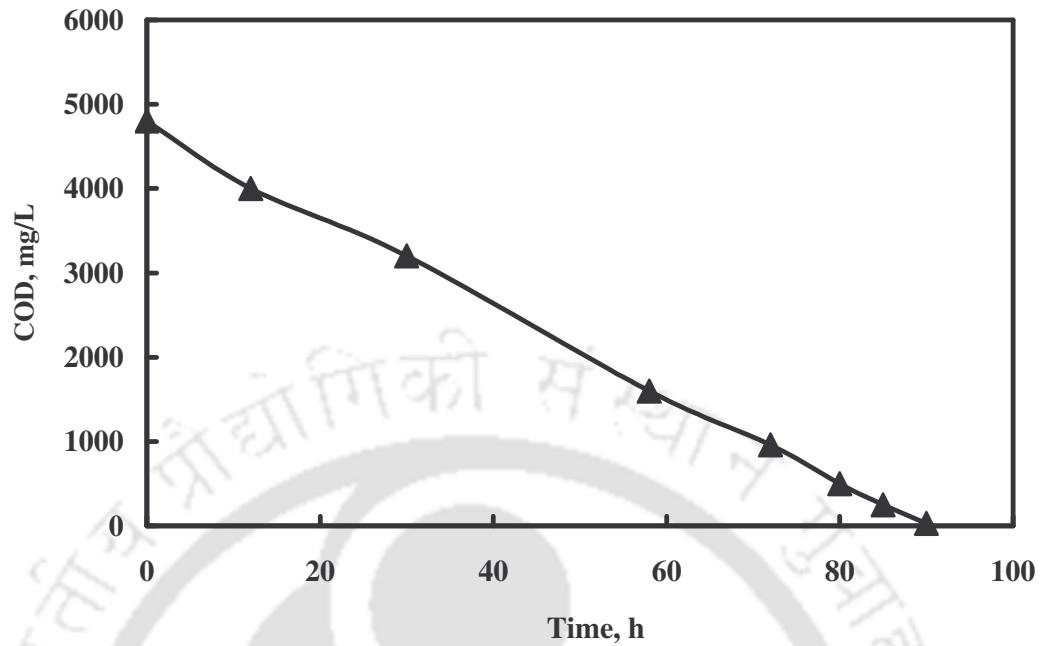


Fig. 4.21: COD removal profile of the pH adjusted refinery wastewater as a function of time.

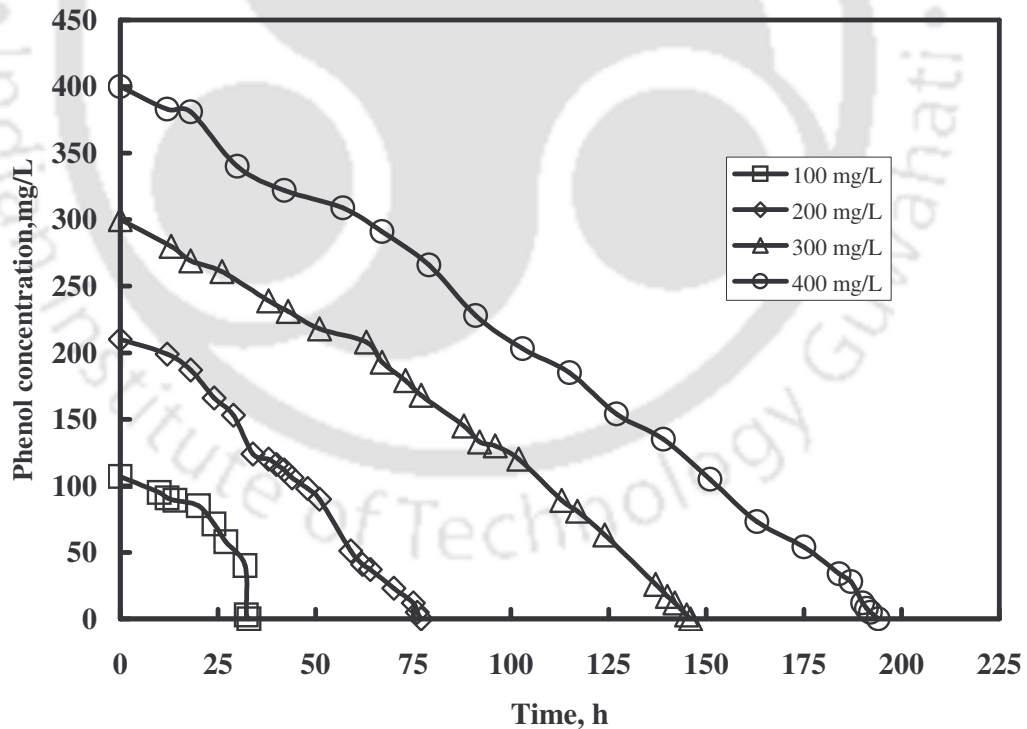


Fig. 4.22: Time profile of phenol degradation at different initial phenol concentrations in the BSTR.

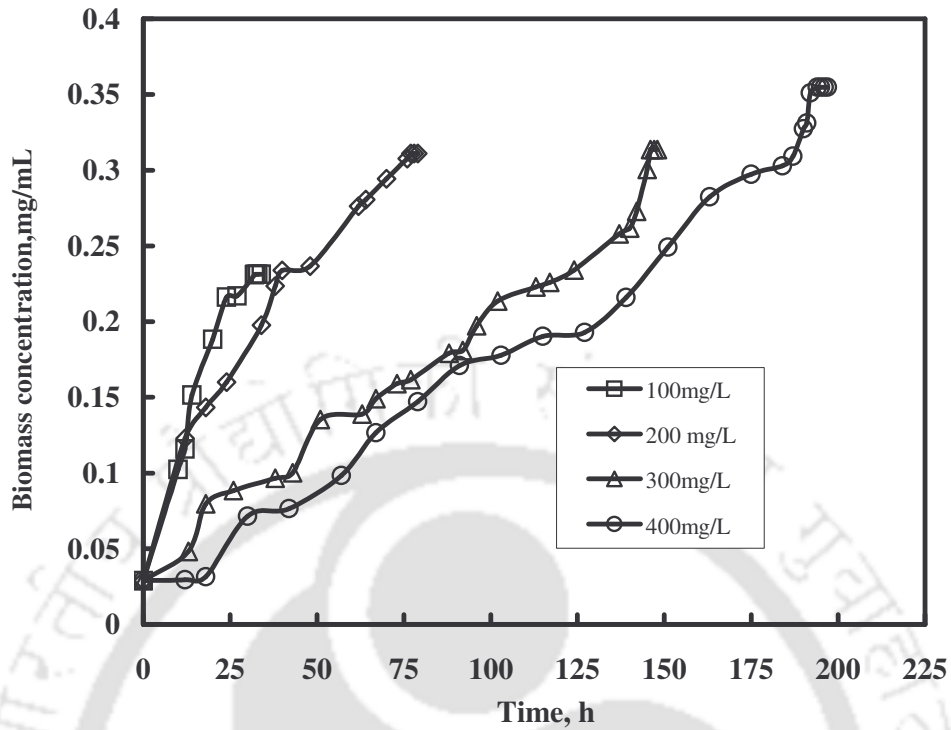


Fig. 4.23: Time profile of biomass output at different initial phenol concentrations in the BSTR.

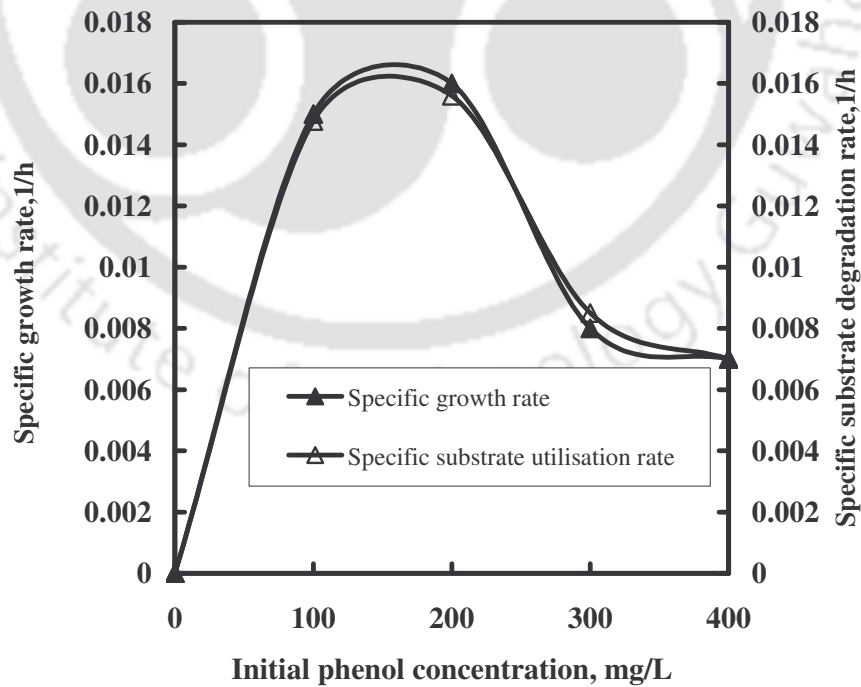


Fig. 4.24: Comparison of specific growth and substrate degradation rates at different initial phenol concentrations.

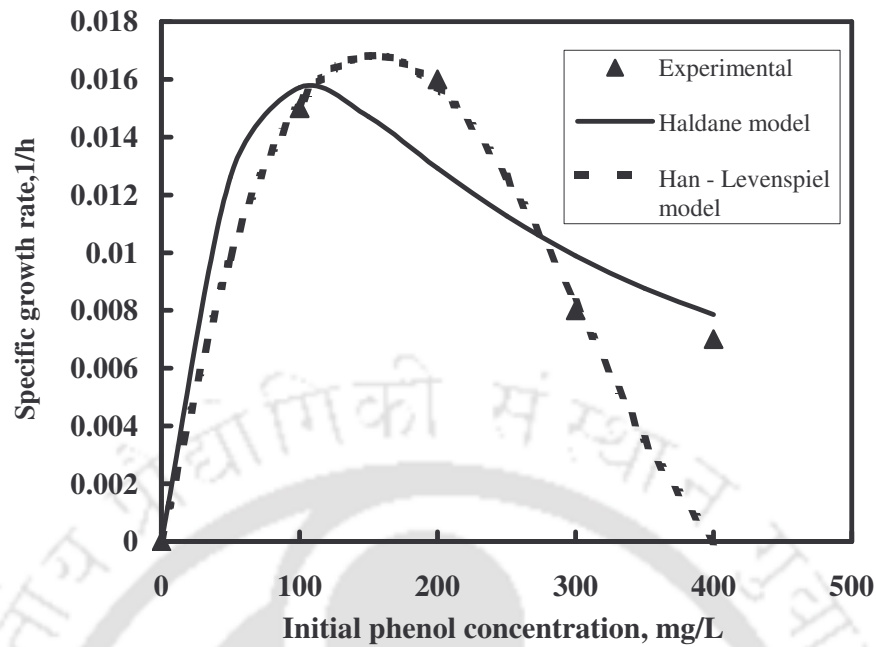


Fig. 4.25: Experimental and predicted specific growth rate of the culture obtained by applying Haldane and Han-Levenspiel substrate inhibition models.

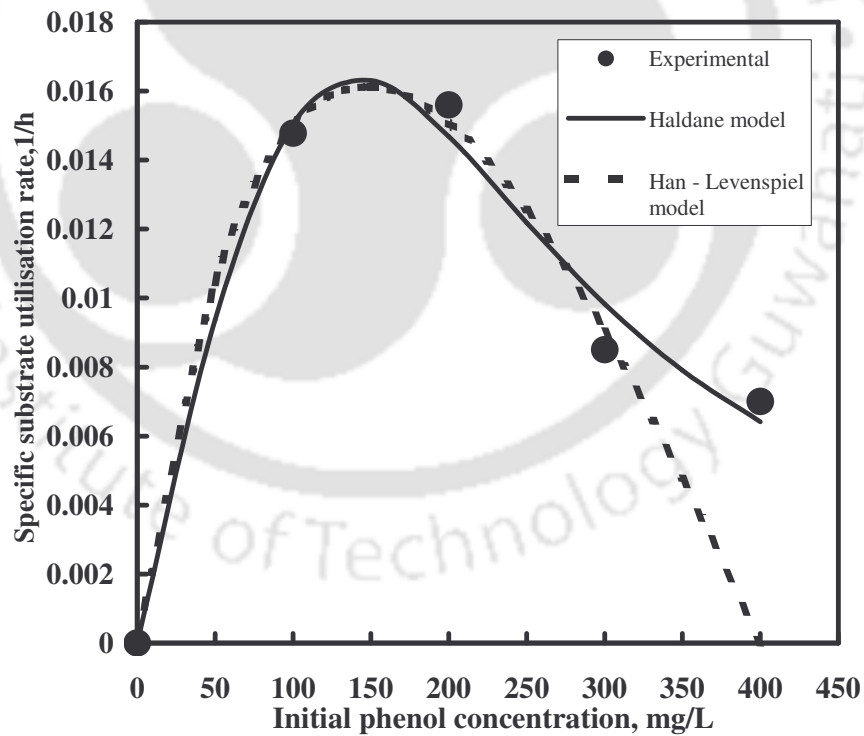


Fig. 4.26: Experimental and predicted specific substrate degradation rate obtained by applying Haldane and Han-Levenspiel substrate inhibition models.

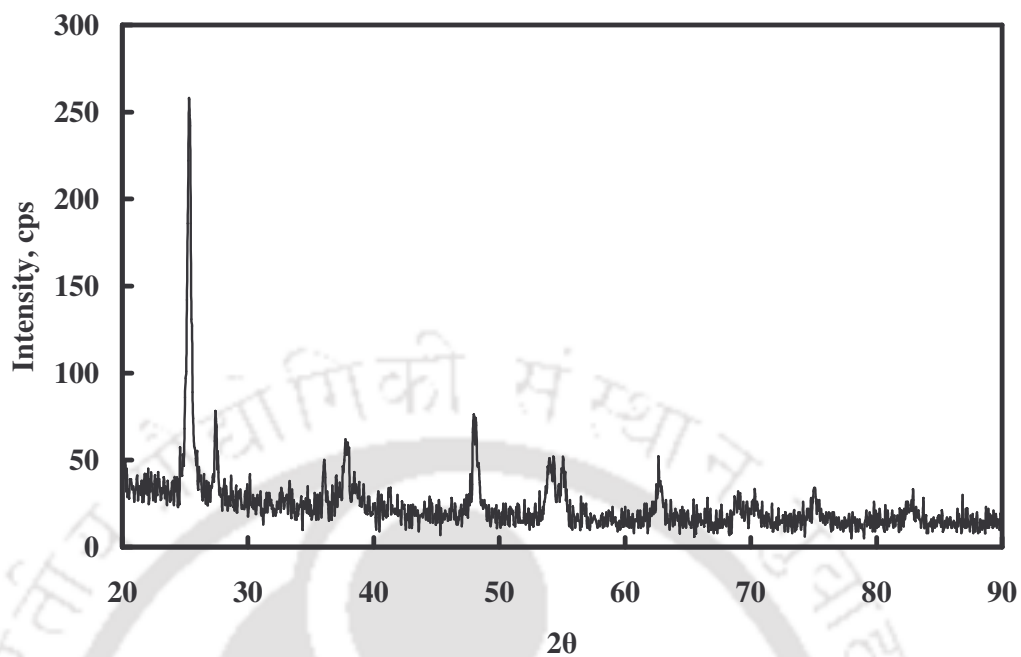


Fig. 4.27: XRD pattern of the Anjatox[®] TiO₂ photocatalyst.

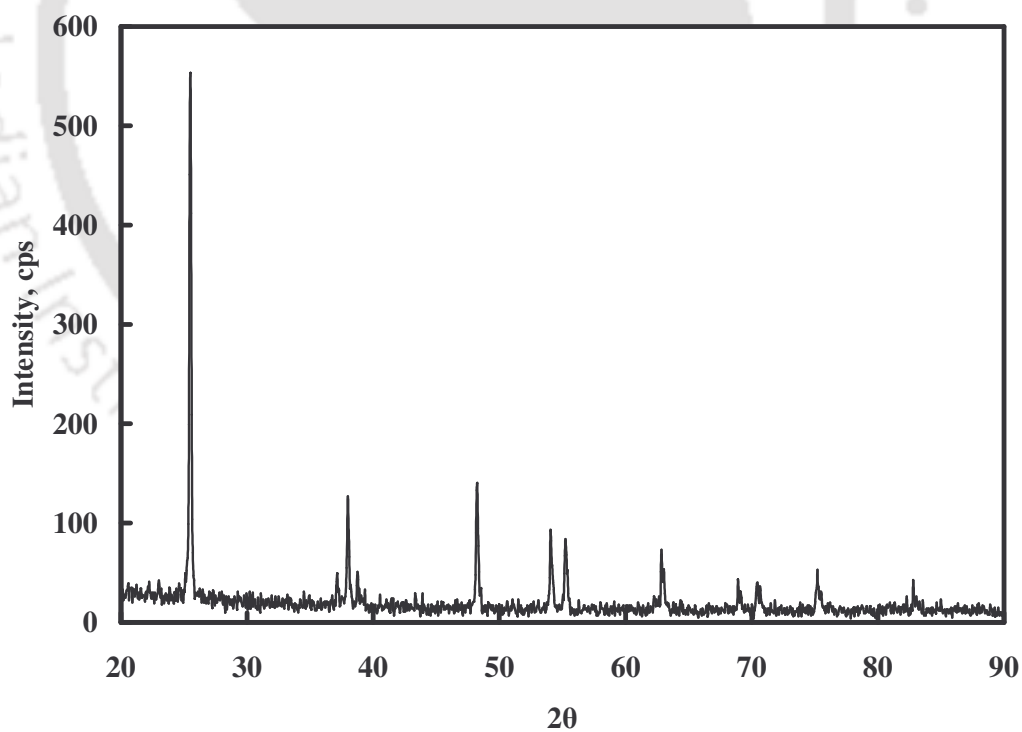


Fig. 4.28: XRD pattern of the Degussa P-25[®] TiO₂ photocatalyst.

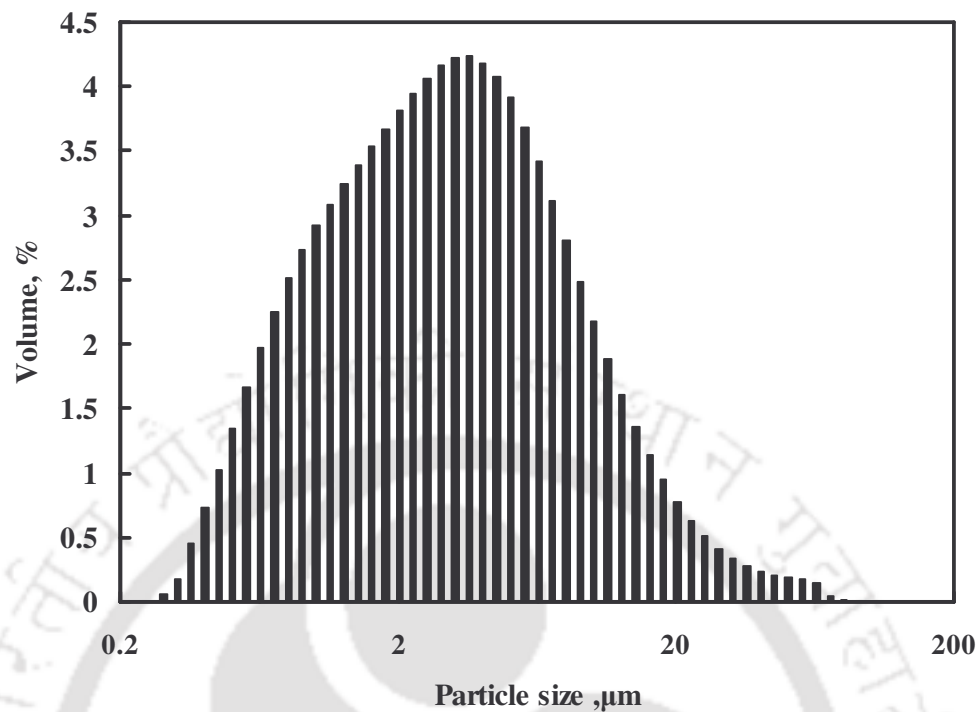


Fig. 4.29: Particle size distribution of Degussa P-25[®] TiO₂ photocatalyst.

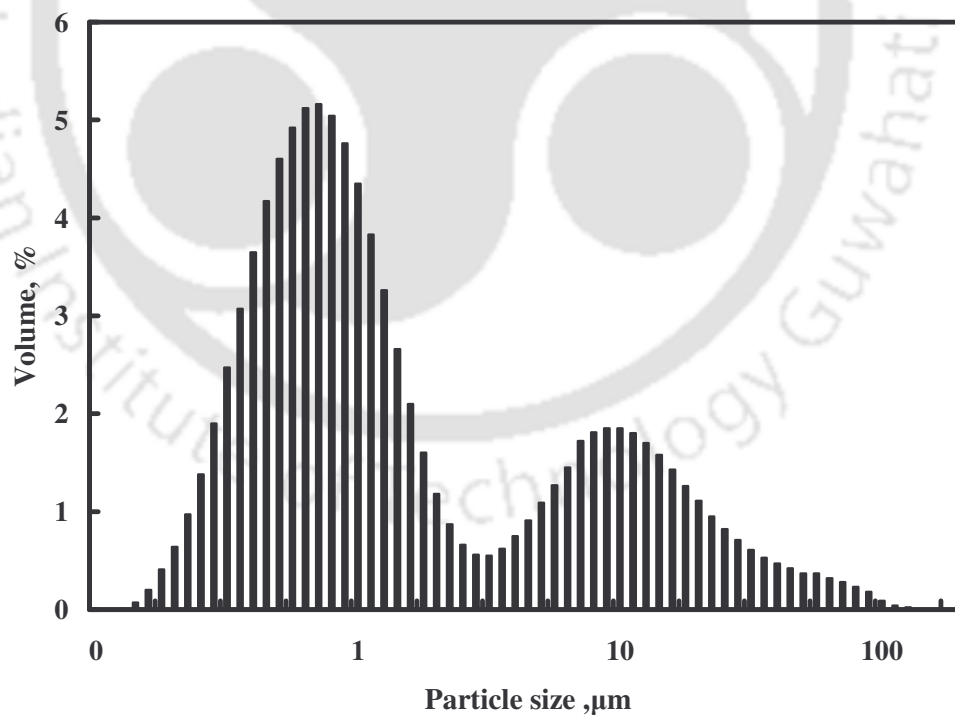


Fig. 4.30: Particle size distribution of Anjatox[®] TiO₂ photocatalyst

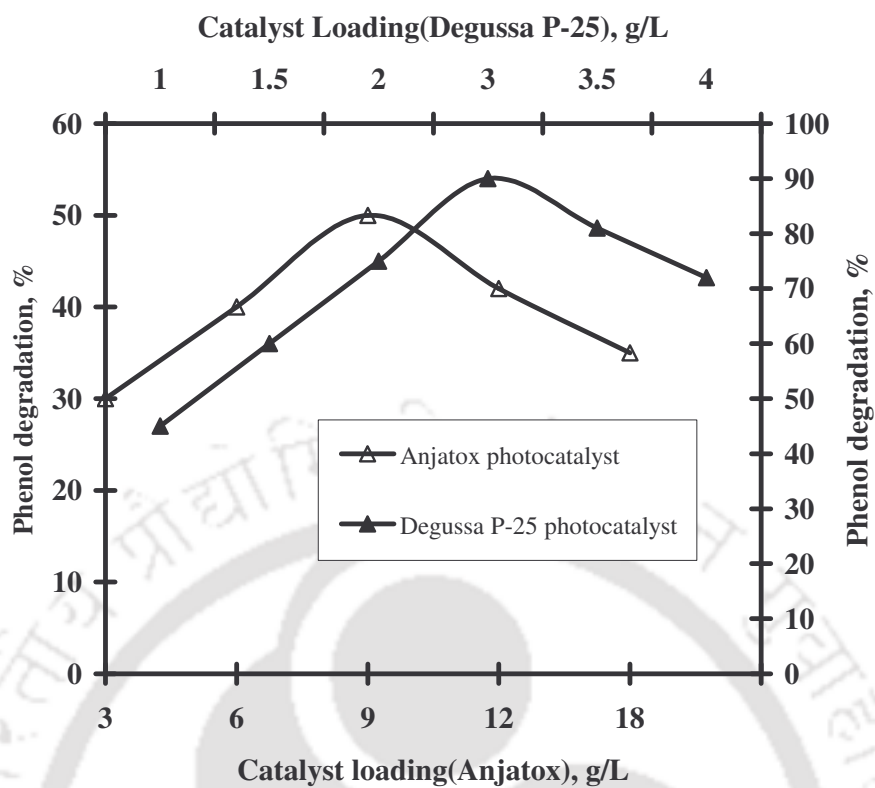


Fig. 4.31: Effect of concentration of Anjatox[®] and Degussa P-25[®] TiO₂ photocatalysts on phenol degradation (Initial phenol concentration = 100 mg/L).

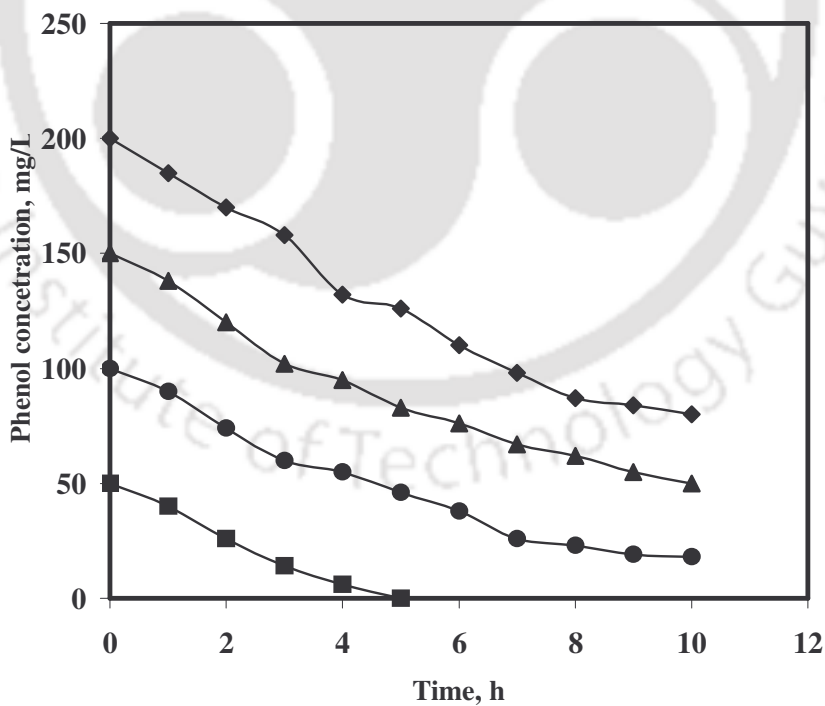


Fig. 4.32: Effect of initial concentration of phenol on its degradation using Degussa P-25[®] TiO₂ at an optimum concentration of 3 g/L.

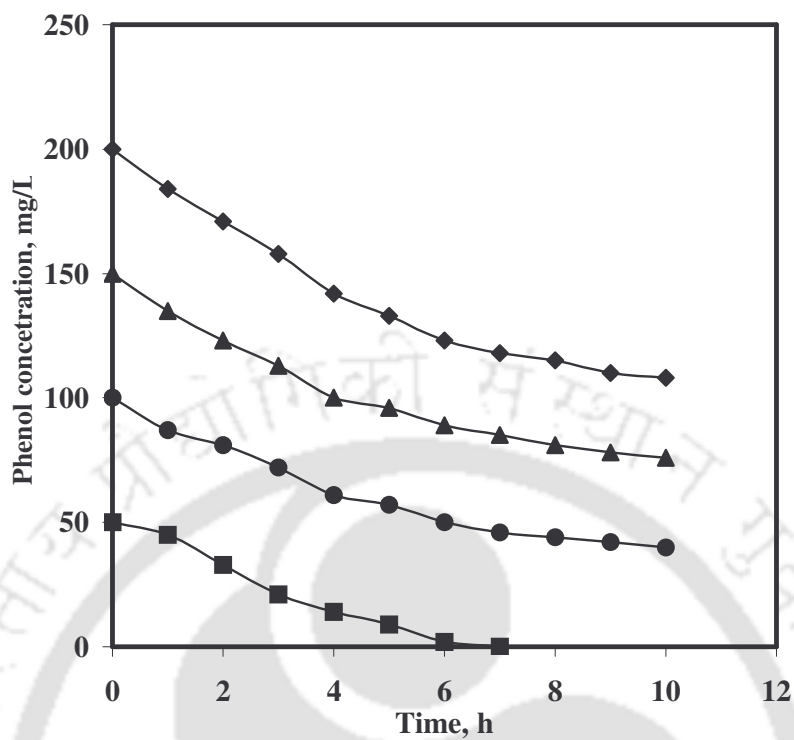


Fig. 4.33: Effect of initial concentration of phenol on its degradation using Anjatox[®] TiO₂ at an optimum concentration of 9 g/L.

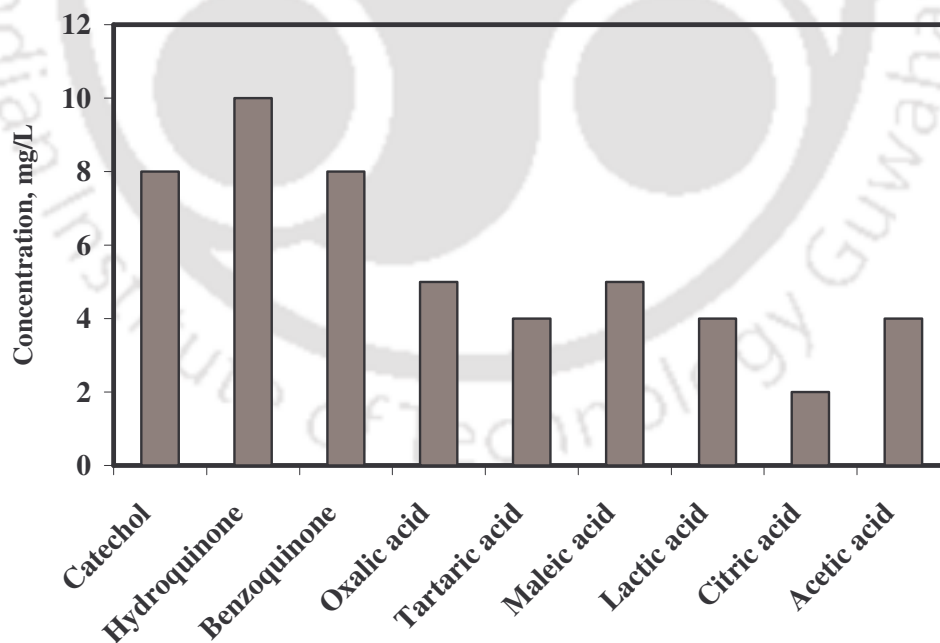


Fig 4.34: Intermediates identified in the photocatalytic degradation along with its concentrations (Initial phenol concentration = 100 mg/L).

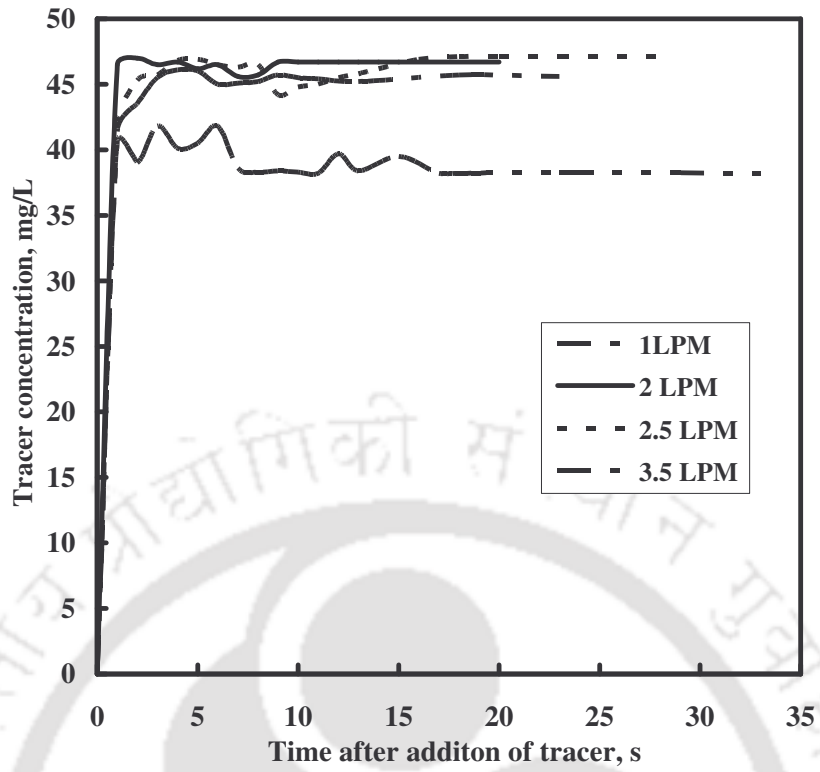


Fig. 4.35: Results of RTD in the ILALR at various superficial gas flow rate.



Fig. 4.36: Photograph of the bubble used for the analysis.

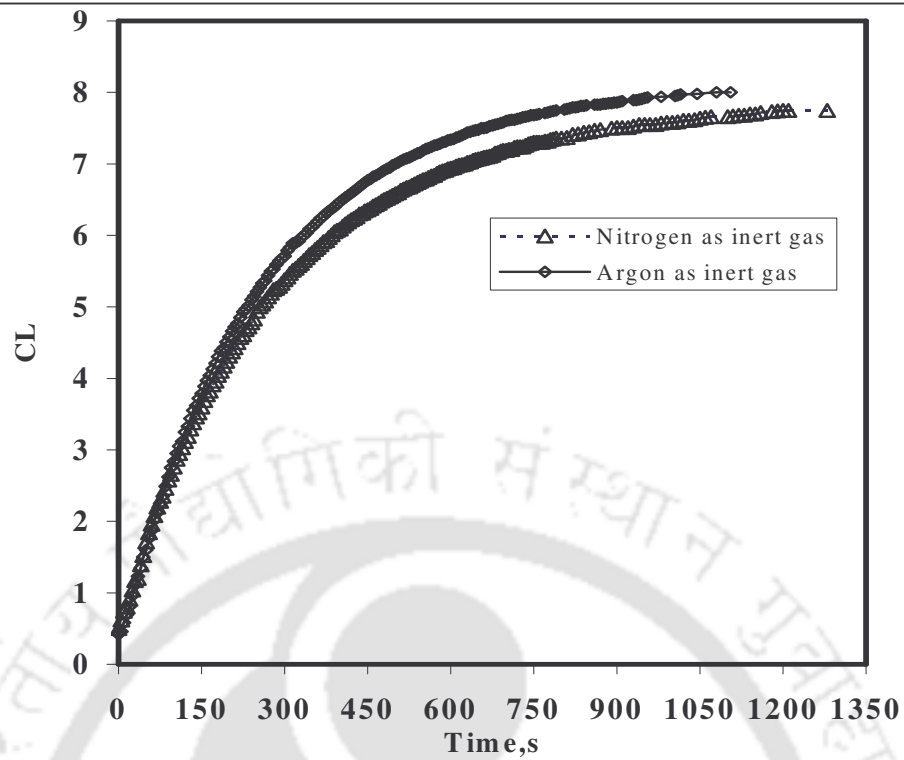


Fig. 4.37: DO profile (C_L) in estimating k_La in the ILALR for a non-living system by the dynamic gassing out method (superficial airflow rate = 2 L/min).

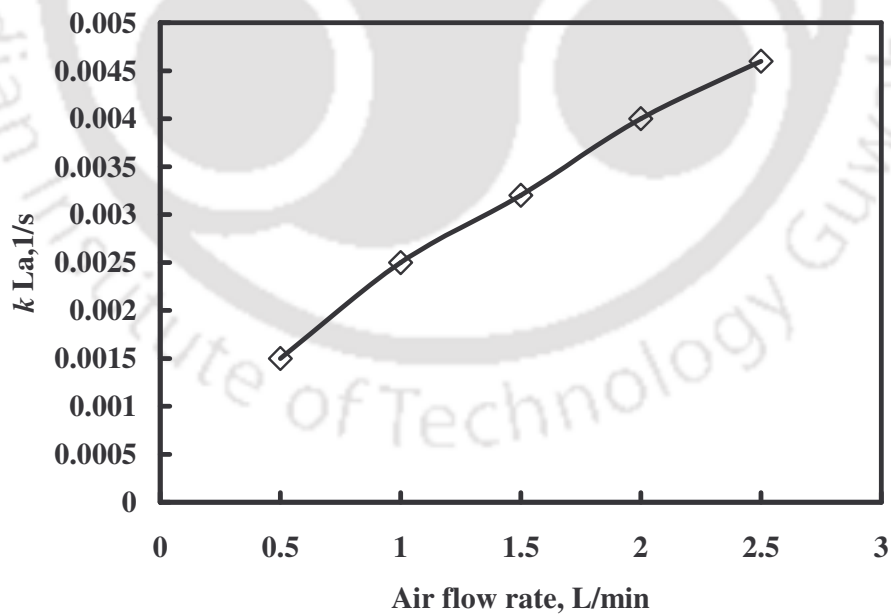


Fig. 4.38: Variation of k_La in the ILALR for non-living system at different superficial airflow rates.

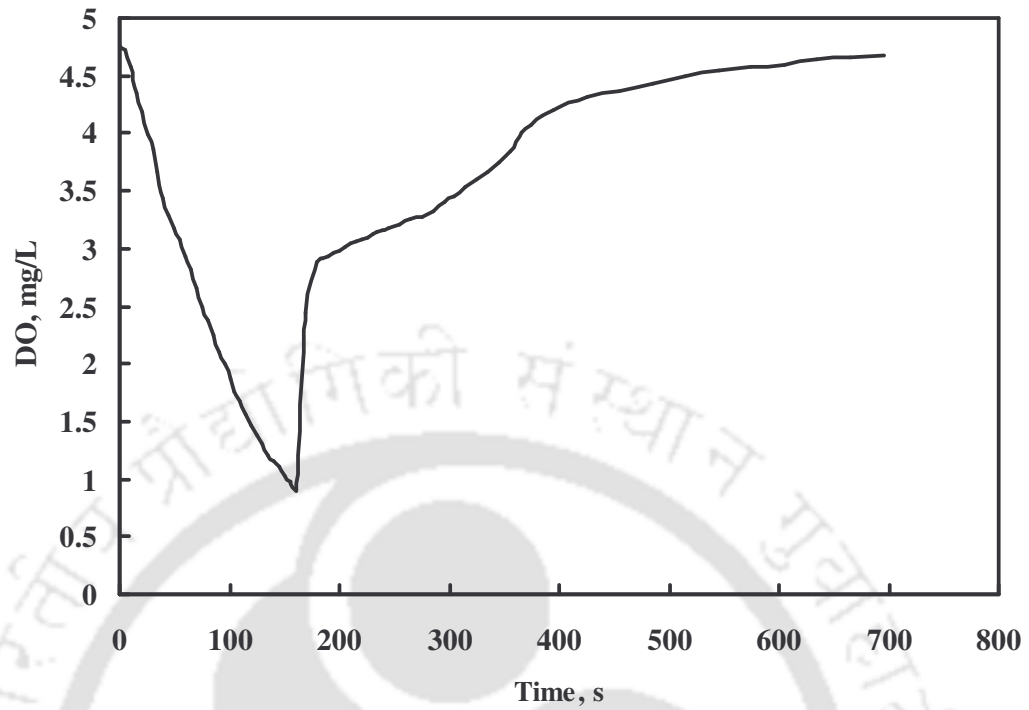


Fig. 4.39: DO profile (C_L) obtained by the dynamic gassing out method in estimating $k_L a$ in the ILALR for a living system (superficial airflow rate = 2 L/min).

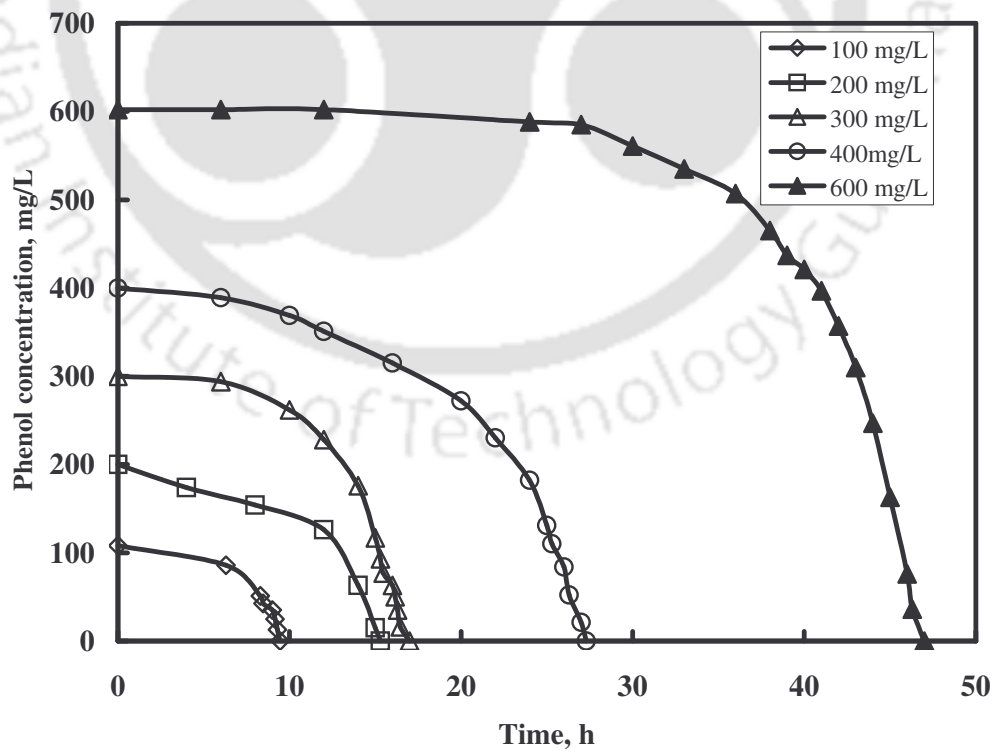


Fig. 4.40: Batch biodegradation profile of phenol obtained in the ILALR.

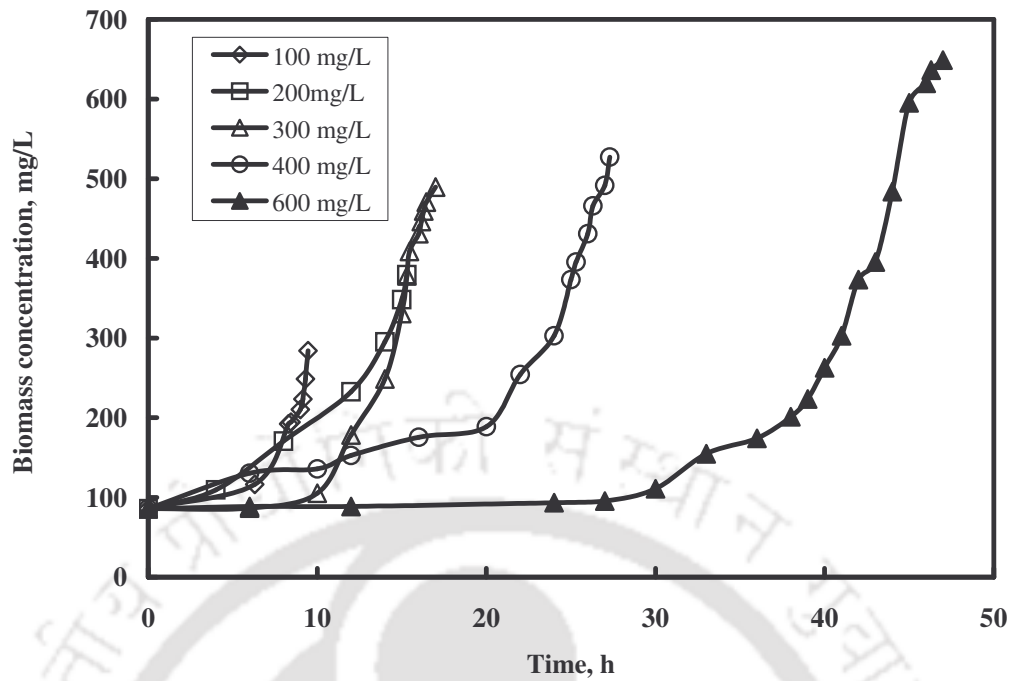


Fig. 4.41 Biomass profile of the culture obtained at various initial phenol concentrations in the batch operated ILALR.

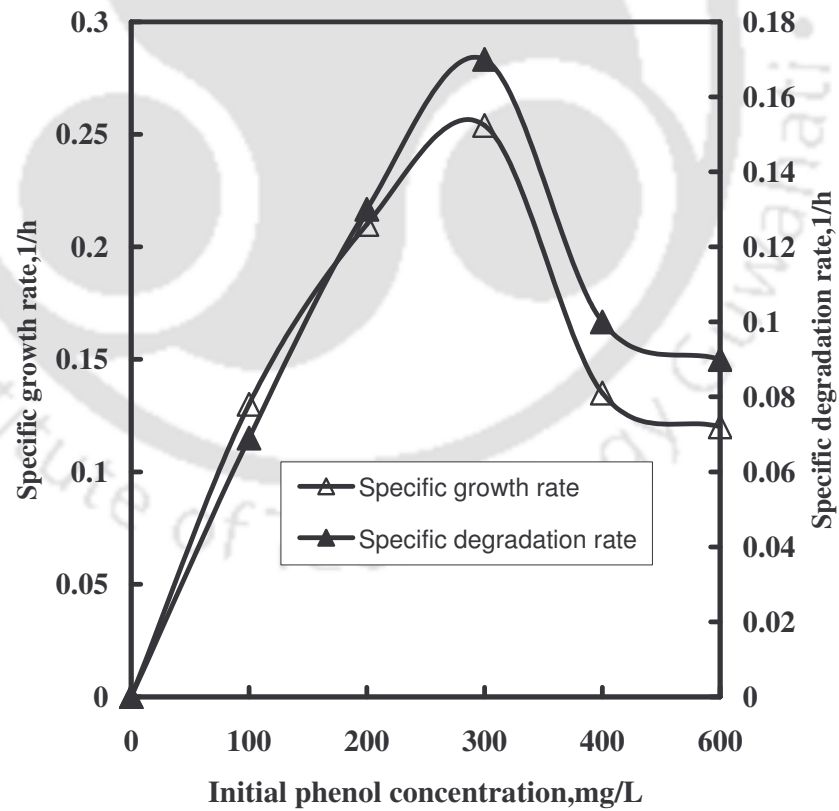


Fig. 4.42: Comparison of specific growth and degradation rates at different initial phenol concentrations in the ILALR.

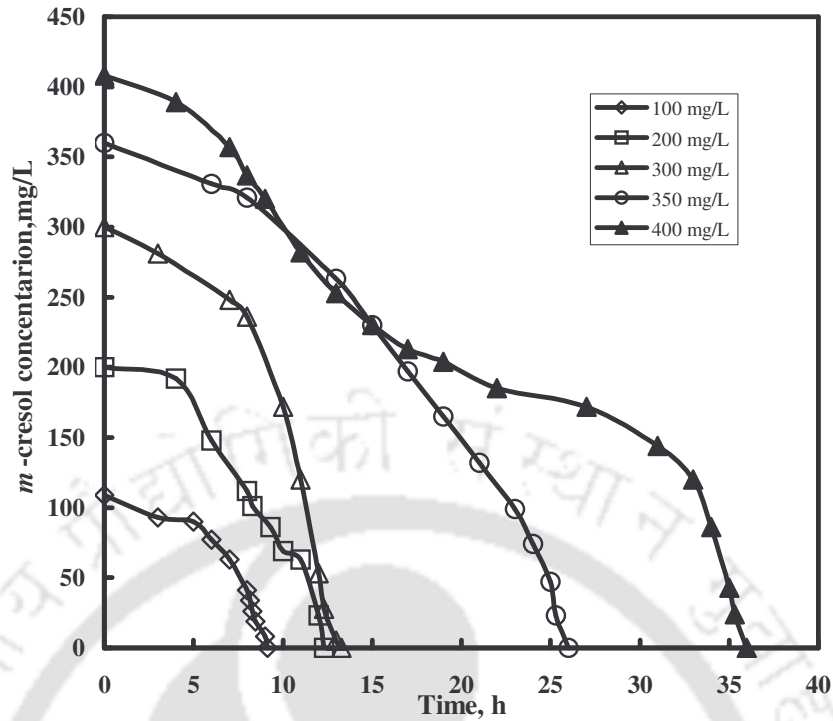


Fig. 4.43: Batch biodegradation profile of *m*-cresol obtained in the ILALR.

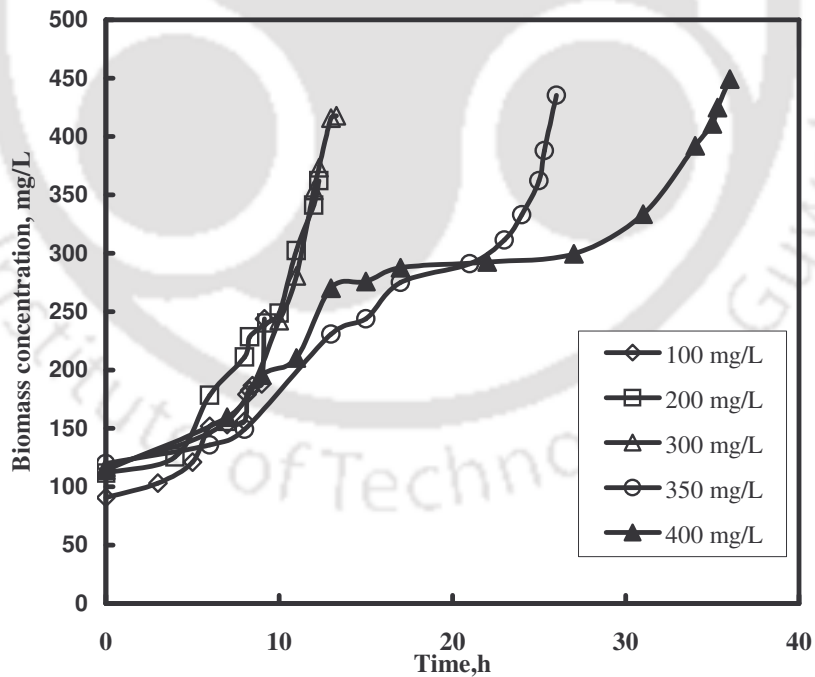


Fig. 4.44: Biomass profile of the culture obtained at various initial *m*-cresol concentrations in the batch operated ILALR.

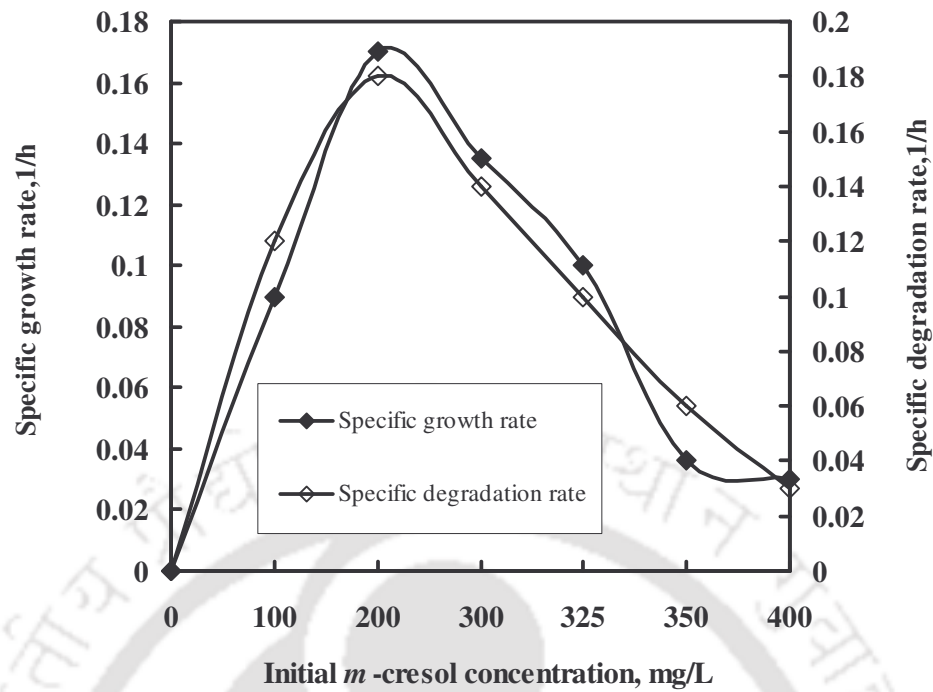


Fig. 4.45: Comparison of specific growth and degradation rates at different initial *m*-cresol concentrations in the ILALR.

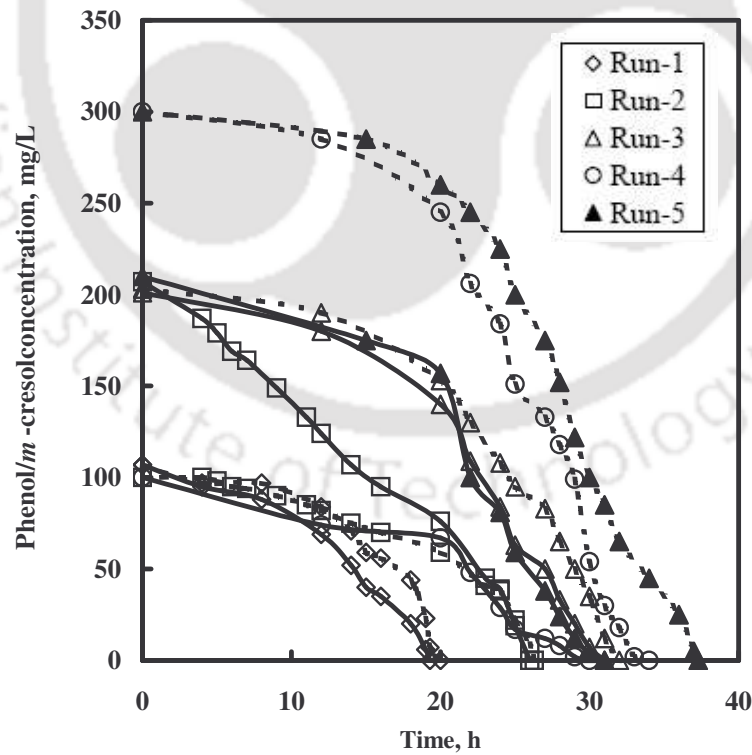


Fig. 4.46: Biodegradation patterns of phenol and *m*-cresol in the mixed substrate system in the ILALR [(—) Phenol; (-----) *m*-cresol].

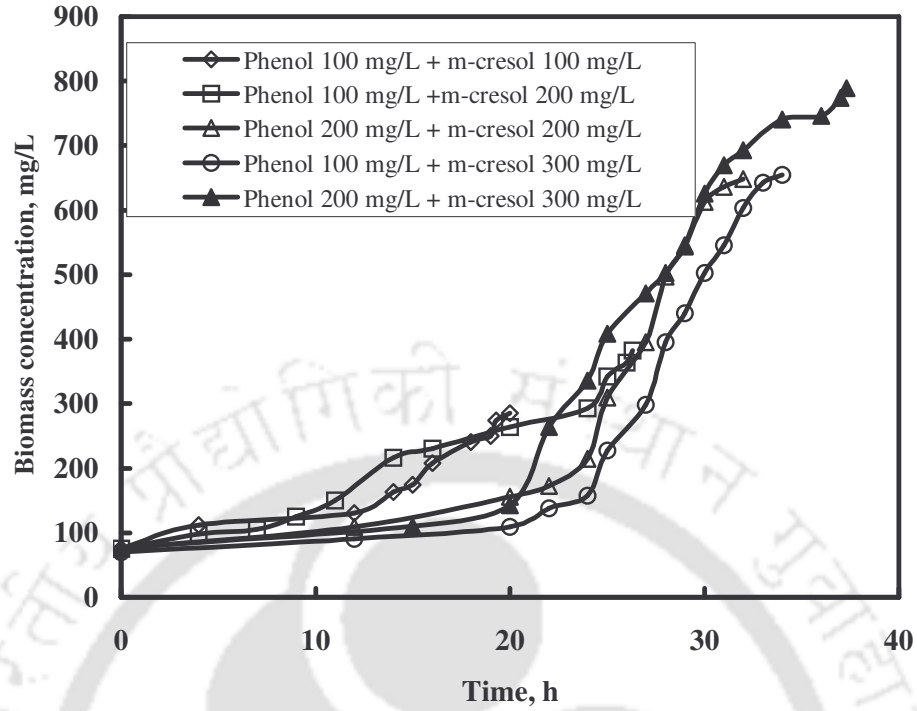


Fig. 4.47: Biomass concentration profile due to phenol and *m*-cresol in the mixed substrate system in the ILALR.

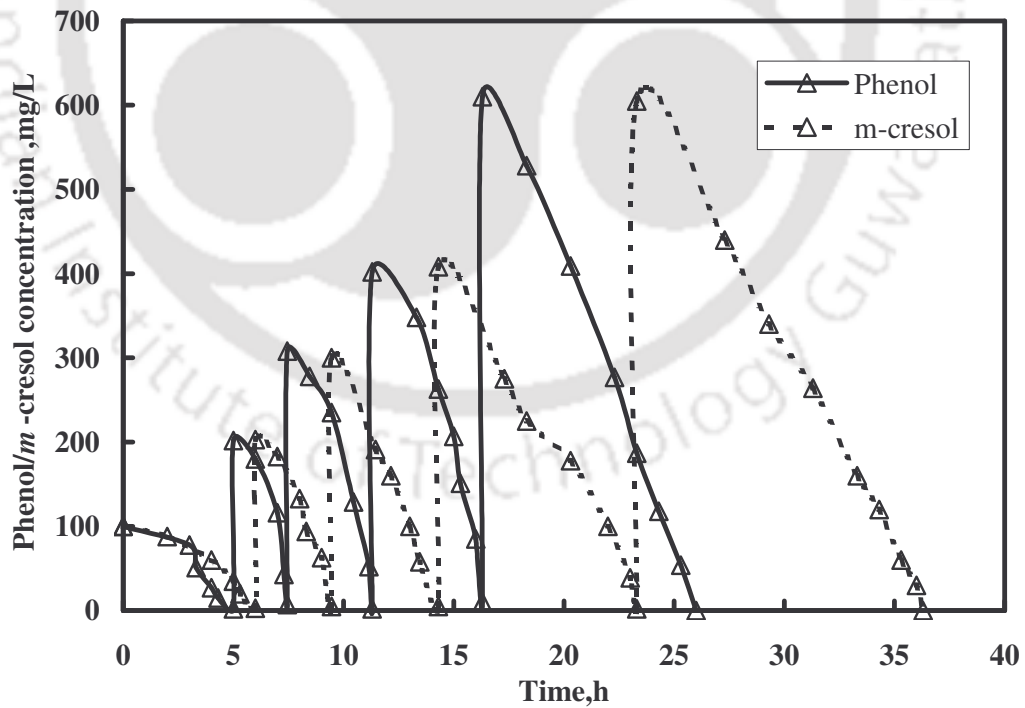


Fig. 4.48: Biodegradation of phenol and *m*-cresol as single substrate system in the fed-batch operated ILALR

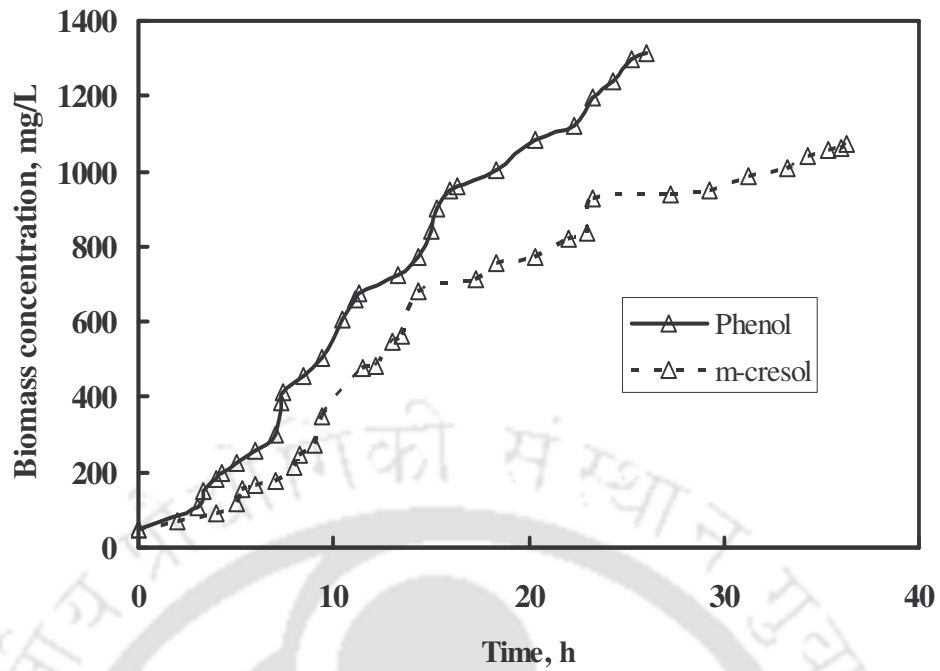


Fig. 4.49: Biomass profile obtained in the fed-batch operated ILALR during degradation of phenol and *m*-cresol in single substrate system.

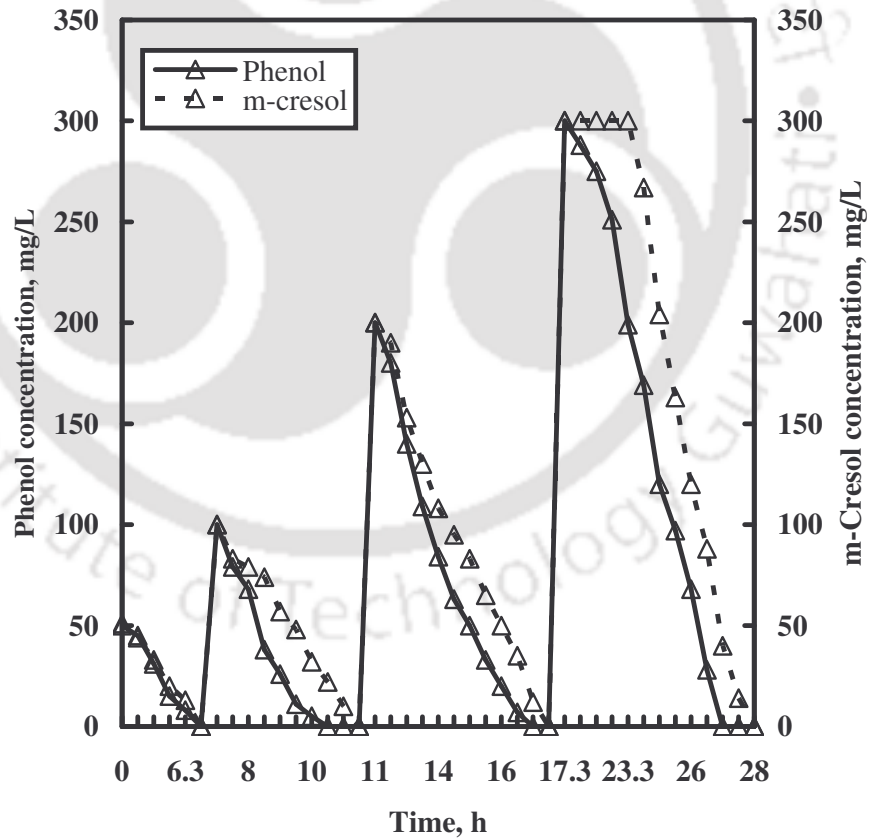


Fig. 4.50: Biodegradation of phenol and *m*-cresol in mixed substrate system in the ILALR operated under fed-batch mode.

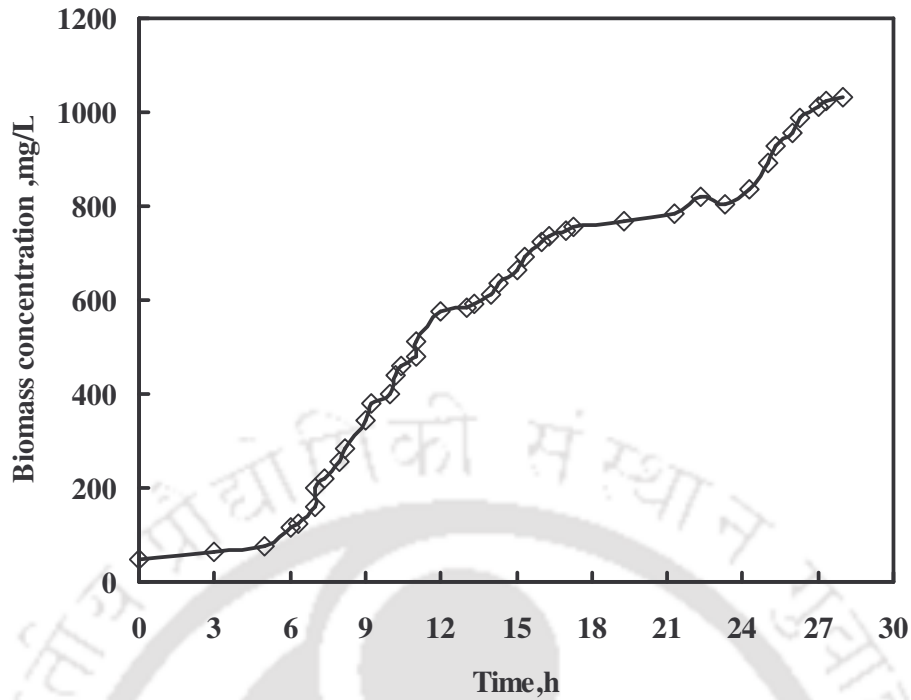


Fig. 4.51: Biomass profile of the culture in mixed substrate system in the fed-batch operated ILALR.

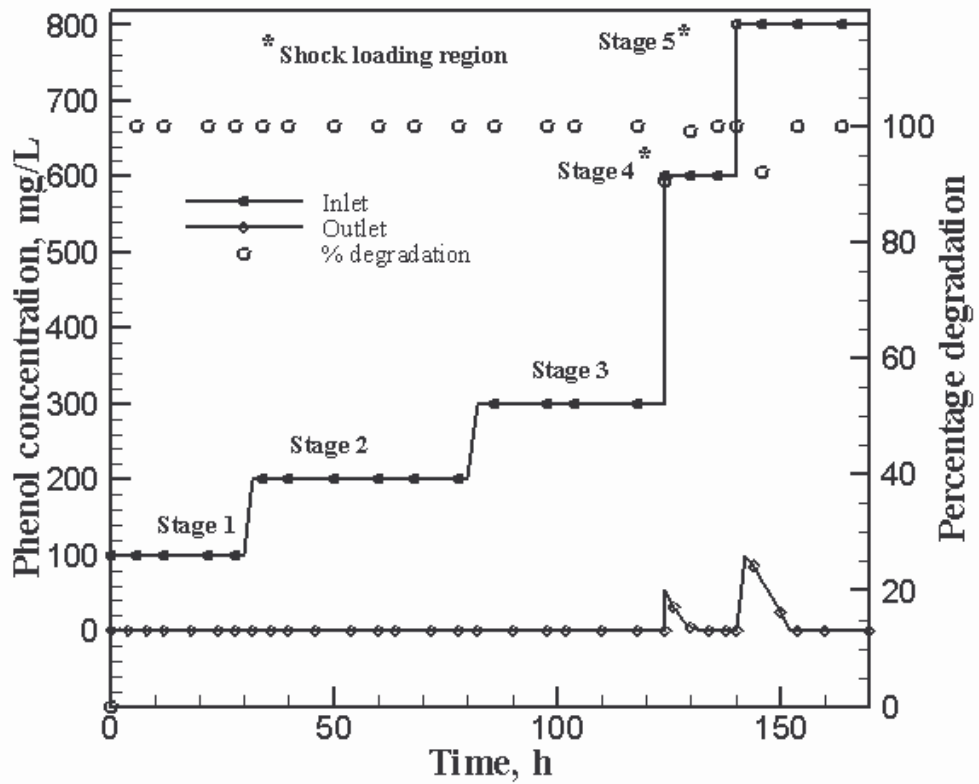


Fig.4.52: Phenol degradation in single substrate system in the continuously operated ILALR at 8.3 h HRT along with the shock loading effect in the reactor.

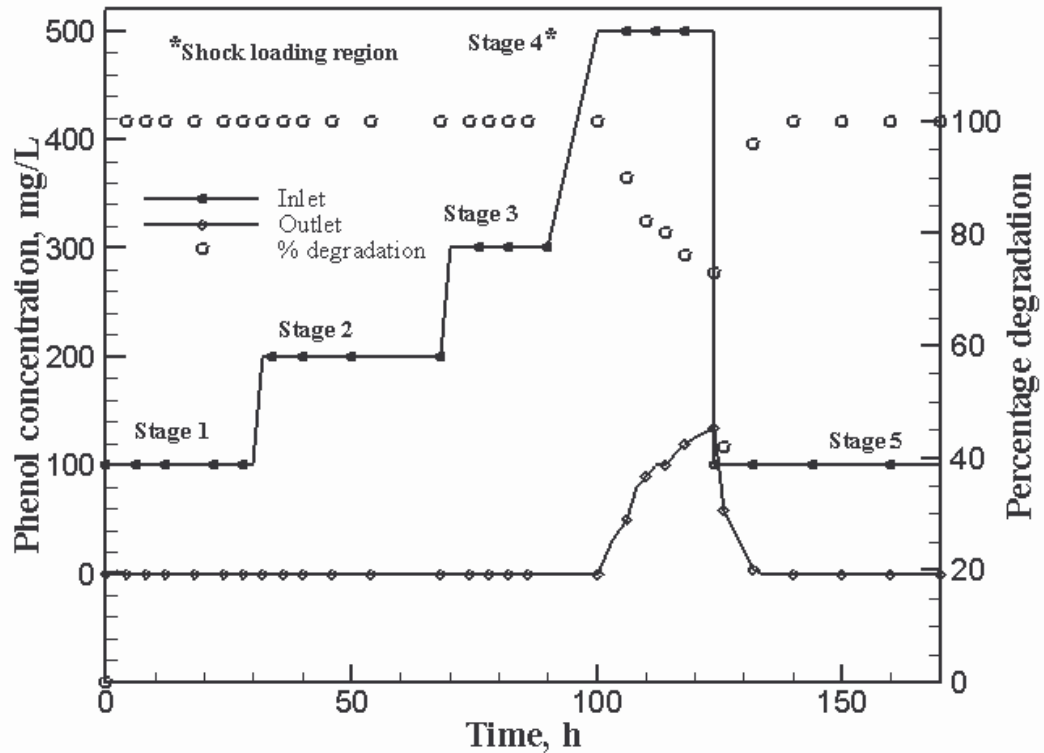


Fig.4.53: Phenol degradation in single substrate system in the continuously operated ILALR at 4.1 h HRT along with the shock loading effect in the reactor.

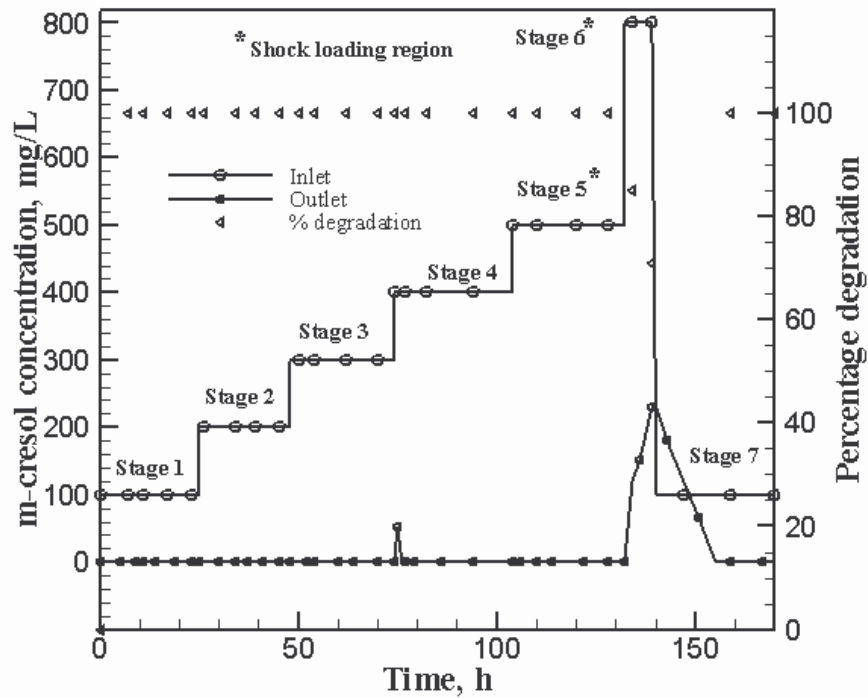


Fig.4.54: *m*-Cresol degradation in single substrate system in the continuously operated ILALR at 8.3 h HRT along with the shock loading effect in the reactor.

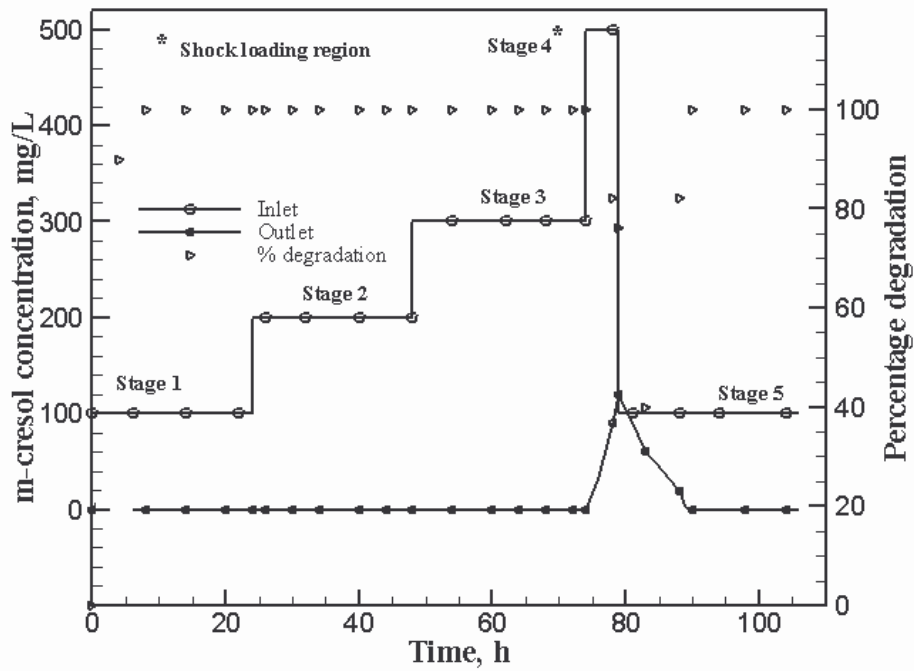


Fig.4.55: *m*-Cresol degradation in single substrate system in the continuously operated ILALR at 4.1 h HRT along with the shock loading effect in the reactor.

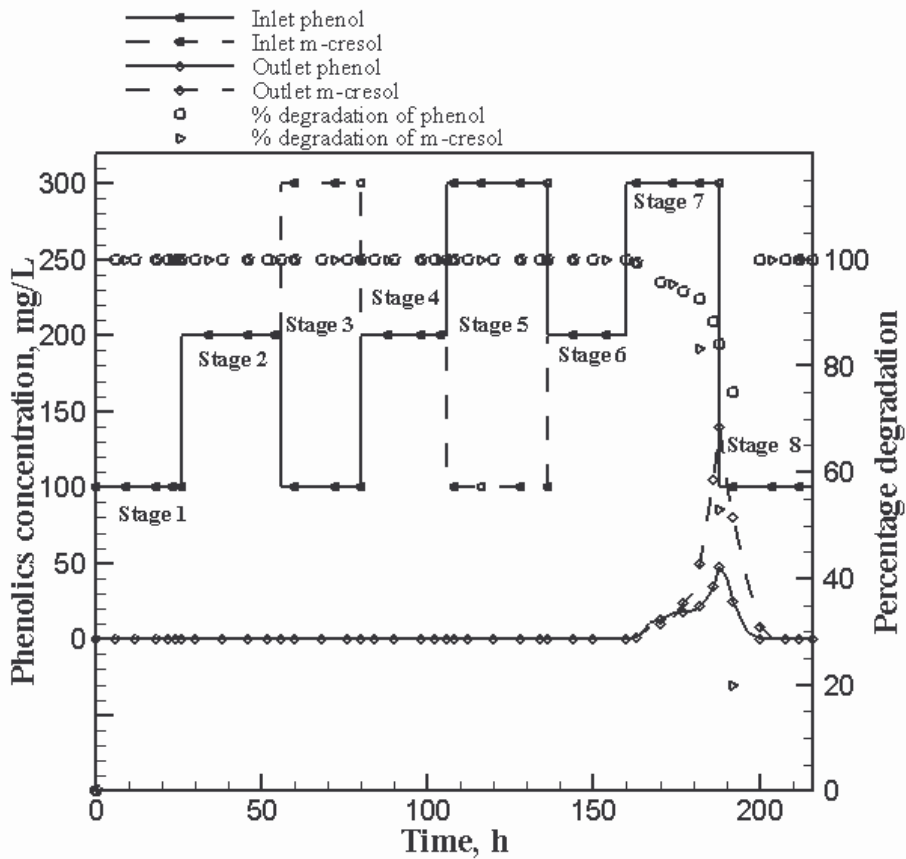


Fig.4.56: Degradation of phenol and *m*-cresol in mixed substrate system in the continuously operated ILALR at 8.3 h HRT

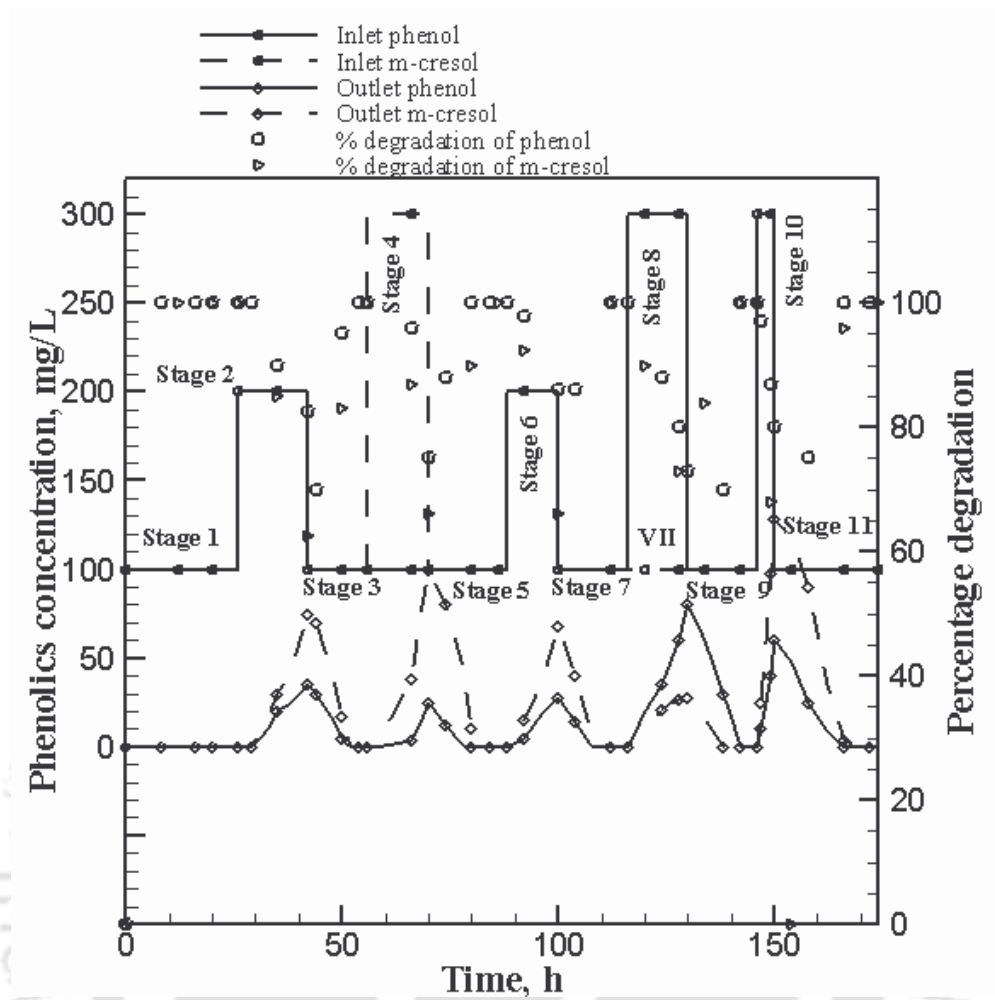


Fig.4.57: Degradation of phenol and *m*-cresol in mixed substrate system in the continuously operated ILALR at 4.1 h HRT

CHAPTER 5

SUMMARY AND CONCLUSIONS

- ❖ Phenol and *m*-cresol were identified as two major phenolic pollutants that emanate from various industrial effluents. An efficient treatment method for these pollutants is sought.
- ❖ An indigenous mixed microbial culture was isolated from a sewage treatment plant and enriched/acclimatized to grow and degrade phenolic compounds – phenol and *m*-cresol. The microbial culture was identified to be predominantly *Pseudomonas* spp. by staining, complete biochemical characterization tests and scanning electron microscopy.
- ❖ Batch degradation studies were carried out with the individual phenolic compounds at initial concentrations ranging from 100 – 800 mg/L (for phenol) and 100 – 900 mg/L (for *m*-cresol). The study conducted in batch shake flasks showed that phenol was degraded faster than *m*-cresol by the culture.
- ❖ Intermediates analyzed during phenol degradation by the culture were very less in amount; however, they were totally absent at the end of the degradation time.
- ❖ Mixed substrate with various combinations of initial concentrations of phenol and *m*-cresol were tested for finding the ability of the mixed culture to grow and degrade these compounds simultaneously in batch shake flasks. Experiments in

this particular study were based on statistically planned full factorial design of experiments. The obtained results were interpreted statistically in the form of ANOVA and student 't' test, which rendered useful interpretations of the main and interaction effects of the two substrates on their degradations as well as the culture growth.

- ❖ The bio-kinetic parameters such as maximum specific growth rate (μ_m), half saturation constant (K_s) and inhibition coefficient (K_i) were estimated from suitable substrate inhibition models by fitting these models to the experimental data on specific growth rate of the culture obtained in the single substrate degradation studies. Interaction parameters for phenol and *m*-cresol degradation were also estimated by fitting the sum kinetics model to the data obtained in the mixed substrate degradation system.
- ❖ An industrial wastewater sample from a petroleum refinery containing considerably high carbonaceous oxygen demand (COD) was tested for evaluating the potential of the mixed culture in treating a real industrial effluent. Complete removal of COD was obtained in the process.
- ❖ Phenol degradation by three different reactor systems – batch stirred tank reactor and internal loop airlift reactor (ILALR), both employing the acclimatized mixed microbial culture and a photo catalytic reactor were studied under batch operational mode. Among the three lab scale reactors operated under batch mode, ILALR was found to be most efficient in degrading phenol.
- ❖ Procedure for identifying the best set of mixing and aeration conditions in the ILALR has been suggested based on the hydrodynamic studies. The same settings were applied for operating the ILALR for biodegradation studies under batch, fed-batch and continuous modes.

- ❖ Degradation of phenol and *m*-cresol, under batch, fed-batch and continuous modes of operation were performed in the ILALR employing the mixed culture. The performance of the ILALR was evaluated by the removal efficiency of the pollutant(s). The ILALR batch study showed a good potential in degrading the phenol and *m*-cresol in both single and mixed substrate systems. The scale up study with the ILALR of 2.5 L working volume showed similar performance to that of the batch shake flask study with 100 mL working volume. However, substrate inhibition due to *m*-cresol above 300 mg/L severely affected its performance in single and mixed substrate systems in the batch operated ILALR.
- ❖ Operating the ILALR under fed-batch mode proved highly efficient in degrading phenolics at much high concentration compared to simple batch operation of the reactor thus overcoming the problem of substrate inhibition due to the phenolics at high concentrations.
- ❖ The performance of the ILALR in continuous operation was found to be good with a maximum phenolics degradation efficiency of 100% at both the HRTs of 8.3 h and 4.1 h. There were only slight fluctuations in the degradation efficiency in case of mixed substrate system, which was nevertheless found only at higher concentrations.
- ❖ Stability of the reactor was evaluated by subjecting the ILALR to operations leading to intermittent and shock loading conditions. Under these conditions with a concentration as high as 800 mg/L of phenol and 500 mg/L of *m*-cresol at both the HRTs (8.3 and 4.1 h), the reactor was nearly stable in its performance.

Scope for Future Work

- 1) Studies with real industrial wastewater to evaluate and optimize airlift bioreactor for field application.
- 2) Identification of the exact bacterial strains of the mixed *Pseudomonas* spp. by precise molecular techniques.
- 3) Evaluation of a hybrid treatment system containing photocatalytic oxidation coupled with the biological process in phenol degradation.
- 4) Mathematical modeling of the biodegradation of the phenolics in the continuously operated ILALR for better understanding and predictability of the system performance.
- 5) A new mathematical model for kinetics studies could be development.

BIBLIOGRAPHY

Abuhamed, T., Bayraktar, E., Mehmetoğlu, T. and Mehmetoğlu, U. (2004) Kinetics model for the growth of *Pseudomonas putida* F1 during benzene, toluene and phenol biodegradation. *Process Biochemistry* 39(8): 983-988.

Aday, S.S., Chen, M. Y., Lee, D.J. and Ren, N. O. (2007) Degradation of phenol by *Acinetobacter* strain isolated from aerobic granules. *Chemosphere* 67(8): 1566-1572.

Alexander, M. (1999) Biodegradation and bioremediation, Academic press, United Kingdom.

Alnaizy, R. and Akgerman, A. (2000) Advanced oxidation of phenolic compounds. *Advances in Environmental Research* 4(3): 233-244.

Annettone, J.P.G. (2006) Hydrodynamics of two – phase in a deep airlift reactor, PhD thesis, University of Minnesota, USA.

Anselmo, A. M., Mateus, M., Cabral, J. M. S. and Novais, J. M. (1985) Degradation of phenol by immobilized cells of *Fusarium flocciferum*. *Biotechnology Letters* 7(12): 889-894.

Bahnemann D.W. (2004) Photocatalytic water treatment: solar energy applications. *Solar Energy* 77(5): 445-459.

Bahnemann, D.W., Bockelmann, D. and Goslich, R. (1991) Mechanistic studies of water detoxification in illuminated TiO₂ suspensions. *Solar Energy materials* 24(1-4): 564-583.

Bai, J., Wen, J.P., Li, H.M. and Jiang Y. (2007) Kinetic modeling of growth and biodegradation of phenol and *m*-cresol using *Alcaligenes faecalis*. *Process Biochemistry* 42(4): 510-517.

Bandyopadhyay B, Humphery A.E. and Taguchi H. (1967) Dynamic measurement of the volumetric oxygen transfer coefficient in fermentation systems. *Biotechnology and Bioengineering* 9(4): 533-544.

Banerjee, I., Modak, J.M., Bandopadhyay, K., Das, D. and Maiti, B.R. (2001) Mathematical model for evaluation of mass transfer limitations in phenol biodegradation by immobilized *Pseudomonas putida*. *Journal of Biotechnology* 87(3): 211-223.

Barros L.M., Macedo, G.R., Duarte, M.M.L., Silva, E.P. and Lobato, A.K.C.L. (2003) Biosorption of cadmium using the fungus *Aspergillus niger*. *Brazilian Journal of Chemical Engineering* 20(3): 229-239.

Boudenne, J., Cercleir, O., Galéa, J. and Van Der Vlist, E. (1996) Electrochemical oxidation of aqueous phenol at a carbon black slurry electrode. *Applied Catalysis A: General* 143 (2): 185-202.

Brillas, E., Calpe, J.C. and Casado, J. (2000) Mineralization of 2,4-D by advanced electrochemical oxidation processes, *Water Research* 34 (8): 2253-2262.

Brillas, E., Sauleda, R. and Casado, J. (1998) Degradation of 4-chlorophenol by anodic oxidation, electro-Fenton, photo electro-Fenton and peroxicoagulation processes. *Journal of the Electrochemical Society* 145(3): 2253-2262.

Brown, A.E. (2001) Bensen's microbiological application, Laboratory manual in general microbiology. 5th edition. McGraw-Hill.

Brunner, W. and Focht, D.D. (1984) Deterministic three-half-order kinetics model for microbial degradation of added carbon substrates in soil. *Applied and Environmental microbiology* 47(1): 167-172.

Buswell, J. A. (1975) Metabolism of phenol and cresols by *Bacillus stearothermophilus*. *Journal of Bacteriology* 124(3): 1077-1083.

Calleja, G., Serna, J. and Rodríguez, J. (1993) Kinetics of adsorption of phenolic compounds from wastewater onto activated carbon. *Carbon* 31(5): 691-697.

- Camarasa, E., Carvalho, E., Meleiro, L.A.C., Filho, R.M., Domingues, A., Wild, G., Poncin, S., Midoulx, N. and Bouillard, J.** (2001) A hydrodynamic model for airlift reactors. *Chemical Engineering and Processing* 40(2): 121- 128.
- Cañizares, P., Domínguez, J. A., Rodrigo, M. A., Villaseñor, J. and Rodríguez, J.** (1999) Effect of the Current intensity in the electrochemical oxidation of aqueous phenol wastes at an activated carbon and steel anode. *Industrial and Engineering Chemistry Research* 38 (10): 3779-3785.
- Carmona, M.R., da Silva, MA.P. and Leite, S.G.F.** (2005) Biosorption of chromium using factorial experimental design. *Process Biochemistry* 40(2): 779-788.
- Clescerl, L. S., Greenberg, A. E. and Eaton, A D.** (Eds) Standard methods for the examination of water and wastewater. American public health association (APHA) 20th Edition
- Couvert, A., Bastoul, D., Roustan, M. and Chatellie, .P,** (2004) Hydrodynamics and mass transfer study in a rectangular three-phase airlift loop reactor. *Chemical Engineering and Processing* 43(11):1381-1387.
- Curcó, D., Malato, S., Blanco, J., Giménez, J. and Marco, P.** (1996) Photocatalytic degradation of phenol: Comparison between pilot-plant-scale and laboratory results. *Solar Energy* 56(5): 387-400.
- Dapaah, S.Y. and Hill, G.A.** (1992) Biodegradation of chlorophenol mixtures by *Pseudomonas putida*. *Biotechnology and Bioengineering* 40(11): 1353-1358.
- Dargaville, T. R., Guerzoni, F. N., Looney, M. G. and Solomon D. H.** (1996) The adsorption of multinuclear phenolic compounds on activated carbon. *Journal of Colloid and Interface Science* 182(1): 17-25.
- Dikshitulu, S., Baltzis, B. C., Lewandowski, G. A. and Pavlou, S.** (1993) Competition between two microbial populations in a sequencing fed-batch reactor: theory, experimental verification, and implications for waste treatment applications. *Biotechnology and Bioengineering* 42(5): 643-656.

Eckenfelder, W., Argaman, Y. and Miller, E. (1989) Process selection criteria for the biological treatment of industrial wastewaters. *Environmental Progress* 8(1): 40-45.

EPA (1998) Handbook Advanced Photochemical Oxidation Processes United States Environmental Protection Agency. Office of Research and Development Washington, USA.

Fang, H. H. P. and Zhou, G.M. (2000) Degradation of phenol and *p*-cresol in reactors. *Water Science and Technology* 42(5-6): 237-244.

Feng, W., Wen, J., Liu, C., Yuan, Q., Jia, X. and Sun, Y. (2007) Modeling of local dynamic behavior of phenol degradation in an internal loop airlift bioreactor by yeast *Candida tropicalis*. *Biotechnology Bioengineering* 97(2): 251 - 264.

Fox, M.A. and Dulay, M.T. (1993) Heterogeneous photocatalysis. *Chemical Reviews* 93(1):341-357.

Gaal, A. and Neujahr, H. Y. (1979) Metabolism of phenol and resorcinol in *Trichosporon cutaneum*. *Journal of Bacteriology* 137(1): 13-21.

Gallego, A., Fortunato, M.S., Foglia, J., Rossi, S., Gemini, V., Gomez, L., Gomez, C.E., Higa, L.E. and Korol S.E. (2003) Biodegradation and detoxification of phenolic compounds by pure and mixed indigenous cultures in aerobic reactors. *International Biodeterioration & Biodegradation* 52(4): 261-267.

García, G.I., Peña, P.R. J., Venceslada, J.L. B., Martín, A. M., Santos, M.A. M. and Gómez, E.R. (2000) Removal of phenol compounds from olive mill wastewater using *Phanerochaete chrysosporium*, *Aspergillus niger*, *Aspergillus terreus* and *Geotrichum candidum*. *Process Biochemistry* 35(8), 751-758.

Gernjak, W., Maldonado, M. I., Malato, S., Cáceres, J., Krutzler, T., Glaser, A. and R. Bauer (2004) Pilot-plant treatment of olive mill wastewater (OMW) by solar TiO₂ photocatalysis and solar photo-Fenton. *Solar Energy* 77(5): 567-572.

Givens, S., Brown, E., Gelman, S., Grady, C. and Skedsvold, D. (1991) Biological process design and pilot testing for carbon oxidation, nitrification and denitrification system. *Environmental Progress* 10(1): 133-146.

Glaze, W., Lay, Y. and Kang, J. (1995) Advanced oxidation processes. A kinetic model for the oxidation of 1,2-dibromo-3-chloropropane in water by the combination of hydrogen peroxide and UV radiation. *Industrial and Engineering Chemistry Research* 34(7): 2314-2323.

Gotz, P. and Reuss, M. (1997) Dynamics of microbial growth: modelling time delays by introducing a polymerization reaction. *Journal of Biotechnology* 58(2): 101-114.

Goudar, C. T., Ganji, S. H., Pujar, B. G. and Strevett, K. A. (2000) Substrate inhibition kinetics of phenol biodegradation. *Water Environment Research*, 72(1): 50-55.

Gowthaman, M.K., Rakshit S.K., Krishnaiah, K. and Baradarajan, A. (1991) Studies on RTD and continuous culture (SCP) in cylindrical and tapered reactors. *Bioprocess Engineering* 7(1-2):41-46.

Guillard, C., Disdier, J., Herrmann, J. M., Lehaut, C., Chopin, T., Malato, S. and Blanco, J. (1999) Comparison of various titania samples of industrial origin in the solar photocatalytic detoxification of water containing 4-chlorophenol. *Catalysis Today* 54(2):217-228.

Guillon, S., Glaze, W., Duguet, J. and Wable, O. (1991) Characterization of natural waters for potential to oxidize organic pollutants with ozone *Proceedings of 10th Ozone World Congress, Zürich, Switzerland.*

Han, K. and Levenspiel, O. (1988) Extended monod kinetics for substrate, product, and cell inhibition. *Biotechnology and Bioengineering* 32(4): 430-437.

Hannaford, A.M. and Kuek, C. (1999) Aerobic batch degradation of phenol using immobilized *Pseudomonas putida*. *Journal of Industrial Microbiology & Biotechnology* 22(2): 121-126.

Hao, O.J., Kim, M.H., Seagren, E.A. and Kim, H. (2002) Kinetics of phenol and chlorophenol utilization by *Acinetobacter* species. *Chemosphere* 46(6):797-807.

Herrmann, J.M., Duchamp, C., Karkmaz, M., Hoai, B.T., Lachheb, H., Puzenat, E. and Guillard, C. (2007) Environmental green chemistry as defined by photocatalysis. *Journal of Hazardous Materials* 146(3):624-629.

Hill G.A, Robinsin C.W. (1975) Substrate inhibition kinetics: phenol degradation by *Pseudomonas putida*. *Biotechnology and Bioengineering* 17(11): 1599-1615.

Hill, G. A. and Robinson, C. W. (1975) Substrate inhibition kinetics: phenol degradation by *pseudomonas putida*. *Biotechnology Bioengineering* 17(11): 1599-1615

Hincapié, M., Maldonado, M.I., Oller, I., Gernjak, W., Sánchez-Pérez, J.A., Ballesteros, M.M. and Malato, S. (2005) Solar photocatalytic degradation and detoxification of EU priority substances. *Catalysis Today* 101 (3-4): 230-210.

Hoffmann, M.R, Martin, S.T., Choi, W. and Bahnemann, D.W. (1995.) Environmental Applications of semiconductor catalysis. *Chemical Reviews* 95(1): 69-96.

Hofmann, K. H. and Kruger, A. (1985) Induction and inactivation of phenol hydroxylase and catechol oxygenase in *Candida maltosa* L4 in dependence on the carbon source. *Journal of Basic Microbiology* 25(6): 373-379.

Hopper, D.J. and Taylor, D. G. (1975) Pathways for the Degradation of m-Cresol and p-Cresol by *Pseudomonas putida*. *Journal of Bacteriology* 122(1):1-6.

Hughes, E. J., Bayly, R. C. and Skurray, R. A. (1984) Evidence for isofunctional enzymes in the degradation of phenol, m- and p-toluic acid, and p-cresol via catechol meta cleavage pathways in *Alcaligenes eutrophus*. *Journal of Bacteriology* 158(1): 79-83.

Hutchison D.H. and Robinson C.W. (1990) A microbial regeneration process for granular activated carbon II. Regeneration studies. *Water Research* 24(10): 1217-1223.

Imandi, S.B., Bandaru, V.V.R., Somalanka, S.R., Bandaru, S.R. and Garapati, H.R. (2008) Application of statistical experimental designs for the optimization of medium constituents for the production of citric acid from pineapple waste. *Bioresource Technology* 99 (10):4445-4450.

Jajuee, B., Margaritas, A., Karamanev, D. and Bergougnou, M.A. (2007) Kinetics of biodegradation of *p*-xylene and naphthalene and oxygen transfer in a novel airlift immobilized bioreactor. *Biotechnology and Bioengineering* 96(2): 232 – 243.

Jamshidi AM, Sohrabi M, Vahabzadeh F and Bonakdarpour B. (2001) Hydrodynamic and mass transfer characterization of a down flow jet loop bioreactor. *Bio chemical Engineering Journal* 8(3): 241-250.

Jin, B., Yin, P. and Lant, P. (2006) Hydrodynamics and mass transfer coefficient in three – phase air- lift reactors containing activated sludge. *Chemical Engineering and Processing* 45(7): 608-617.

Juang, R.S. and Tsai, S.Y. (2006) Growth kinetics of *Pseudomonas putida* in the biodegradation of single and mixed phenol and sodium salicylate. *Biochemical Engineering Journal* 31(2): 133-140.

Kameya, T., Murayama, T., Kitano, M. and Urano, K. (1995) Testing and classification methods for the biodegradabilities of organic compounds under anaerobic conditions. *The Science of The Total Environment* 170(1-2): 31-41.

Kamp, F., Wase, D.A.J., McManamey, W.J., Mendoza, O. and Thayanythy, K. (1987) A comparison of some methods of estimating volumetric mass-transfer coefficients in an external-loop airlift fermentor. *Biotechnology and Bioengineering* 30(2): 179- 186.

Kanai, T., Uzumaki, T. and Kawase, Y. (1996) Simulation of airlift bioreactors: Steady – state performance of continuous culture processes. *Computers and Chemical Engineering* 20(9): 1089-1099.

Kar, S., Swaminathan, T. and Baradarajan, A. (1997) Biodegradation of phenol and cresol isomer mixtures by *Arthrobacter*. *World Journal of Microbiology and Biotechnology* 13(6): 659-663.

Kargi, F. and Eker, S. (2005) Removal of 2,4-dichlorophenol and toxicity from synthetic wastewater in a rotating perforated tube biofilm reactor. *Process Biochemistry*, 40: 2105-2111

Karigar, C., Mahesh, A., Nagenahalli, M. and Yun, D.J. (2006) Phenol degradation by immobilized cells of *Arthrobacter citreus*. *Biodegradation* 17(1): 47–55.

Kelvin, J., Vincente, A.A. and Teixeira, J.A. Study of hydrodynamics and mixing in an airlift reactor with an enlarged separator using magnetic tracer method. Proceedings of the 3rd International Symposium on Two-Phase Flow Modeling and Experimentation, Pisa, 22-24 September 2004.

Kennes, C., Mendez, R. and Lema, J.M. (1997) Methanogenic degradation of p-cresol in batch and in continuous UASB reactors. *Water Research* 31(7): 1549-1554.

Kidak, R. and Ince, N.H. (2006) Ultrasonic destruction of phenol and substituted phenols: A review of current research. *Ultrasonics Sonochemistry* 13(3): 195–199.

Kim, J.H., Oh, K. K., Lee, S. T., Kim, S.W. and Hong, S.I. (2002) biodegradation of phenol and chlorophenols with defined mixed culture in shake-flasks and a packed bed reactor. *Process Biochemistry* 37(12): 1367-1373.

Korpijarvi, J., Oinas, P. and Reunanen, J. (1999) Hydrodynamics and mass transfer in an airlift reactor. *Chemical Engineering Science* 54 (13-14): 2255-2262

Kotturi, G., Robinson, C. W. and Inniss, W. E. (1991) Phenol degradation by a psychrotrophic strain of *Pseudomonas putida*. *Applied Microbiology & Biotechnology* 34(4): 539-543.

Krug, M. and Straube, G. (1986) Degradation of phenolic compounds by the yeast *Candida tropicalis* HP15. II. Some properties of the first two enzymes of the degradation pathway. *Journal of Basic Microbiology* 26(5): 271-281.

Kubo, M., Matsuoka, K., Takahashi, A., Shibasaki-Kitakawa, N. and Yonemoto, T. (2005) Kinetics of ultrasonic degradation of phenol in the presence of TiO₂ particles. *Ultrasonics Sonochemistry* 12(4): 263-269.

Kumar, A., Kumar, S. and Kumar, S. (2005) Biodegradation kinetics of phenol and catechol using *Pseudomonas putida* MTCC 1194. *Biochemical Engineering Journal* 22(2): 151-159.

Kumaran, P. and Paruchuri, Y.L. (1996) Kinetics of phenol biotransformation. *Water Research* 31(1): 11-22.

Kuo, W.S., Chiang, Y.H. and Lai, L.S. (2008) Solar photocatalysis of carbarylinsate promoted by dye photosensitization. *Dyes and Pigments* 76(1): 82-87.

Lefrancois, L., Mariller, C. G. T., and Mejane, J. V. (1955) Efectionnements aux Procèdes de Cultures Forgiques et de Fermentations Industries Brevet D'Invention, France, No. 1,102,200, Delivree le 4 Mai (in French).

Legrini, O., Oliveros, E., Braun, A.M. (1993) Photochemical processes for water treatment. *Chemical. Reviews* 93(2): 671- 698.

Léonard, D. and Lindley, N. D. (1998) Carbon and energy flux constraints in continuous cultures of *Alcaligenes eutrophus* grown on phenol. *Microbiology* 144(1): 241-248

Léonard, D., Youssef, B. C., Destruhaut, C., Lindley, N. D and Queinnec, I. (1999) Phenol degradation by *Ralstonia eutropha*: Colorimetric determination of 2-hydroxymuconate-semialdehyde accumulation to control feed strategy in fed-batch fermentations. *Biotechnology and Bioengineering* 65(4): 407- 415.

- Leyva, E., Moctezuma, E, Ruíz , M. G. and Torres-Martínez , L.** (1998) Photo degradation of phenol and 4-chlorophenol by BaO–LiO₂–TiO₂ catalysts. *Catalysis Today* 40(4): 367–376
- Li, J.K. and Humphrey, A. E.** (1989) Kinetic and fluorometric behavior of a phenol fermentation. *Biotechnology Letters* 11(3): 177-182.
- Li, K., Chang, S. and Yu, C.** (2000) Treatment of chlorohydrocarbon contaminated groundwater by air stripping. *International Conference on Remediation of Chlorinated and Recalcitrant Compounds*, 2nd, Monterey, CA, United States, May 22-25:293-300.
- Litter, M.** (1999) Heterogeneous photocatalysis transition metals ions in photocatalytic systems. *Applied Catalysis B: Environmental* 23(2): 89-114.
- Livingston A.G. and Chase H.A.** (1989) Modeling phenol degradation in a fluidized bed bioreactor. *AICHE* 35 (12): 1980-1992.
- Loh, K. C. and Ranganath. S.** (2005) External-loop fluidized bed airlift bioreactor (EFBAB) for the co metabolic biotransformation of 4-chlorophenol (4-cp) in the presence of phenol *Chemical Engineering Science* 60(22): 6313 - 6319.
- Loh, K. C. and Wang, S. J.** (1998) Enhancement of biodegradation of phenol and a non-growth substrate 4-chlorophenol by medium augmentation with conventional carbon sources. *Biodegradation* 8(5): 329-338.
- Loh, K.C. and Liu, J.** (2001) External loop inversed fluidized bed airlift bioreactor (EIFBAB) for treating high strength phenolic wastewater. *Chemical Engineering Science* 56(21): 6171–6176.
- Luong, J. H. T.** (1987). Generalization of Monod kinetics for analysis of growth data with substrate inhibition. *Biotechnology Bioengineering* 29(2): 242-248
- Maeda, M., Itoh, A. and Kawase, Y.** (2005) Kinetics for aerobic biological treatment of *o*-cresol containing wastewaters in a slurry bioreactor: biodegradation by utilizing waste activated sludge. *Biochemical and Engineering Journal* 22(2): 97–103.

Mahanty, B., Pakshirajan, K. and Dasu, V.V. (2008) Biodegradation of pyrene by *Mycobacterium frederiksbergense* in a two-phase partitioning bioreactor system. *Bioresource Technology* 99 (7): 2694-2698.

Malato, S., Blanco, J., Alarcón, D. C., Maldonado, M.I., Fernández-Ibáñez, P. and Gernjak, W. (2007) Photocatalytic decontamination and disinfection of water with solar collectors *Catalysis Today* 122(1-2):137-149.

Martin, S., Herrmann, H. and Hoffmann, M. (1994) Time-resolved microwave conductivity, Part 2. Quantum sized TiO₂ and the effect of adsorbates and light intensity on charge-carrier dynamics. *Journal of the Chemical Society, Faraday Transaction* 90(21): 3323-3330.

Marugán, J., Aguado, J., Gernjak, W. and Malato, S. (2007) Solar photocatalytic degradation of dichloroacetic acid with silica-supported titania at pilot-plant scale. *Catalysis Today* 129(1-2): 59-68.

Matthews, R. (1990) Purification of water with near-UV illuminated suspensions of titanium dioxide. *Water Resesearch* 24(5): 653-660.

Matthews, R.W. (1991) Environment: photochemical and photocatalytic process. Degradation of organic compounds: In Photochemical conversion and storage of solar energy. Pelizzetti, E. and Schiavello, M. Editors, Kluwer academic publishers: Dordrecht, The Netherlands. 427-449.

Mendonça, E., Martins, A. and Maria Anselmo, A. (2004) Biodegradation of natural phenolic compounds as single and mixed substrates by *Fusarium flocciferum*. *Electronic Journal of Biotechnology* 7(1): 30-37.

Metcalf. and Eddy. Inc (2003) Wastewater engineering: Treatment, disposal and reuse 4th eds. Tata-McGraw-Hill, New Delhi, India.

Mills, A. and Hunte, S.L. (1997) An overview of semiconductor photocatalysis. *Journal of Photochemistry and Photobiology A: Chemistry* 108(1): 1-35.

Minero, C., Pelizzetti, C., Piccini, P. and Vinceti, M. (1994) Photocatalyzed transformation of nitrobenzene on TiO₂ and ZnO *Chemosphere* 28(6): 1229-1244.

Monod, J. (1949) The growth of bacterial cultures. *Annual Reviews of Microbiology* 3: 371-394.

Monteagudo, J.M., Durán, A., Guerra, J, García-Peña F. and Coca, P. (2008) Solar TiO₂-assisted photocatalytic degradation of IGCC power station effluents using a Fresnel lens. *Chemosphere* D.O.I: 10.1016/2007.10.067.

Monteiro A. A. M. G., Boaventura R. A. R. and Rodrigues A. E. (2000) Phenol biodegradation by *Pseudomonas putida* DSM 548 in a batch reactor. *Biochemical Engineering Journal* 6(1): 45-49.

Montgomery D. C. (2004) Design and analysis of experiments. 6th edition. John Wiley & Sons.

Mulchandani, A. and Luong, J.H.T. (1989) Microbial inhibition kinetics revisited *Enzyme Microbial Technology* 11(2): 66-73.

Murialdo, S.E., Fenoglio, R., Haure P.M. and González, J.F. (2003) Degradation of phenol and chlorophenols by mixed and pure cultures. *Water SA* 2(4), 457-463.

Neujahr, H. Y. and Gaal, A. (1973) Phenol hydrolase from yeast. Purification and properties of the enzyme from *Trichosporon cutaneum*. *European Journal Biochemistry* 35(2): 386-400.

Neujahr, H. Y., Lindsjö, S. and Varga, J. M. (1974) Oxidation of phenol by cells and cell-free enzymes from *Candida tropicalis*. *Antonie van Leeuwenhoek*, 40(2): 209-216.

Niccolai, A., Fontani, S., Kapat, A. and Olivier, R. (2003) Maximization of recombinant *Helicobacter pylori* neutrophil activating protein production in *Escherichia coli*: improvement of a chemically defined medium using response surface methodology. *FEMS microbiology Letters* 22(2): 257-262.

Nieto, J., Freer, J., Contreras, D., Candal, R.J., Sileo E.E. and Mansilla, H.D. (2007) Photocatalyzed degradation of flumequine by doped TiO₂ and simulated solar light. *Journal of Hazardous Materials* D.O.I 10.1016/2007.11.026.

Nuhoglu, N. and Yalcin, B. (2005). Modeling of phenol removal in a batch reactor. *Process Biochemistry*, 40 (3-4): 1233-1239.

Okaygun, M.S, Green, L.A and Akgerman, A. (1992) Effects of consecutive pulsing of an inhibitory substrate on biodegradation kinetics. *Environmental Science and Technology* 26(9): 1746-1752.

Okpokwasili, G.C. and Nweke, C.O. (2005) Microbial growth and substrate utilization kinetics. *African Journal of Biotechnology* 5(4): 305-317.

Pakshirajan, K., Chugh, D. and Saravanan, P. (2008) Feasibility of *m*-cresol degradation using an indigenous mixed microbial culture with glucose as co-substrate. *Clean Technology Environmental policy*. D.O.I 10.1007/s10098-007-0120-9.

Paller, G., Hommel, R. K. and Kleber, H.P. (1995) Phenol degradation by *Acinetobacter calcoaceticus* NCIB 8250. *Journal of Basic Microbiology* 35(5): 325-335.

Pawlowsky, U. and Howell, J. A. (1973) Mixed culture biooxidation of phenol. I. Determination of kinetic parameters. *Biotechnology and Bioengineering* 15(5): 889-896.

Peternele, W.S., Winkler-Hechenleitner, A.A and Pineda, E.A.G. (1999) Adsorption of Cd (II) and Pb (II) onto functionalized formic lignin from sugarcane bagasse. *Bioresource Technology*, 68(1): 95-100.

Peyton, G. and Glaze, W. (1988) Destruction of pollutants in water with ozone in combination with ultraviolet radiation. 3. Photolysis of aqueous ozone. *Environmental Science and Technology* 22(7): 761-767.

Przepiórski, J. (2006) Enhanced adsorption of phenol from water by ammonia-treated activated carbon. *Journal of Hazardous materials* 135(1-3): 453-456.

Punima, B.C. and Jain, A. (1998) Wastewater Engineering. Laxmi Publications (p)Ltd. New Delhi, India

Quan, X., Shi, H., Zang, Y., Wang, J. and Qian, Y. (2004) Biodegradation of 2,4 dichlorophenol and phenol in an airlift inner loop bioreactor immobilized with *Achromobacter* sp. *Separation and Purification Technology* 34(1-3): 97-103.

Radehaus, P.M. and Schmidt, S.K. (1992) Characterization of a novel *Pseudomonas* sp. that mineralizes high concentrations of pentachlorophenol. *Applied and Environmental Microbiology* 58(9): 2879-2885.

Reardon, K.F., Mosteller, D.C. and Bull Rogers, J.D. (2000) Biodegradation kinetics of benzene, toluene, and phenol as single and mixed substrates for *Pseudomonas putida* F1. *Biotechnology and Bioengineering* 69(4): 385-400.

Reddy, L.V.A., Wee, Y.J., Yun, J.S. and Ryu, H.W. (2008) Optimization of alkaline protease production by batch culture of *Bacillus* sp. RKY3 through Plackett–Burman and response surface methodological approaches. *Bioresource Technology*, 99(7): 2242-2249

Robert, D. and Malato.S. (2002) Solar photocatalysis: a clean process for water detoxification *The Science of The Total Environment* 291(1-3): 85-97.

Robertson, P. (1996) Semiconductor photocatalysis: an environmentally acceptable alternative production technique and effluent treatment process. *Journal of Cleaner Production* 4(3-4): 203-212.

Rodriguez, G.V., Youssef, C.B. and Vilanova, J.W. (2006). Two-step modeling of the biodegradation of phenol by an acclimated activated sludge. *Chemical Engineering Journal*, 117 (3): 245-252.

Ruiz-Ordaz, N., Ruiz-Lagunez, J.C., Castañón-González, J.H., Hernández-Manzano, E., Cristiani-Urbina, E. and Galíndez-Mayer, J. (2001). Phenol biodegradation using a repeated batch culture of *Candida tropicalis* in a multistage bubble column. *Revista Latinoamericana de Microbiología* 43(1):19-25.

Ryan, D.R., Leukes, W.D. and Burton, S.G. (2005) Fungal bioremediation of phenolics wastewaters in an airlift reactor. *Biotechnology Progress* 21(4): 1066-1074.

Sacher, F., Karrenbrock, F., Knepper, T. and Lindner, K. (2001) Adsorption studies of organic compounds for the assessment of their relevancies for drinking water production. *Vom Wasser* 96: 173-191.

Sahinkaya, E. and Dilek, F. B. (2007) Biodegradation kinetics of 2,4-dichlorophenol by acclimated mixed cultures. *Journal of Biotechnology* 127(4): 716-726.

Santos, V.L. and Valter, R. L. (2004) Biodegradation of phenol by a filamentous fungi isolated from industrial effluents-identification and degradation potential. *Process Biochemistry* 39 (8): 1001-1006.

Schmidt, S.K., Simkins, S. and Alexander, M. (1985) Models for the kinetics of biodegradation of organic compounds not supporting growth. *Applied and Environmental Microbiology* 50 (2): 323-331.

Sen, R. and Swaminathan, T. (2004) Response surface modeling and optimization to elucidate and analyze the effects of inoculum age and size on surfactin production. *Biochemical Engineering Journal* 21(2): 141-148.

Spanning, Å. and Neujahr, H. Y. (1987) Growth and enzyme synthesis during continuous culture of *Trichosporon cutaneum* on phenol. *Biotechnology and Bioengineering* 29(4): 464-468.

Stoilova, I., Krastanov, A., Stanchev, V., Daniel, D., Maria, G. and Alexieva, Z. (2006). Biodegradation of high amounts of phenol, catechol, 2,4-dichlorophenol and 2,6-dimethoxyphenol by *Aspergillus awamori* cells. *Enzyme and Microbial Technology* 39(5): 1036-1041.

Sun, S., Liu, C., Wei, W. and Bao, X. (2006) Hydrodynamic of an annulus airlift reactor. *Powder Technology* 162(3): 201-207.

- Tsai, S.Y. and Juang, R.S.** (2006) Biodegradation of phenol and sodium salicylate mixtures by suspended *Pseudomonas Putida* CCRC 14365. *Journal of Hazardous Materials*, 138 (1): 125-132.
- Urano, K. and Kato, Z.** (1986) Evaluation of biodegradation ranks of priority organic compounds. *Journal of Hazardous Materials*, 13(2): 147-149.
- Vandu C.O., Ellenberger, J. and Krishna, R.** (2005) Hydrodynamics and mass transfer in an up flow monolith loop reactor. *Chemical Engineering and Processing* 44 (3):363-374
- Vázquez, I., Rodríguez-Iglesias, J., Marañón, E., Castrillón L. and Álvarez, M.** (2007). Removal of residual phenols from coke wastewater by adsorption. *Journal of Hazardous materials* 147(1-2): 395-400.
- Viggiani, A., Olivieri, G., Siani, L., Di Donato, A., Marzochella, A., Salatino, P., Barbieri, P. and Galli, E.** (2006) An airlift biofilm reactor for the biodegradation of phenol by *Pseudomonas stutzeri* OX1. *Journal of Biotechnology* 123(4): 464-477.
- Vinod, V.A. and Reddy, G.V.** (2005) Simulation of biodegradation process of phenolic wastewater at higher concentrations in a fluidized-bed bioreactor. *Biochemical Engineering Journal* 24(1), 1-10.
- Vione, D., Minero, C., Maurino, V., Carlotti, M.E., Picatonotto, T. and Pelizzetti, E.** (2005) Degradation of phenol and benzoic acid in the presence of a TiO₂-based heterogeneous photocatalyst. *Applied Catalysis B: Environmental* 58(1-2): 79-88
- Viraraghavan, T. and Alfaro, F. de. M.** (1998) Adsorption of phenol from by wastewater by peat, fly ash and bentonite. *Journal of Hazardous materials* 57(1-3): 59-70.
- Wang, S .J. and Loh K.C.** (1999) Modeling the role of metabolic intermediates in kinetics of phenol biodegradation. *Enzyme and Microbial Technology* 25(3): 177-184.
- Wang, Y.** (1992) Effect of chemical oxidation on anaerobic biodegradation of model phenolic compounds. *Water Environment Research* 64(3): 268-273.

Wang, Q., Hou, Y., Xu, Z., Miao, J. and Li, G. (2008a) Optimization of cold-active protease production by the psychrophilic bacterium *Colwellia* sp. NJ341 with surface response methodology. *Bioresource Technology* 99(6): 1926-1931.

Wang, Y.H., Li, Y.P., Zhang, O. and Zhang, X. (2008b) Enhanced antibiotic activity of *Xenorhabdus nematophila* by medium optimization. *Bioresource Technology* 99(6): 1708-1715.

Wiesmann, U. and Putnaerglis, A. (1986) Influence of oxygen concentration on substrate degradation in activated sludge reactors. *German Chemical Engineering* 9(5): 284-291.

Wu, J., Bewtra, J., Biswas, N. and Taylor, K. (1994) Effect of H₂O₂ addition mode on enzymatic removal of phenol from wastewater in the presence of polyethylene glycol. *Canadian Journal of Chemical Engineering* 72(5): 881-886.

Yan, J., Jianping, W., Bai, J., Daoquan, W. and Zongding, H. (2006) Phenol biodegradation by the yeast *Candida tropicalis* in the presence of *m*-cresol. *Biochemical Engineering Journal* 29(3): 227-23.

Yang, R. D. and Humphrey, A. E. (1975) Dynamic and steady state studies of phenol biodegradation in pure and mixed cultures. *Biotechnology and Bioengineering* 17(8): 1211-1235.

Yano, T. and Koga, S. (1969) Dynamic behaviour of the chemostat subject to substrate inhibition. *Biotechnology and Bioengineering* 11(2): 139-153.

Yoon, H., Klinzing, G. and Blanch, H.W. (1977) Competition for mixed substrates by microbial populations. *Biotechnology and Bioengineering* 19(8): 1193-1210.

Zhang, L., Kanki, T., Norikai, S. and Toyoda, A. (2001) Photocatalytic degradation of organic compounds in aqueous solution by a TiO₂ -coated rotating-drum reactor using solar light. *Solar Energy* 70(4): 331-337.



APPENDIX

Details of the biochemical characterization test for microbes along with the principle and result interpretation as described in the Hi mobility™ Biochemical kit

Sl.No.	Test	Reagent to be added after incubation	Principle	Original colour of the medium	Positive reaction	Negative reaction
1.	ONPG	Nil	Detects β -galactosidase activity	Colourless	Yellow	Colourless
2.	Lysine decarboxylase	Nil	Detects Lysine decarboxylation	Olive green	Purple	Yellow
3.	Ornithine decarboxylase	Nil	Detects Ornithine decarboxylase	Olive green	Purple	Yellow
4.	Urease	Nil	Detects Urease activity	Orangish yellow	Pink	Orangish yellow
5.	Phenylalanine deamination	2-3 drops of TDA reagent	Detects Phenylalanine deamination activity	Colourless	Green	Colourless
6.	Nitrate reduction test	1-2 drops of sulphanilic acid and 1-2 drops of N,N-Dimethyl-1-Nphthylamine	Detects Nitrate reduction	Colourless	Pinkish red	Colourless
7.	Vogers proskauer's Test	Add 2-3 drops of Britt reagent A and 1 drop of Baritt reagent B.	Detects acetoin production	Colourless	Pinkish red	Colourless / Slight copper
8.	H ₂ S production	Nil	Detects H ₂ S production	Orangish yellow	Black	Orangish yellow

9.	Citrate utilization	Nil	Detects capability of organism to utilize citrate as a sole carbon source	Yellowish-green	Blue	Yellowish-green
10.	Methyl Red Test	Add 1-2 drops of Methyl Red reagent	Detects acid production	Colourless	Red	Yellow
11.	Indole	1-2 drops of Kovac's reagent	Detects deamination of tryptophan	Colourless	Pinkish red	Colourless
12.	Malonate	Nil	Detects capability of organism to utilize sodium malonate as a sole carbon source	Light green	Blue	Light green
13.	Esculin	Nil	Esculin hydrolysis	Cream	Black	Cream
14.	Arbinose	Nil	Arbinose utilization	Red	Yellow	Red/Pink
15.	Xylose	Nil	Xylose utilization	Red	Yellow	Red/Pink
16.	Adonitol	Nil	Adonitol utilization	Red	Yellow	Red/Pink
17.	Rhamnose	Nil	Rhamnose utilization	Red	Yellow	Red/Pink
18.	Cellobiose	Nil	Cellobiose utilization	Red	Yellow	Red/Pink
19.	Melibiose	Nil	Melibiose utilization	Red	Yellow	Red/Pink
20.	Saccharose	Nil	Saccharose utilization	Red	Yellow	Red/Pink

21.	Raffinose	Nil	Raffinose utilization	Red	Yellow	Red/Pink
22.	Trehalose	Nil	Trehalose utilization	Red	Yellow	Red/Pink
23.	Glucose	Nil	Glucose Utilization	Red	Yellow	Red/Pink
24.	Lactose	Nil	Lactose utilization	Red	Yellow	Red/Pink
25.	Oxidase	Nil	Done on oxidase disc separately. Detects cytochrome oxidase production	White	Deep purple with in 10 sec	White/ purple after 60 sec
26.	Motility + Esculin	Nil	Detects motility and esculin hydrolysis	Cream	Movement of growth in the second well with simultaneous blackening	No change in second well
27.	Catalase	3% H ₂ O ₂	Detects catalase activity	Cream	Effervescence when treated with 3 % H ₂ O ₂	No effervescence
28.	α -methyl-D mannose	Nil	Carbohydrate utilization	Red	Yellow	Red/pink
29.	Ribose	Nil	Carbohydrate utilization	Orangish Red	Yellow	Orangish red
30.	Mannitol	Nil	Carbohydrate utilization	Red	Yellow	Red/pink

LIST OF PUBLICATIONS

Published/Accepted in Refereed International Journals

1. Saravanan, P., Pakshirajan, K. and Saha, P. (2008) Growth kinetics of an indigenous mixed microbial consortium during phenol degradation in a batch reactor. *Bioresource Technology*, 99 (1) 205-209.
2. Saravanan, P., Pakshirajan, K. and Saha, P. (2008) Kinetics of phenol and *m*-cresol biodegradation by an indigenous *Pseudomonas* Species isolated from a sewage treatment plant. *Journal of Environmental sciences*. Accepted.
3. Saravanan, P., Pakshirajan, K., and Saha, P. (2008) Biodegradation of phenol and *m*-cresol in a batch and fed batch operated internal loop airlift bioreactor by indigenous mixed microbial culture predominantly *Pseudomonas* sp. *Bioresource Technology*,99(18) 8553-8558.
4. Saravanan, P., Pakshirajan, K. and Saha, P. (2008) Batch growth kinetics of an indigenous mixed microbial culture utilizing *m*-cresol as the sole carbon source. *Journal of Hazardous Materials*. doi/10.1016/j.jhazmat.2008.05.069.Inpress.
5. Saravanan, P., Pakshirajan, K. and Saha, P. (2008) Hydrodynamics and batch biodegradation of phenol in an internal loop airlift bioreactor. *International Journal of Environment and Waste Management*. Accepted.
6. Saravanan, P., Pakshirajan, K. and Saha, P. (2008) Kinetics of growth and multi substrate degradation by an indigenous mixed microbial culture isolated from a wastewater treatment plant in Guwahati, India. *Water Science and Technology*. Accepted.

Communicated/Under Review in Refereed International Journals

7. Saravanan, P., Pakshirajan, K. and Saha, P. (2008) Degradation of phenol by TiO₂-based heterogeneous photocatalysts in presence of sunlight. *Journal of Hydro-Environment Research*. Revised manuscript under review.
8. Saravanan, P., Pakshirajan, K. and Saha, P. (2008) Performance of batch stirred tank bioreactor and internal loop airlift bioreactor in degrading phenol using *Pseudomonas* spp.- A comparative study. *Journal of Environmental Protection Science*. Revised manuscript under review.
9. Saravanan, P., Pakshirajan, K. and Saha, P. (2008) Treatment of phenolics containing synthetic wastewater in an internal loop airlift bioreactor (ILALR) using indigenous mixed strain of *Pseudomonas* sp. under continuous mode of operation. *Process Biochemistry*. Under review.

In Conferences

1. Saravanan, P., Pakshirajan, and K. and Saha, P. Evaluation of indigenous mixed microbial consortium for bioremediation of petroleum refinery effluent. *Proceedings of International Symposium on Sanitary and Environmental Engineering (SIDISA 08)*, Organized by Civil and Environmental Engineering Department University of Florence, Italy, June 24-27, 2008.
2. Saravanan, P., Pakshirajan, K. and Saha, P. Successive batch operation of internal loop airlift bioreactor in degrading phenol and *m* – cresol as single substrate by indigenous mixed microbial consortium isolated from a sewage treatment plant in Proceedings of *Singapore International Water Week 2008*, Jointly organized by PUB and International Water Association (IWA) at Suntech Singapore International Convention and Exhibition center, Singapore, June 23-27, 2008.
3. Saravanan, P., Pakshirajan, K. and Saha, P. Kinetics of growth and multi substrate degradation by an indigenous mixed microbial culture isolated from a wastewater treatment plant in Guwahati, India. *Proceeding of 2nd IWA – ASPIRE Asia-Pacific Regional Group Conference & Exhibition, Water and Sanitation in the Asia-Pacific Region: Opportunities, Challenges and Technology*, Perth, Australia, 28 October - 1 November 2007.

4. Saravanan, P., Pakshirajan, K. and Saha, P. Performance of batch stirred tank reactor in degrading phenol using indigenous mixed microbial consortium. *Proceeding of International Conference on New Horizon in Biotechnology (NHBT)*. Organized by National Institute for Interdisciplinary Science & Technology (NIST), (Formerly Regional Research Laboratory), Trivandrum, India, 26 – 29 November 2007.
5. Saravanan, P., Pakshirajan, K. and Saha, P. Modeling the degradation of phenol by a mixed microbial culture in a batch reactor. Presented in the *59th Annual Session of the Indian Chemical Engineering Congress (CHEMCON 2006)*, Ankleshwar, Gujarat, India. December 27-30, 2006.
6. Saravanan, P., Mandal, B.P. and Saha, P. Solar Photocatalytic treatment of phenolic wastewater, presented in the *58th Annual Session of the Indian Chemical Engineering Congress (CHEMCON 2005)*, New Delhi, India. December 14-17, 2005.

